NASA CR-706

DESIGN AND FABRICATION OF A HIGH-PERFORMANCE BRAYTON CYCLE RADIAL-FLOW GAS GENERATOR

Prepared under Contract No. NAS 3-2778 by
AIRESEARCH MANUFACTURING COMPANY OF ARIZONA
Phoenix, Ariz.

for Lewis Research Center

NATIONAL AERONAUTICS AND SPACE ADMINISTRATION

For sale by the Clearinghouse for Federal Scientific and Technical Information
Springfield, Virginia 22151 – Price $3.00

FOREWORD

The research described herein, which was conducted by the AiResearch Company of Arizona, a Division of the Garrett Corporation, was performed under NASA Contract NAS 3-2778. The work was done under the technical management of Mr. Jack A. Heller, Space Power Systems Division, Lewis Research Center, with Mr. George K. Fischer and Mr. Harold E. Rohlik, both of the Fluid System Components Division, Lewis Research Center, as technical consultants. The report was originally issued as AiResearch Report APS-5200-R.

ABSTRACT

The program described herein consisted of analyses, design, gas bearing development and fabrication of a radial-flow gas generator (turbocompressor) for performance evaluation by the NASA. The respective turbine and compressor components, identical to those in the gas generator, were delivered in separate research packages utilizing oil-lubricated ball bearings for detail aerodynamic performance investigations. A gas generator was delivered that operated satisfactorily on its gas journal and thrust bearings at 38, 500 rpm design speed at 500^{o} F turbine inlet temperature.

TABLE OF CONTENTS

TABLE OF CONTENTS (Contd.)

DESIGN AND FABRICATION OF A HIGH-PERFORMANCE BRAYTON CYCLE RADIAL-FLOW GAS GENERATOR

AIRESEARCH MANUFACTURING COMPANY OF ARIZONA

SUMMARY

The NASA-Lewis Research Center is presently engaged in an investigation of Brayton-cycle space-power systems that use solar or nuclear energy as the heat source and an inert gas as the working fluid. The turbomachinery required for the system and component investigations was defined by the NASA for both radial and axial-flow machinery. Under Contract NAS3-2778, three pieces of radial turbomachinery were designed and fabricated, as follows:

Compressor and Turbine Research Packages - The two compressor and turbine research packages each include a high-performance single-stage radial wheel and attendant components and a suitable set of running gear with oil-lubricated bearings. Both research packages are to be used to evaluate component aerodynamic performance.

Gas Generator - This unit combines the turbine and compressor of the two research packages into a single hot unit, with the running gear including gas-lubricated bearings. The gas generator will be used to evaluate the Brayton-cycle radial turbomachinery in a ground test loop.

This report describes the selection of the gas generator design speed and the design, fabrication, inspection, instrumentation, and testing of the gas generator prior to delivery to the NASA. Shown below is the specified design point of the turbine and compressor as individual components and as included in the radial turbomachinery gas generator:

	Turbine	Compressor	Gas Generator
Working fluid	Argon	Argon	Argon
Flow rate, lbs per sec.	1.184	0.621	0.611
Turbine inlet temperature, ^{o}R	520	-	1950
Turbine inlet pressure, psia	13.2	-	13.2
Turbine total pressure ratio	1.56	-	1.56
Compressor inlet temperature, ^{o}R	-	520	536
Compressor inlet pressure, psia	-	6.0	6.0
Compressure pressure ratio	-	2.30	2.30

Two cold research packages each of the turbine and compressor were delivered to the NASA for aerodynamic performance investigations. Two gas generators were fabricated and also delivered to the NASA; one as a complete unit and the second as separate parts. Successful dynamic and mechanical integration of the thrust and journal gas bearings with the gas generator was accomplished. Prior to shipment to the NASA, the assembled unit was subjected to an Acceptance Test which demonstrated satisfactory performance on air at approximately $500^{o}F$ turbine inlet temperature.

1.0 INTRODUCTION

The NASA-Lewis Research Center is presently conducting an evaluation of closed, recuperated Brayton-cycle space power systems that use solar or nuclear energy as the heat source and an inert gas as the working fluid. Both axial- and radial-flow types of turbomachinery will be evaluated. This contract (NAS3-2778) calls for the design and fabrication of the following radial-flow turbomachinery:

Compressor and Turbine Research Packages - The two compressor and turbine research packages each include a high-performance single-stage radial wheel and attendant components and a suitable set of running gear with oil-lubricated bearings. Both research packages are to be used to evaluate component aerodynamic performance.

Gas Generator - This unit combines the turbine and compressor of the two research packages into a single hot unit, with the running gear including gas-lubricated bearings. The gas generator will be used to evaluate the Brayton-cycle radial turbomachinery in a ground test loop.

The gas generator is but one of the components utilized in the closed Brayton-cycle space power system. However, it is perhaps the most critical from a performance and reliability standpoint. The gas generator consists of a single-stage radial compressor utilized for the compression of the inert working fluid (argon) mounted on a shaft supported by gas journal and thrust bearings, driven by a single-stage, radial-inflow power turbine (mounted on the same shaft). The gas, partially expanded, is exhausted from the gas generator compressor drive turbine into a second-stage free turbine which drives an alternator on the same shaft. This latter package is separate from the gas generator unit.

The contract effort, performed to design, fabricate, and acceptance test the radial-flow gas generator, is summarized in Section 3.0 of this report. The program included the scaling of existing AiResearch turbine and compressor designs, and development of the mechanical and dynamic integration of the gas bearings into the gas generator.

The significance of the program is the integration of gas bearings with turbomachinery that culminates as a gas-bearing gas generator designed for operation on inert gas in a zero-g environment--a first of its kind. Gas bearings appear to be a promising solution to the bearing requirements of long-life Brayton-cycle space power turbomachinery.

The guidance and assistance given to this contractor by Messrs. J. A. Heller, H. E. Rohlik, and G. K. Fischer of NASA-Lewis are acknowledged. The technical assistance and consultation provided by The Franklin Institute (Dr. E. J. Gunter, Jr.), and by Dr. V. Castelli, in the design of gas journal bearings is also acknowledged.

2.0 SELECTION OF DESIGN SPEED

Figure 1 shows a schematic of the NASA Brayton-cycle space power system. Contract NAS3-2778 calls for the design and fabrication of a turbine research test package, a compressor research test package, and a gas generator with the same aerodynamic components as were used in the test packages, As specified by the contract, the gas generator and research test packages have identical design conditions when corrected mass-flow rates are compared. Table 1 presents a summary of the design conditions as specified by the contract. In addition to the conditions listed in Table 1, the most important remaining turbomachinery variables are:

(a) Shaft speed, N_1

(b) Compressor specific speed, N_{S_c}

From the expression of compressor specific speed

$$N_{S_c} = \frac{N_1}{60} \left(\frac{1}{R_1 T_1}\right)^{1/4} \left(\frac{\overset{o}{m}}{P_1}\right)^{1/2} \left[\frac{(\gamma - 1)M}{\gamma g(r_c^{\theta_1} - 1)}\right]^{3/4}$$

it can be seen that the compressor specific speed is a function only of shaft speed, since the remaining variables are fixed by the contract. (A list of the symbols used throughout this report can be found in the Glossary, Appendix I.) Therefore, the shaft speed is the only remaining variable to be specified.

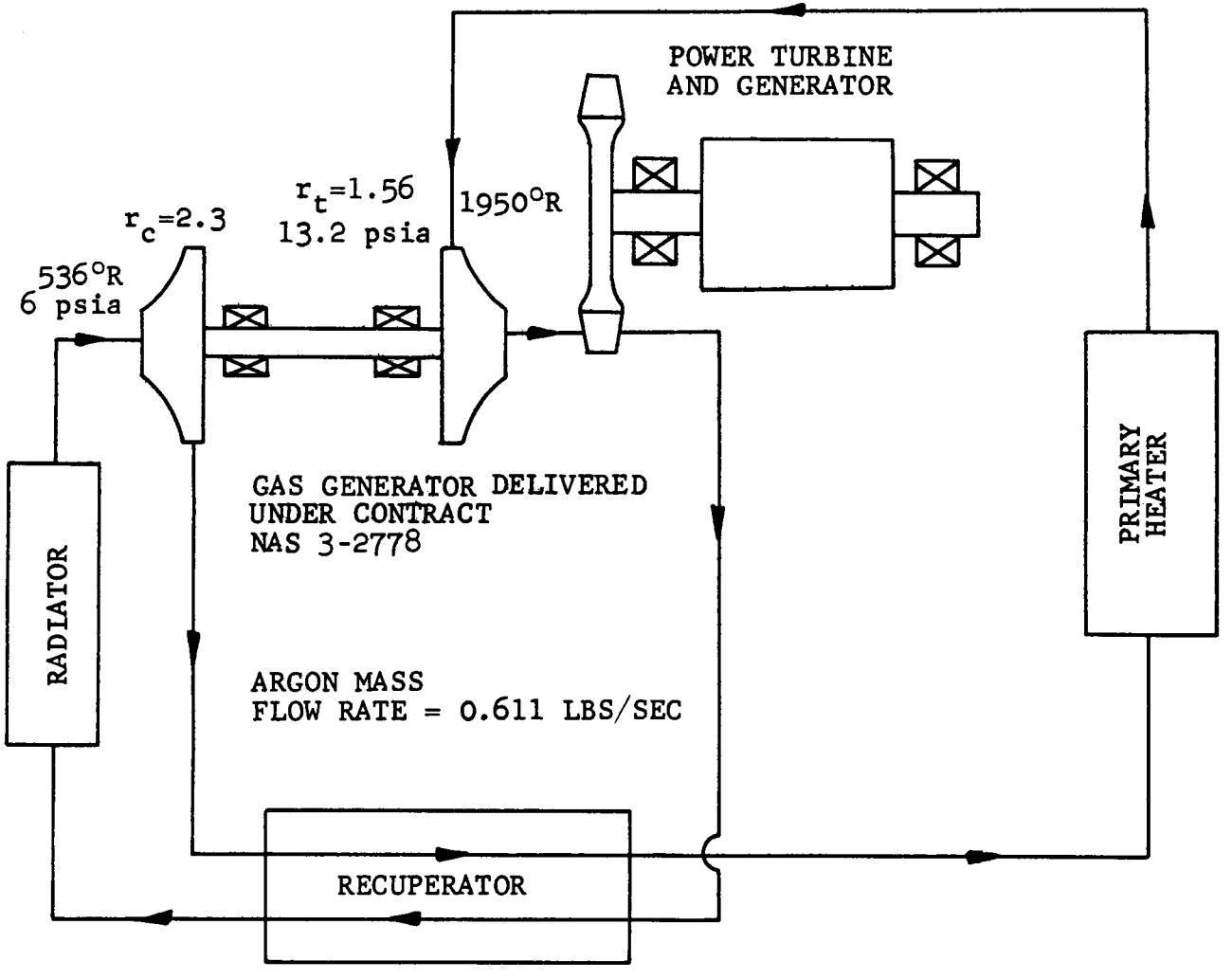

NASA BRAYTON-CYCLE-POWER SYSTEM

FIGURE 1

TABLE 1

DESIGN PARAMETERS FIXED BY
CONTRACT NAS 3-2778

	Turbine Package	Compressor Package	Gas Generator
Working fluid	Argon	Argon	Argon
Mass flow rate, W - lbs per sec.	1.184	0.621	0.611
Turbine inlet temperature, T_3, $^{\circ}R$	520	-	1950
Turbine inlet pressure, P_3, psia	13.2	-	13.2
Turbine pressure ratio, r_{t_1}	1.56	-	1.56
Compressor inlet temperature, T_1, $^{\circ}R$	-	520	536
Compressor inlet pressure, P_1, psia	-	6.0	6.0
Compressor pressure ratio, r_c	-	2.30	2.30
Corrected mass flow rate:			
$W\sqrt{\theta}/\delta$ turbine, lbs per sec.	1.318	-	1.318
$W\sqrt{\theta}/\delta$ compressor, lbs per sec.	-	1.521	1.521

With the design-point conditions listed in Table 1, a recuperator effectiveness (E_R) of 0.85, and a pressure-loss parameter (β) of 0.90, a gas generator design-point study was conducted to establish the gas generator thermodynamic and aerodynamic operating conditions. Figures 2 and 3 illustrate the variation of wheel diameters, component and cycle efficiencies, component specific speeds, and turbine pressure ratio over a range of shaft speeds with the turbine and compressor matched. As noted on the figures, a shaft speed of 38,500 rpm was selected as discussed below.

(a) The compressor specific speed of 0.106, corresponding to a shaft speed of 38,500 rpm, makes AiResearch compressor experience with similar specific speeds directly applicable. A more favorable specific speed of 0.09, based on a system weight optimization to reduce the weight 5 percent, would result in a speed of 33,000 rpm, which is undesirable, as discussed in (c) below.

(b) Reasonable adiabatic efficiencies occur for the compressor and turbines at a shaft speed of 38,500 rpm, whereas at lower speeds the component efficiency and, thus, the cycle efficiency drop off rapidly.

(c) Turbine and compressor wheel diameters of 6 inches occur at a shaft speed of 38,500 rpm with reasonably obtainable adiabatic efficiencies. An increase in the shaft speed would reduce the wheel size and result in more restrictive manufacturing tolerances necessary to maintain hydraulically smooth aerodynamic passages.

COMPRESSOR INLET TEMPERATURE, T_1 = 536°R
TURBINE INLET TEMPERATURE, T_3 = 1950°R
RECUPERATOR EFFECTIVENESS, E_R = 0.85
WORKING FLUID = ARGON

$\frac{\text{TURBINE PRESSURE RATIO}}{\text{COMPRESSOR PRESSURE RATIO}}$, β = 0.90

COMPRESSOR PRESSURE RATIO, r_c = 2.30
COMPRESSOR INLET PRESSURE, P_1^c = 6.0 PSIA
MASS FLOW RATE, $\dot{m}$ = 0.611 LBS PER SEC

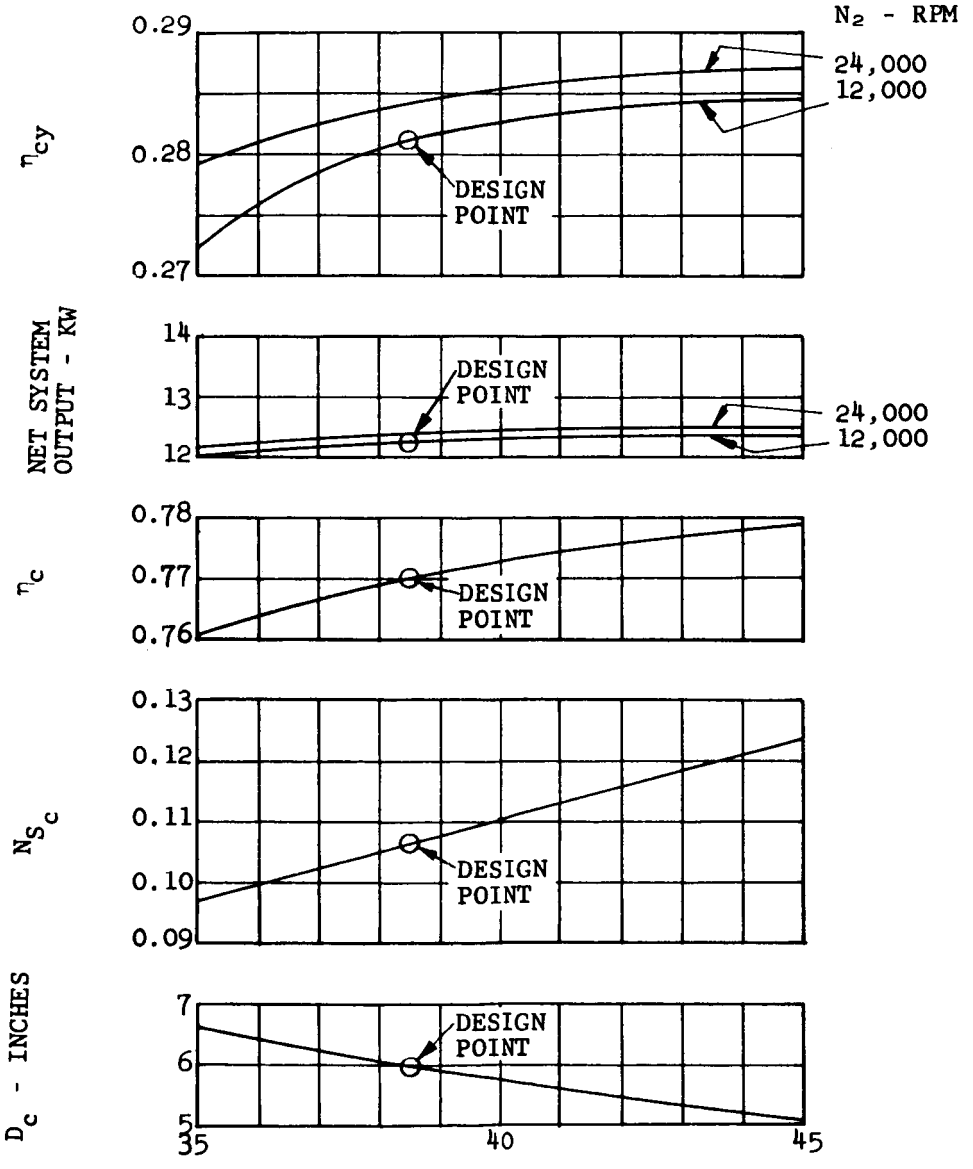

COMPRESSOR DESIGN POINT
STUDY RESULTS
FIGURE 2

COMPRESSOR INLET TEMPERATURE, T_1 = 536°R
TURBINE INLET TEMPERATURE, T_3 = 1950°R
RECUPERATOR EFFECTIVENESS, E_R = 0.85
WORKING FLUID = ARGON

$\frac{\text{TURBINE PRESSURE RATIO}}{\text{COMPRESSOR PRESSURE RATIO}}$, β = 0.90

COMPRESSOR PRESSURE RATIO, r_c = 2.30
COMPRESSOR INLET PRESSURE, P_1 = 6.0 PSIA
MASS FLOW RATE, $\dot{m}$ = 0.611 LBS PER SEC

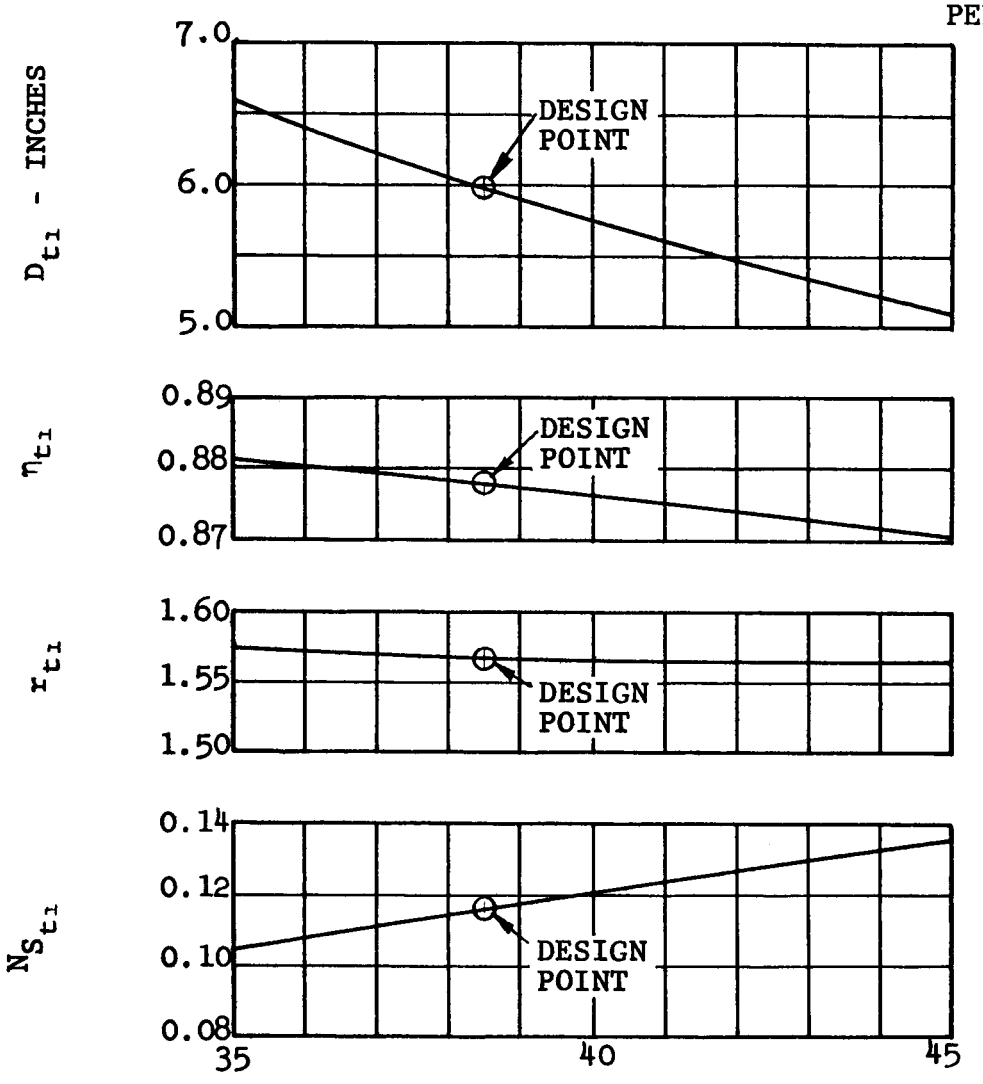

TURBINE DESIGN POINT
STUDY RESULTS
FIGURE 3

3.0 GAS GENERATOR DESIGN

3.1 Gas Generator Description

Figure 4 shows a schematic of the final gas generator configuration. The compressor and turbine wheels are mounted on a common shaft into which is incorporated a double-acting thrust bearing slider. Pivoted-pad gas-journal bearings support the shaft, one on each side of the thrust bearing next to the turbine and compressor wheels. These bearings are of the hydrodynamic type (self acting) with hydrostatic lift-off capability for starting and stopping. Between the journal bearing carriers are located the hydrostatic and hydrodynamic thrust bearing stators. The wheels, shaft, and bearings are mounted in the main frame, on which is also mounted the compressor scroll and diffuser and the turbine nozzle and scroll.

The following sections describe the design and development of the various components incorporated into the gas generator. Design details of the turbine and compressor have been minimized in the interest of brevity. However, the gas bearing development and integration of the components are included.

3.2 Compressor and Turbine

The compressor and turbine components of the gas generator were first designed, fabricated, and tested on cold research packages shown in Figures 5 and 6.

The compressor research package consists of a 6.0-inch-diameter radial impeller with attendant scroll and diffuser mounted on an oil-bearing test rig. Performance testing was accomplished on this rig and cutback tests were run to determine the optimum impeller cutback for the design conditions. Figure 7 shows the final map for the compressor. A complete discussion of the compressor design,

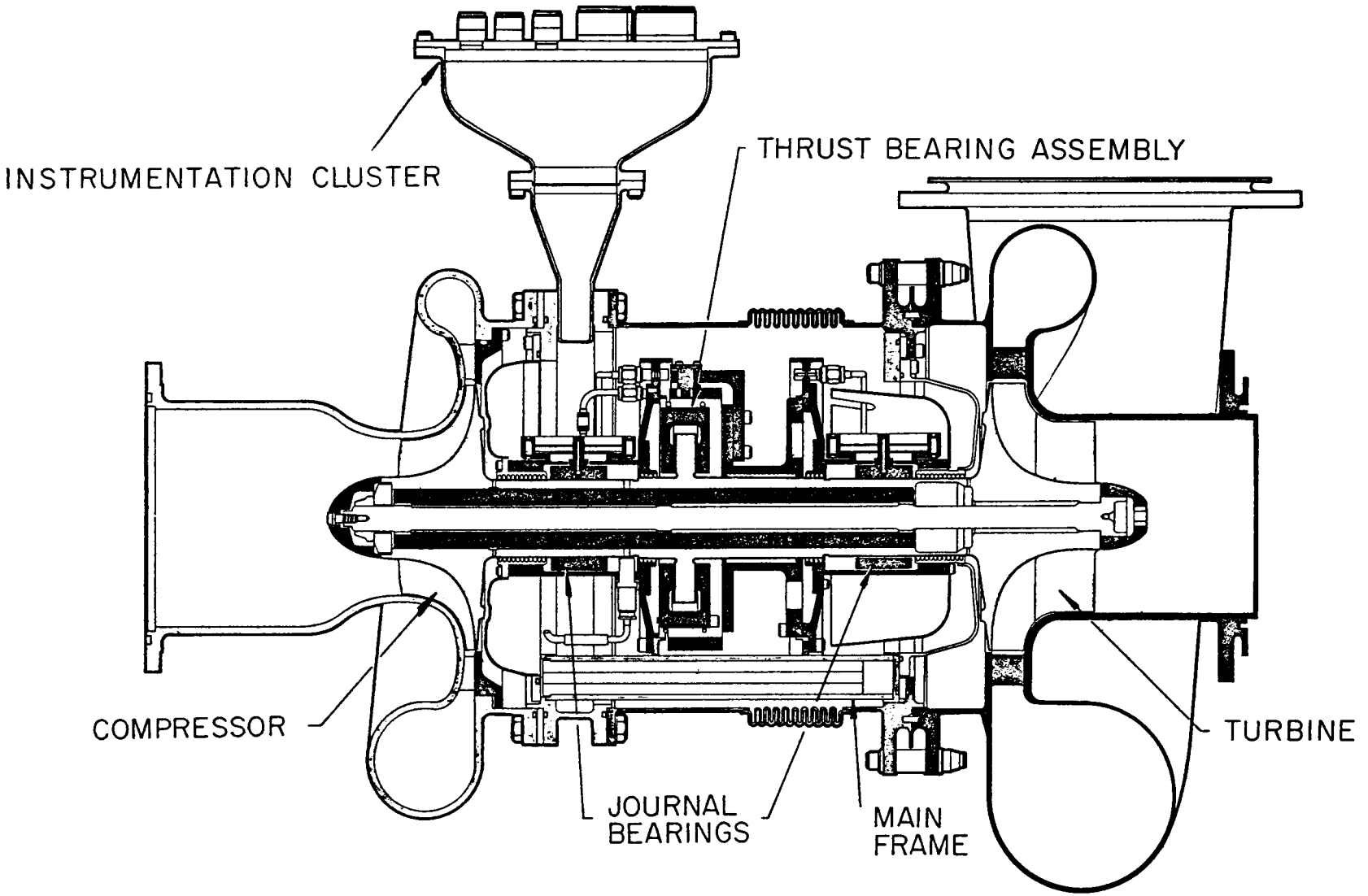

NASA BRAYTON-CYCLE RADIAL GAS GENERATOR

FIGURE 4

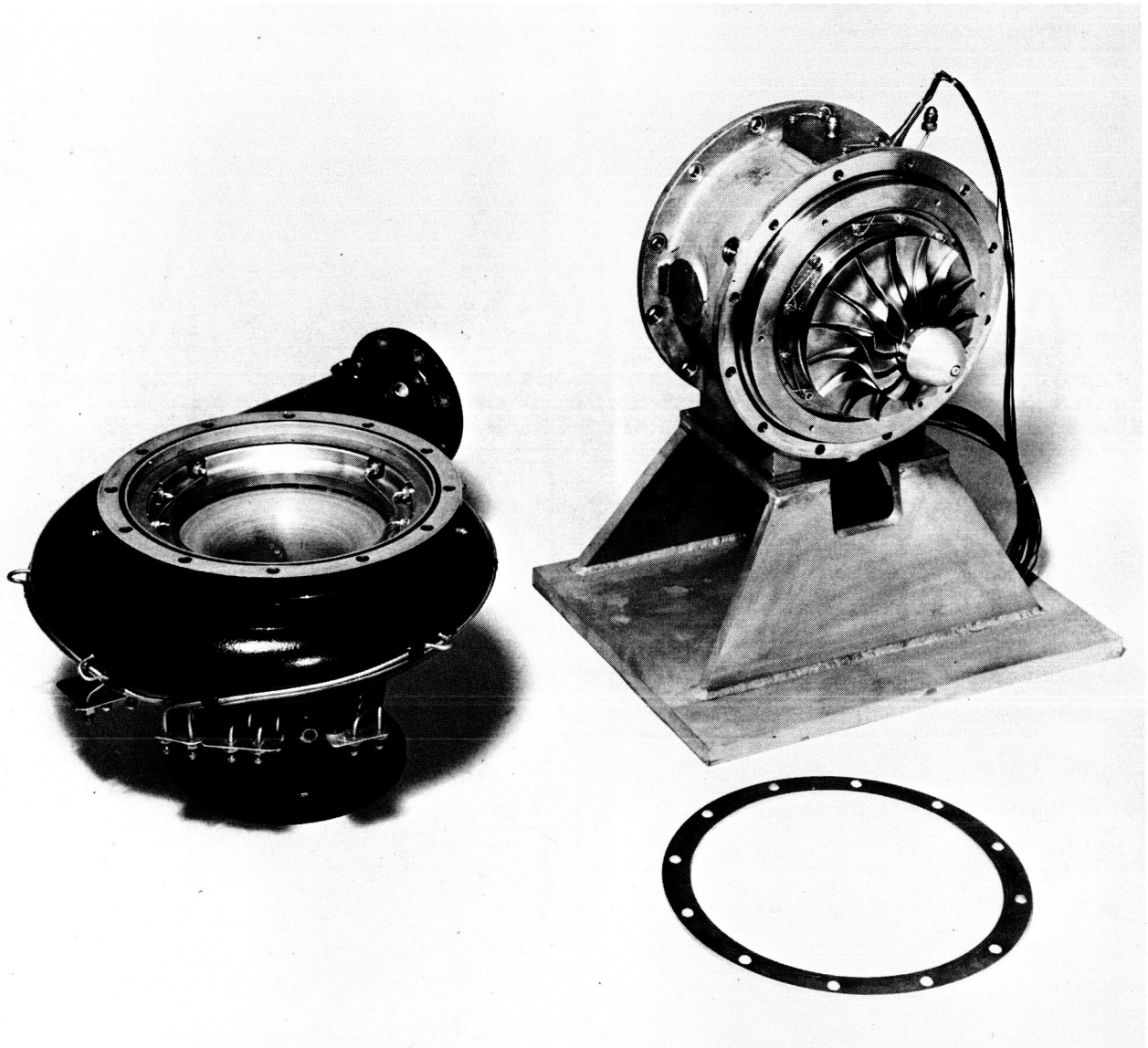

NASA COMPRESSOR RESEARCH PACKAGE

FIGURE 5

NASA TURBINE RESEARCH PACKAGE

FIGURE 6

TEST FLUID - ARGON
COMPRESSOR INLET TOTAL PRESSURE - 12.0 TO 12.5 IN. Hg ABS
COMPRESSOR INLET TOTAL TEMPERATURE - 536°R
100 PERCENT $N/\sqrt{\theta}$ = 37,900 RPM

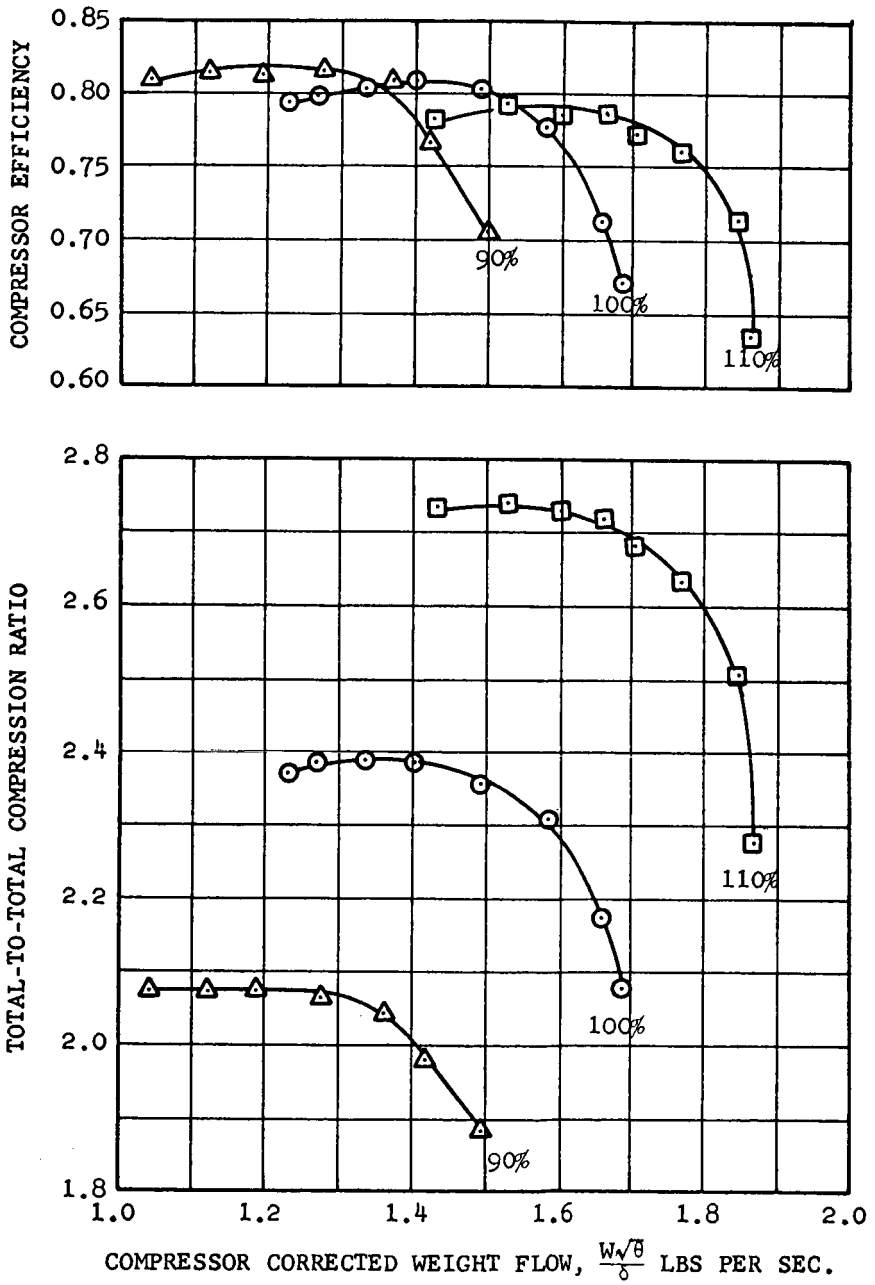

6-IN.-DIAMETER COMPRESSOR TEST RESULTS
FIGURE 7

fabrication, and acceptance testing can be found in NASA Report CR-54368 entitled Design and Development of a High-Performance Brayton-Cycle Compressor Research Package (AiResearch Report APS-5109-R). Two compressor research packages were delivered to the NASA.

The turbine research package consists of a 6.0 inch diameter radial turbine wheel with attendant scroll and nozzle mounted on an oil-bearing test rig. Development testing was accomplished on this rig. A complete discussion of the turbine design, fabrication, and acceptance testing can be found in NASA Report CR-54367 entitled Design and Development of a High-Performance Brayton-Cycle Turbine Research Package (AiResearch Report APS-5108-R). Two turbine research packages were delivered to the NASA.

3.3 Dynamic Analysis

At the initiation of the gas-generator design, four possible gas-bearing/turbine and compressor wheel configurations were analyzed to determine the best configuration from critical speed and design considerations. The four systems, shown in Figure 8, consisted of a double overhung system, a compressor overhung system, a turbine overhung system, and a system wherein the bearings are mounted outside the turbine and compressor wheels. Of the four configurations analyzed, the double overhung system was chosen for continued analysis since it presented fewer overall design problems.

A bearing load and critical speed analysis was then conducted for the double overhung system with a range of bearing spacings (6.0 to 14.5 inches) and overall resilient gas bearing spring rates (5,000 to 20,000 pounds per inch). The resiliently mounted

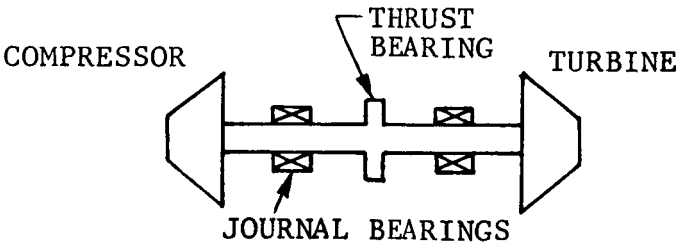

DOUBLE OVERHUNG SYSTEM

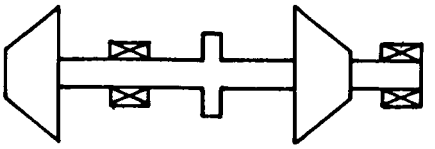

COMPRESSOR OVERHUNG SYSTEM

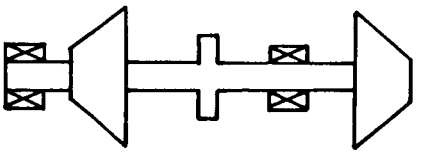

TURBINE OVERHUNG SYSTEM

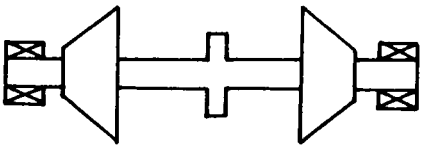

DOUBLE STRADDLE MOUNTED SYSTEM

GAS GENERATOR CONFIGURATIONS
FIGURE 8

bearings tend to minimize the critical speeds and bearing loads (see Section 3.4 for a discussion of the resiliently mounted bearings). Figure 9 shows the results of the critical speed analysis. For the variable spacing and bearing combined gas film and mount spring rates, the bearing loads at design operating speed were approximately 20 pounds per 0.001 inch c.g. eccentricity (i.e., the c.g. of both the turbine and compressor masses are displaced 0.001 inch in the same direction from the rotational center). Bearing spacings from 6.0 to 13.0 inches were initially chosen to be utilized in the gas bearing testing and as limits for the gas generator. The 14.5-inch bearing spacing was rejected since the third critical speed is too close to the 38,500 rpm operating speed.

These results were obtained by utilizing an AiResearch critical-speed computer program. This program has the capability of considering gyroscopic moments, shaft flexibilities, bearing (and support) flexibilities, static and dynamic rotor unbalance, and rotor distributed properties. The rotor may be lumped into a maximum of 30 mass stations, and at each mass station the mass, polar moment of inertia, diametral moment of inertia, mass unbalance and bearing flexibility may be specified. The whirl ratio may also be prescribed. The program computes bearing loads versus speed and the rotor critical speeds and corresponding rotor modal patterns.

After the design of the gas generator was finalized, the final critical-speed analysis was accomplished, and the results are shown in Figure 10. For this analysis the bearing spacing was 7.0 inches, and the combined rotating group polar moment of inertia was 0.060 inch-lbs-sec^2.

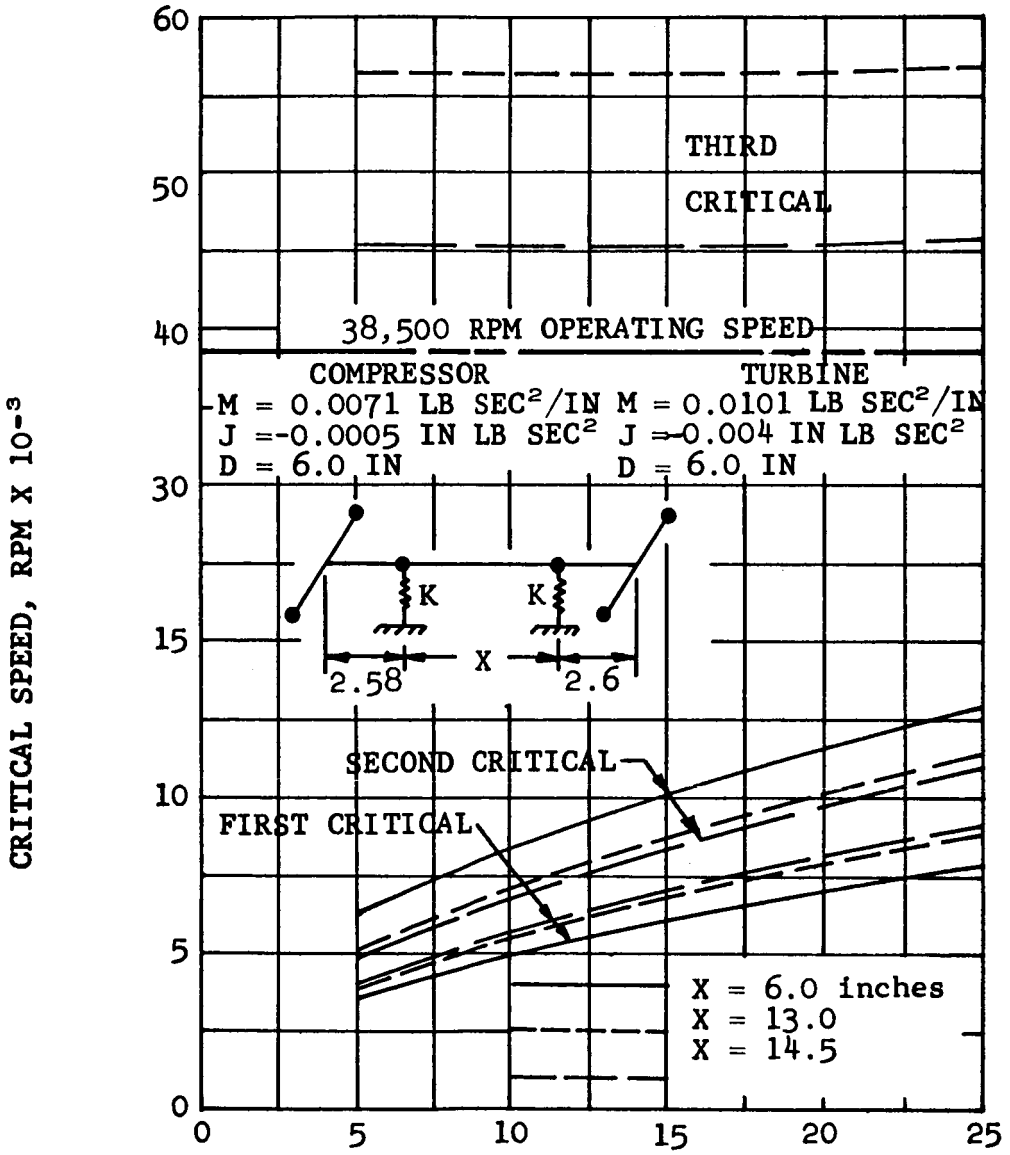

CRITICAL SPEED VS. BEARING SPRING RATE FOR NASA GAS GENERATOR, INITIAL RESULTS

FIGURE 9

$e_1 = e_2 = 0.001$ INCH X = BEARING SPACING = 7.0 INCHES

$k_1 = k_2 = 35{,}800$ POUNDS PER INCH (GAS FILM STIFFNESS)

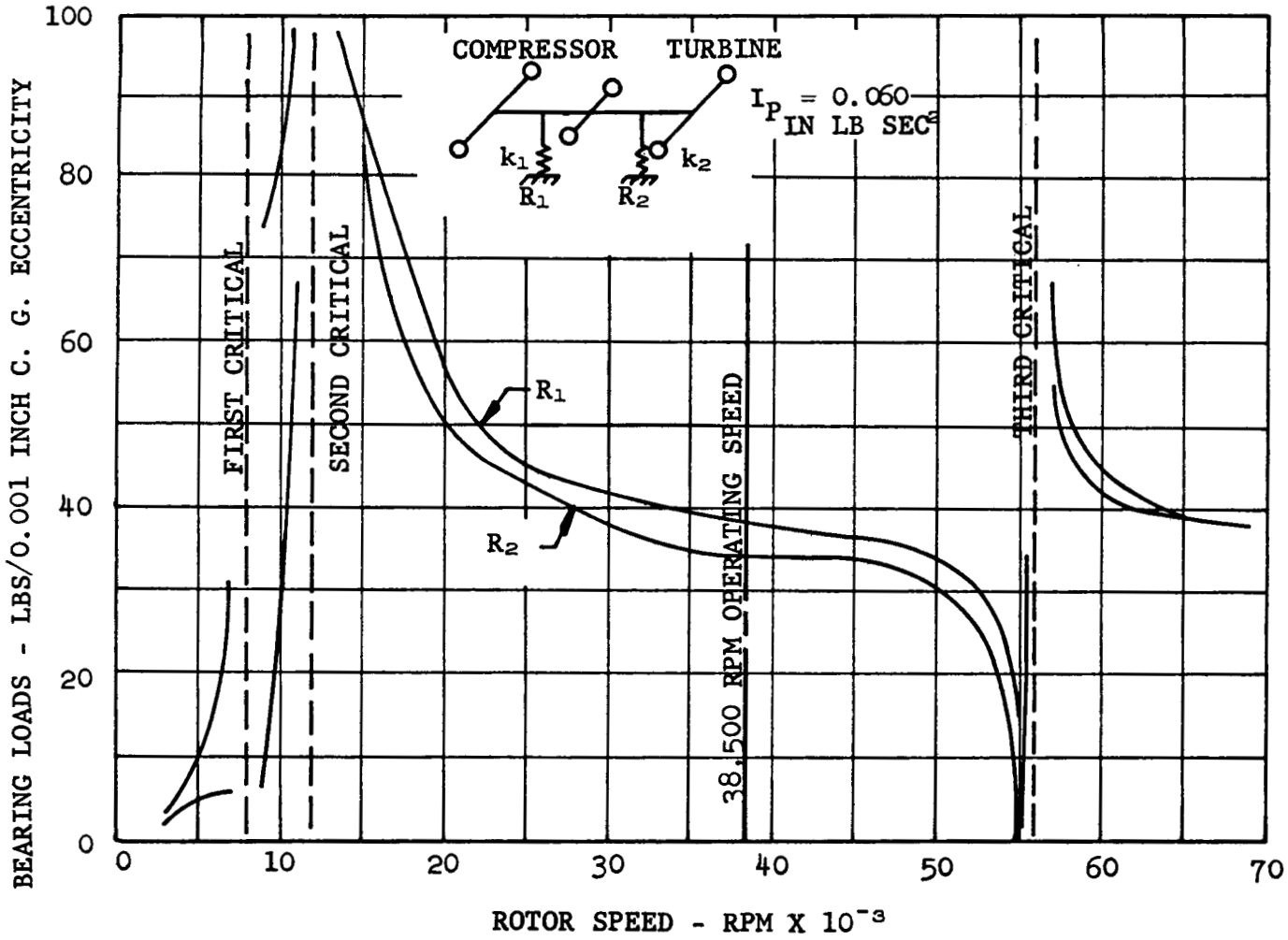

BEARING LOAD VS ROTOR SPEED
NASA GAS GENERATOR FINAL CONFIGURATION

FIGURE 10

It should be noted that the bearing loads shown in Figure 10 are for c.g. eccentricities of 0.001-inch. However, the c.g. eccentricity obtained on both the bearing test rig shafts and the gas generator is in the range of 0.0001-inch which reduces the actual bearing loads by a factor of 10.

3.4 Journal Gas Bearings

3.4.1 Design Considerations and Bearing Selection

The use of gas-lubricated bearings for the rotor support system of the gas generator is contingent upon three requirements:

(a) that an effective means be provided to accommodate dimensional changes and misalignments of the components associated with the bearings.

(b) that rotor dynamic stability be ensured throughout the system operating range.

(c) that the bearings can be self-acting (use process gas) at the rotor design speed (no external pressurization available for long-time operation).

A careful review of the above requirements led to the selection of self-acting partial-arc pivoted-pad bearings. This type of bearing offers attractive mechanical design features such as the ability to accommodate rotor radial misalignments and minor bearing surface imperfections. In addition, rotor dynamic stability is, in general, considerably improved with pivoted shoe bearings as compared to other bearing types such as conventional cylindrical journal bearings.

Based on extensive turbomachinery experience with both anti-friction bearings and conventional oil journal bearings, AiResearch chose to resiliently support the two journal bearing assemblies of the gas generator. The following desirable advantages are realized in the use of resilient mounts:

(a) Rigid rotor critical speeds are influenced by resilient bearing mounts. Proper choice of the support spring rate will ensure that the first two system critical speeds are in the low-speed, low-energy regime.

(b) Large transient rotor dynamic motions, such as occur during acceleration through system critical speeds, are not limited by the gas film thickness, since the resilient mounts will accommodate large movements.

(c) Rotor and bearing dimensional variations as a result of thermal and centrifugal growth are partially accommodated by the deflection of the resilient mounts.

(d) The ability to establish a positive preload on the rotor-bearing group to suppress whirl tendencies in "zero-g" environments (space power systems).

The last advantage cited--that of establishing a positive bearing preload (shoe-rotor interference at zero speed), brings about an additional design consideration of its own--that of external pressurization (a hydrostatic shoe lift-off flotation system) for starting and stopping. This combination of external pressurization during starting and stopping and self-acting ability during normal operation (no external pressurization required) eliminates the possibility of any contact between the tilting shoes of the journal bearing and the surface of the rotor.

The bearing configuration selected for the gas generator bearing development consisted of three bearing shoes, with each shoe encompassing a 100-degree arc. All the shoes were provided with pivotal freedom, and one or more of the shoes at each bearing were provided with radial resiliency. The shoes initially contacted

the journal with a predetermined interference load (preload) which was accommodated by the shoe resilient supports. Each shoe was lifted from the journal prior to rotation by means of hydrostatic orifices incorporated in the bearing shoe surfaces. The hydrostatic gas supply was then removed from the orifices when the shaft assembly had reached its design operating speed.

Figure 11 schematically illustrates the two resilient mounting methods that were developed. In Case 1, each of the shoes is resiliently supported, and the differential dimensional changes are accommodated by the flexibility of each of the lubricant films and of each of the three shoe supports. The equivalent mechanical system simulating this case is one of each shoe being separated from the journal by a nonlinear spring in a parallel with a nonlinear viscous damper. In this case the total film resistance acts in series with the shoe resilient support linear spring. In Case 2 of Figure 11, only one shoe at each bearing is resiliently supported, and all of the differential dimensional change is accommodated within each lubricant film and the single-shoe resilient support.

Figure 12 shows two basic bearing shoe and mount configurations that were evaluated during the testing program. Both the fixed-stem (elastically pivoted) and the ball-and-socket resiliently mounted gas bearing designs utilize the deflection of the circular plate or diaphragm to provide the mount spring rate. The inherent angular stiffness of the fixed-stem design is eliminated by the ball-and-socket design. The hydrostatic lift-off system consists of either a single orifice or four orifices incorporated into the bearing shoe surface.

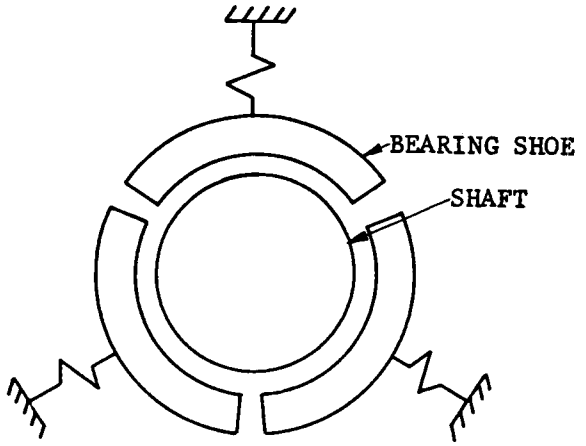

THREE SHOES FLEXIBLY MOUNTED

CASE 1

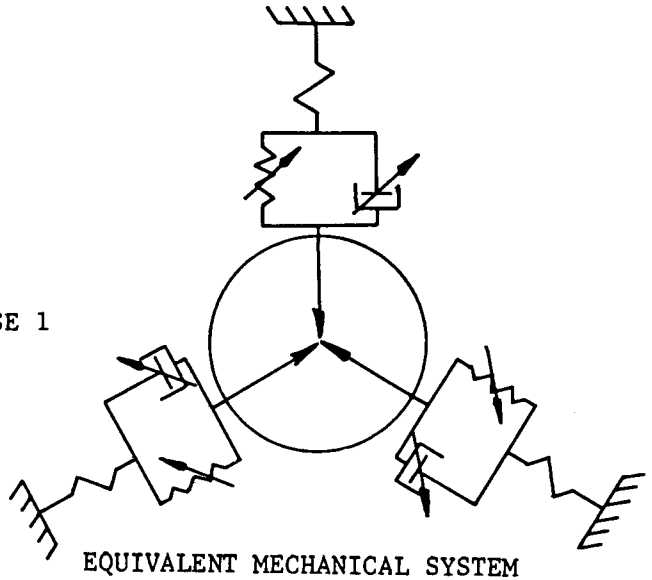

EQUIVALENT MECHANICAL SYSTEM

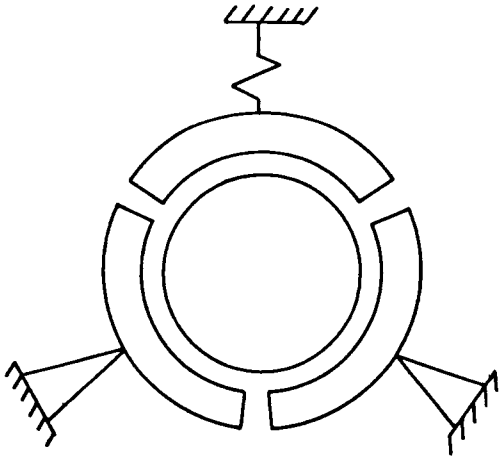

TWO FIXED MOUNTS, ONE FLEXIBLY MOUNTED

CASE 2

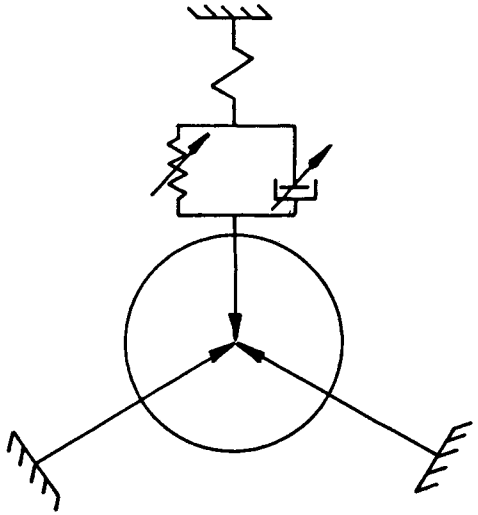

EQUIVALENT MECHANICAL SYSTEM

BEARING MOUNTING METHODS
FIGURE 11

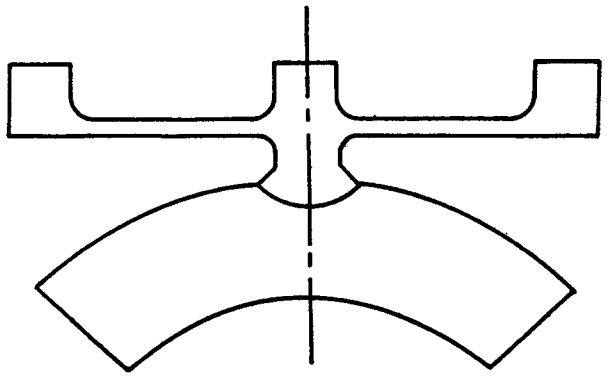

BALL-AND-SOCKET
DIAPHRAGM MOUNT

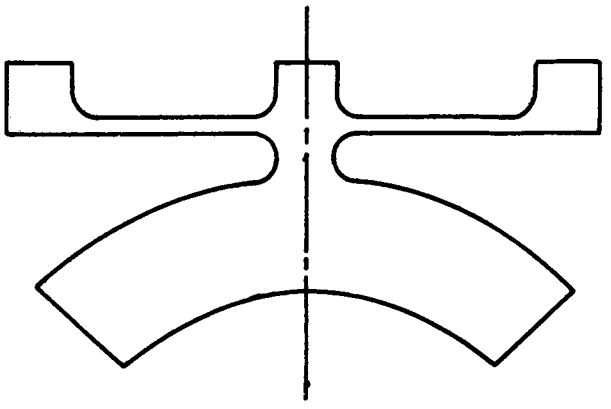

FIXED-STEM
DIAPHRAGM MOUNT

GAS BEARING SHOE MOUNTING METHODS

FIGURE 12

3.4.2 Gas Bearing Analysis

Once the aerodynamic performance of the gas generator was determined (compressor impeller and turbine wheel sizes) preliminary layouts of the main rotating assembly were completed. Tentative bearing span ranges from 6.0 to 13.0 inches were obtained from these layouts. The mass and inertial properties of the aerodynamic components, and assumed rotor dimensions, including the range of bearing spans, plus a range of bearing support flexibilities, were used to determine a range of rigid-body critical speeds, as well as the third critical speed (free-free bending mode).

In general, the rotor diameter size is the governing criterion to keep the shaft free-free bending mode (third critical speed) well above the operating speed. The gas bearing journal size was therefore determined from the above analysis. The final task was to determine whether gas bearings of the prescribed diameter had adequate self-acting load-carrying ability, gas film stiffness, etc., to meet the bearing load requirements.

Analysis of the gas bearings was accomplished by a steady-state digital computer program that is capable of considering either incompressible or compressible fluids operating in either the laminar or turbulent flow regimes. Either a full journal or a single sector may be prescribed with local variation in the surface geometry. In addition, provision is made for considering local hydrostatic lift-off orifices. Thus, externally pressurized, self-acting, or hybrid lubrication may be analyzed for a single shoe.

An iterative numerical technique is employed to solve the Reynolds equation for finite length bearings, and, thus, end-leakage effects are implicit in the analysis. Any combination of journal dynamic motions may be considered that would introduce misalignment, journal eccentricity rate of change, and journal whirl. The program predicts bearing loads, center of pressure coordinates and moments about any specified set of coordinate axes, flow-leakage rates, and pressure distribution for a maximum matrix size of 21 rows and 36 columns.

The journal bearing computer program was utilized to formulate the initial bearing designs committed to the test program. In addition, the computer program greatly simplified the problem of evaluation of test results.

The test rotors were evolved from the aforementioned analysis. The bearing spans ranged from 6.0 to 13.0 inches. The rotors were hollow with approximately 1/4-inch wall thickness at the journals. The journal surfaces were Flame-Plated with tungsten carbide. The mass and inertial properties of each were similar to those of the future gas generator rotating assembly. For the 11-inch bearing span rotor (most frequently used in development testing), these properties were:

Mass: 0.0384 lb sec^2 per inch
Polar moment of inertia: 0.033 in -lb-sec^2
Diametral moment of inertia: 1.271 in-lb-sec^2

The pivoted-pad gas bearing/resilient-mount configurations initially analyzed and tested were:

Pivot = ball/socket and fixed-stem (elastic pivot)
Mount stiffnesses = 20,000 lbs per inch and 10,000 lbs per inch
Lift-off system = 4-orifice and single-orifice
Clearance ratio (C/R) = 0.001
Journal radius (R) = 1.000 inch
Angular span (degrees) = 100
L/R ratio = 1.5
Pivot location = 50° from leading edge

3.4.3 Gas Bearing Testing

Development testing of the gas bearings was accomplished on two development test rigs--the single-shoe test rig, and the dynamic two-bearing test rig. The single shoe test rig was used to investigate isolated behavior of the bearing shoe, such as hydrostatic capability, hydrodynamic performance, misalignment effects, pivotal function, shoe instability, etc., of some of the bearing designs considered in Section 3.4.3.3. The two-bearing test rig was used to evaluate complete bearing systems with the shaft oriented in the vertical plane, since this best simulated zero-g conditions for journal bearings and represented the most critical bearing operation from the standpoint of stability. All testing was undertaken in ambient air conditions, and hydrostatic supplies utilized pressurized air which could be varied from zero to 160 psig as necessary.

3.4.3.1 Single-Shoe Test Rig

This test rig consists of a precision surface rotor mounted on precision ball bearings and driven by an air turbine. The rotor has two capacitance probes imbedded in the surface 180 degrees apart and spaced to sweep under the outer edge of each of the test shoes. Both probes are commonly connected to an axially located

junction which terminates at one end of the rotor. A spring-loaded needle brush, bearing against the rotor end, conveys the capacitance signal to a remotely located distance meter (Photocon Products Dynagage). Thus each revolution of the rotor produces two signals (sweep of each shoe edge) and gives a continuous display of the clearance between the shoe and the rotor. The test bearing shoe is mounted in a bearing carrier and loaded against the rotor. Strain gauges, mounted in a bridge circuit on the bearing resilient circular plate, are used to establish the desired initial preload, and for constantly monitoring bearing operating loads. Figure 13 shows the single shoe test rig.

3.4.3.2 Dynamic Two-Bearing Test Rig

The two-bearing rotor dynamic test rig, shown in Figure 14, is used to investigate the dynamic behavior as well as other aspects of the system comprising the gas bearings and test rotor.

The test rotor is vertically supported in the test rig and is driven by a turbine wheel mounted at the rotor upper end. A hydrostatic thrust bearing supports the rotor at the bottom. Each bearing shoe assembly is secured to a support assembly. This support assembly is mounted to a track directed radially with respect to the rotor, and radial positioning of the assembly is provided by a calibrated screw thread. The track may also be pivoted about an axis parallel to the rotor axis. In addition, the support assembly has provision for pivoting of the bearing shoe assembly about a horizontal axis directed perpendicularly to the track. Thus, the angular attitude of each bearing shoe assembly may be adjusted mechanically about three orthogonal axes, and any desired initial clearance or interference between shoe and shaft may be established. A micrometer adjustment in each support assembly limits the maximum radial deflection of the bearing resilient support. Any type of resilient supporting system with any desired flexibility may be tested with this rig.

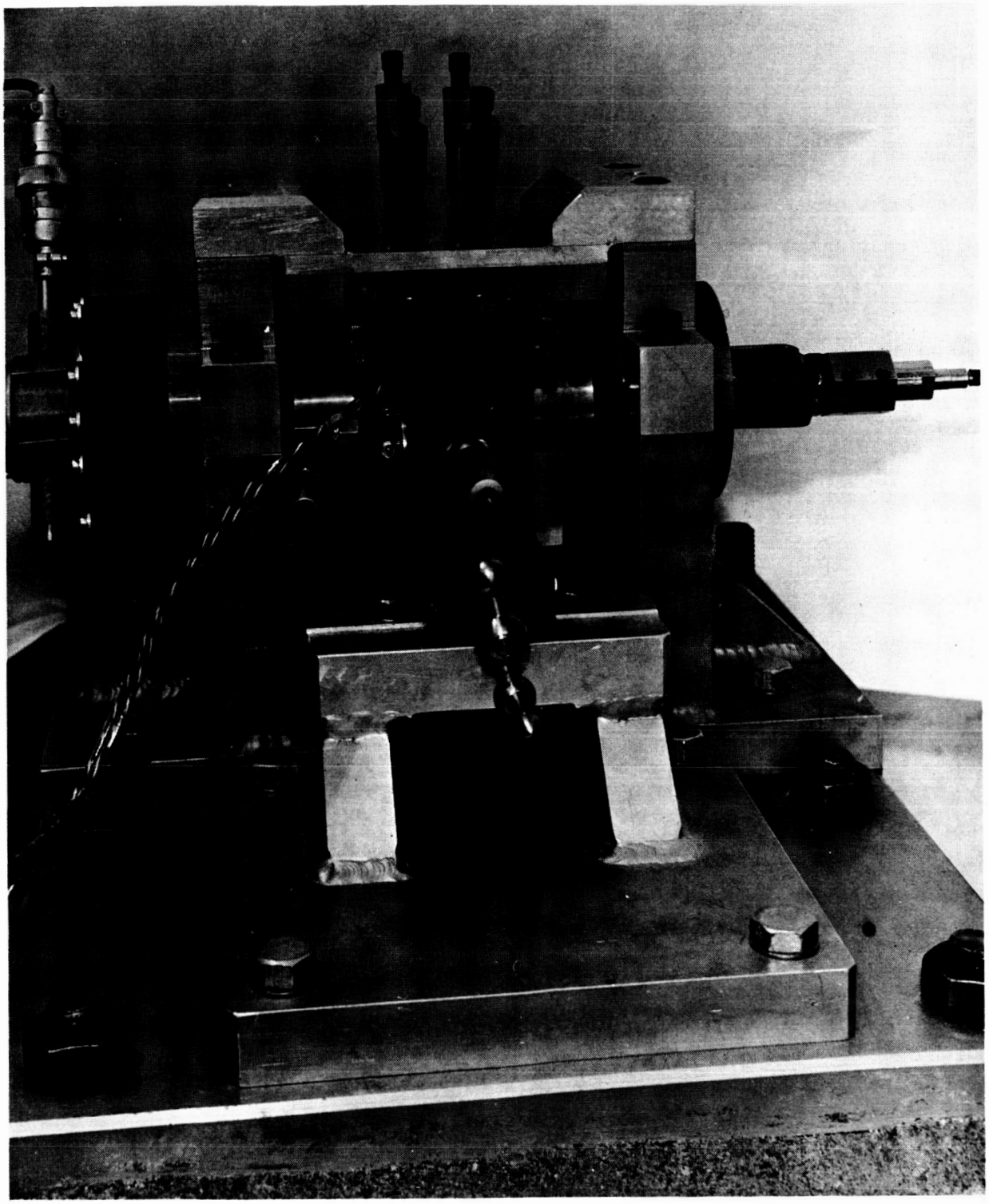

SINGLE-SHOE BEARING TEST RIG

FIGURE 13

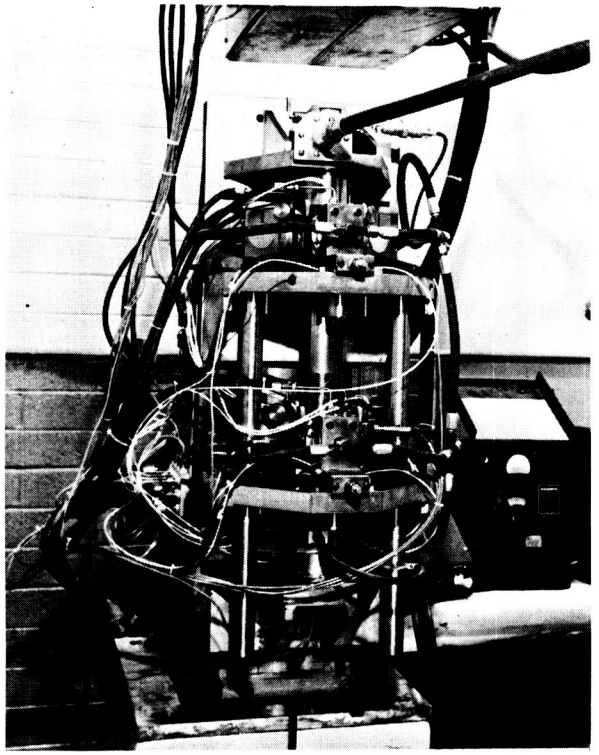

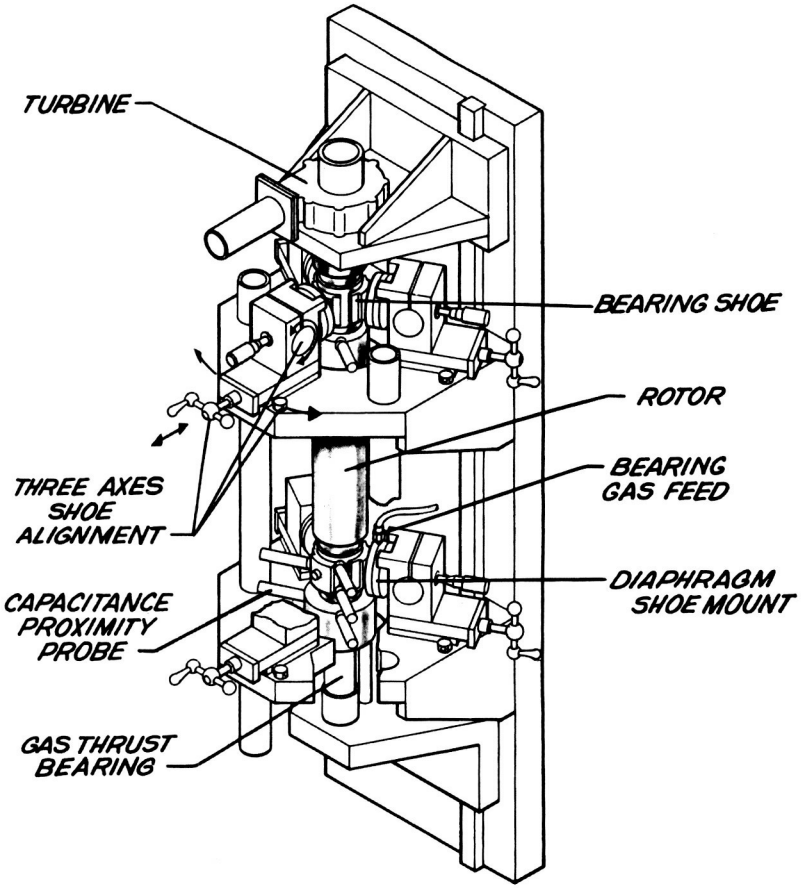

DYNAMIC TWO-BEARING TEST RIG

FIGURE 14

The test-rig bearing support brackets are made so that the bearing span may be varied to accommodate rotors of various lengths.

Capacitance probes (Photocons), mounted in quadrature with respect to the rotor axis on each bearing bracket, monitor shaft dynamic motions in the radial direction near each bearing. In addition, the relative motions of one bearing shoe are monitored by two capacitance probes directed at the upper and lower regions of the shoe leading edge, and also by a third Photocon directed at the shoe trailing edge, thus providing the capability of describing the motion of the shoe in the two planes of pitch and roll. A Photocon at the bottom of the rotor measures the axial motions of the rotor. This instrumentation, as well as speed output, is connected to a 14-channel magnetic tape recorder (see Figure 15 for the bearing test facility instrumentation), thus providing a means of recording the continuous history of test runs from start-up to full speed.

For each test, initial alignment of each bearing shoe may be obtained with the test rotor supported on alignment center pins at each end. After alignment is achieved, the center pins are removed, and the hydrostatic thrust bearing is replaced at the bottom of the shaft. Strain gauges cemented to each bearing shoe resilient plate are calibrated as functions of both linear and angular displacements of the bearing. The outputs from each of these strain gauges are utilized as the basis of establishing the desired radial alignment and initial preload between the bearing and the shaft.

These strain-gauge signals are also utilized to continuously monitor bearing loads during testing. Thermocouples connected to the bearing shoes are used to determine nominal shoe temperature, and signals from the thermocouples and strain gauges are continuously recorded on a Sanborn recorder.

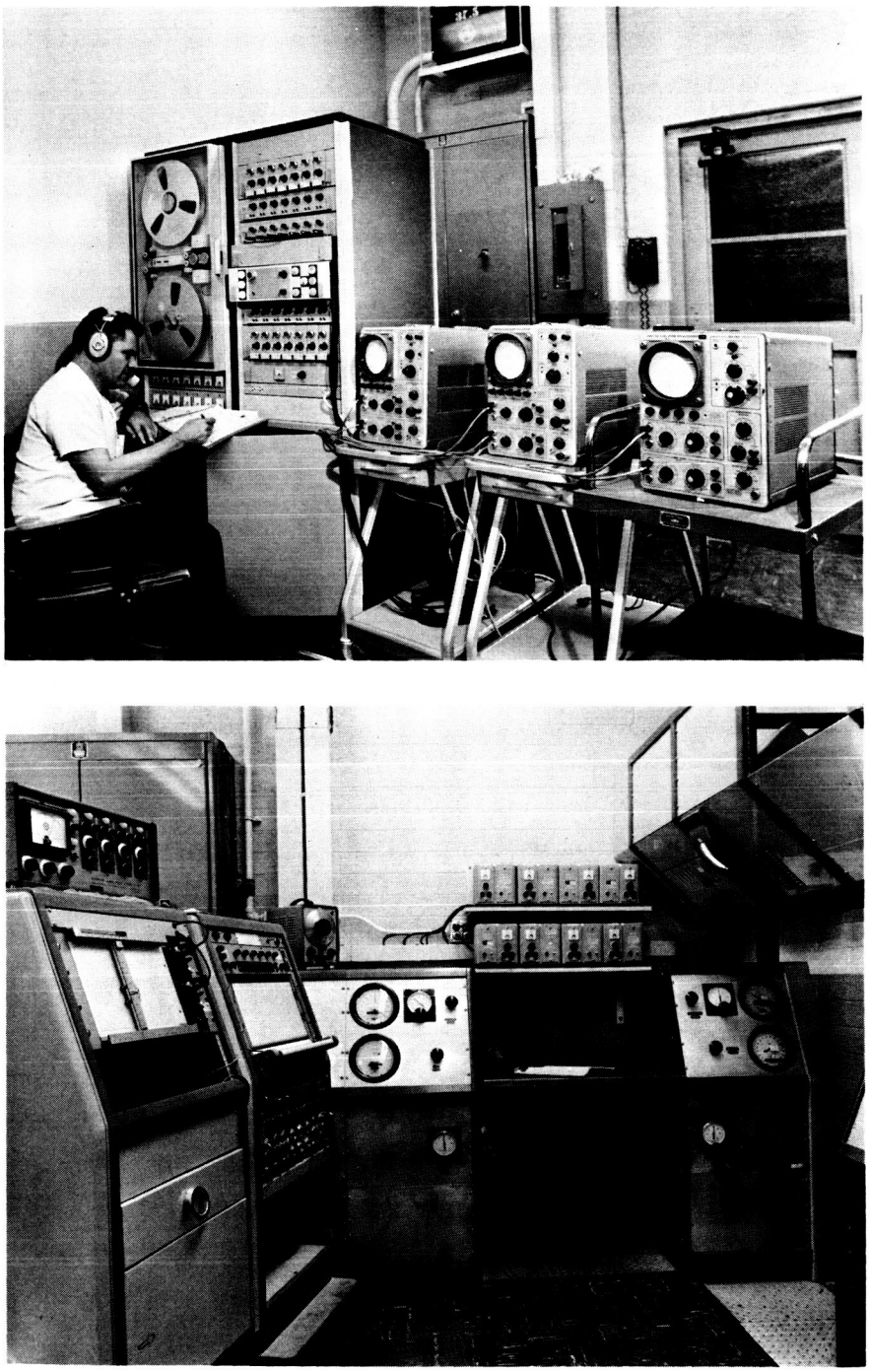

GAS-BEARING TEST FACILITY INSTRUMENTATION
FIGURE 15

3.4.3.3 Test Results

As previously noted on page 29, the four basic pivoted-pad gas bearing configurations initially tested were (in order):

(1) Fixed-stem, four-orifice
(2) Ball-and-socket, four-orifice
(3) Fixed-stem, single-orifice
(4) Ball-and-socket, single-orifice

Each of the above bearing configurations utilized the equal spring mount system shown in Figure 11, Case 1.

The tests of the first bearing configuration (fixed stem, four orifice) were satisfactory and rotor speeds to 50,000 rpm were accomplished without incident. These tests established that a bearing of this type might meet the operating requirements. However, initial alignment problems inherent in the fixed-stem design led to further testing, the goal being to develop a workable ball-and-socket pivot design to alleviate the bearing alignment problems in the final gas generator. Test evaluation of the remaining three configurations indicated that a shoe geometry change was required to provide a wide range of stable rotor operation in the externally pressurized, hybrid, and self-acting bearing regimes. Some of the problems encountered in these tests were shoe flutter and spragging (shoe leading-edge dip).

Results of computer analyses showed that an increase in the shoe clearance ratio and a relocation of the shoe pivot point would tend to optimize the shoe stability characteristics and also provide a reduction in the predicted shoe friction loss.

Based on this information, the bearing shoes were redesigned (both fixed-stem and ball-and-socket types) with the pivot located 65 percent back from the shoe leading edge and the clearance ratio (C/R) increased to 0.0017. Testing of these configurations with the equal spring mount system proved to be satisfactory. The shoe flutter and spragging mentioned above were no longer a problem. The spring rate of this particular system was in the order of 20,000 pounds per inch. In order to decrease the mount spring rate, the mounting system depicted in Figure 11, Case 2 was used (two fixed shoes per bearing and one resilient mount). The composite spring rate of this system was in the order of 5,400 to 6,000 pounds per inch. The stability of this system was excellent, and in addition, the low composite spring rate afforded adequate rotor thermal and centrifugal growth relief.

3.4.4 Gas Generator Journal Bearing Configuration

As a result of the testing discussed above, the gas generator bearing configuration selected was based on a similarity of the bearing compressibility number, λ, between the gas generator bearing and the air test bearings where

$$\lambda = \frac{6\mu\Omega}{P_a} \left(\frac{R}{C}\right)^2$$

μ = lubricant viscosity, lbs per sec per sq inch

R = journal radius, inches

Ω = angular velocity, radians per second

P_a = ambient pressure, psia

c = bearing clearance (difference between bearing and journal radii), inches

λ = bearing number

For the gas generator with a design lambda (λ) $\approx$ 1.5, the journal bearing configuration was thus determined to be:

Journal radius, inches	= 0.875
Clearance ratio	= 0.00263
L/R ratio	= 1.50
Angular span, degrees	= 100
Pivot location (from leading edge), degrees	= 65
Pivot type:	Ball-and-socket
Mounting system:	Two shoes per bearing radially constrained, the third shoe resiliently supported by a 2,500-pound-per-inch diaphragm mount
Number of hydrostatic supply orifices per shoe:	Four

These characteristic requirements are based on the machine design point of 38,500 rpm shaft speed, 12 psia journal ambient pressure, argon gas atmosphere, and a journal ambient temperature level of 500°F.

The four hydrostatic orifices provide easier lift-off action and are utilized instead of the single orifice so that the orifices are located away from the point of peak hydrodynamic pressure.

Figure 16 shows the predicted performance of the bearings at the design conditions.

3.5 Thrust Gas Bearings

3.5.1 Thrust Bearing Design

The design of the thrust bearing was based on the following calculated gas generator operating requirements when operating in the design system:

(a) A maximum start-up thrust load to self-sustained speed of 60 pounds in a direction from the compressor to the turbine (with a turbine back pressure of 3 psia assumed).

(b) At self-sustained speed (approximately 21,000 rpm), the thrust direction reverses and its magnitude becomes approximately 20 pounds.

(c) The thrust load increases from 20 pounds to a maximum value of 30 pounds at operating speed, in a direction from the turbine to the compressor. The normal thrust bearing is to operate hydrodynamically, beginning at self-sustained speed.

BEARING CONFIGURATION

1. ANGULAR SPAN - 100 DEGREES
2. L/R = 1.5
3. AMBIENT PRESSURE = 12 PSIA
4. R = 0.875 INCHES
5. ARGON AT TWO TEMPERATURES

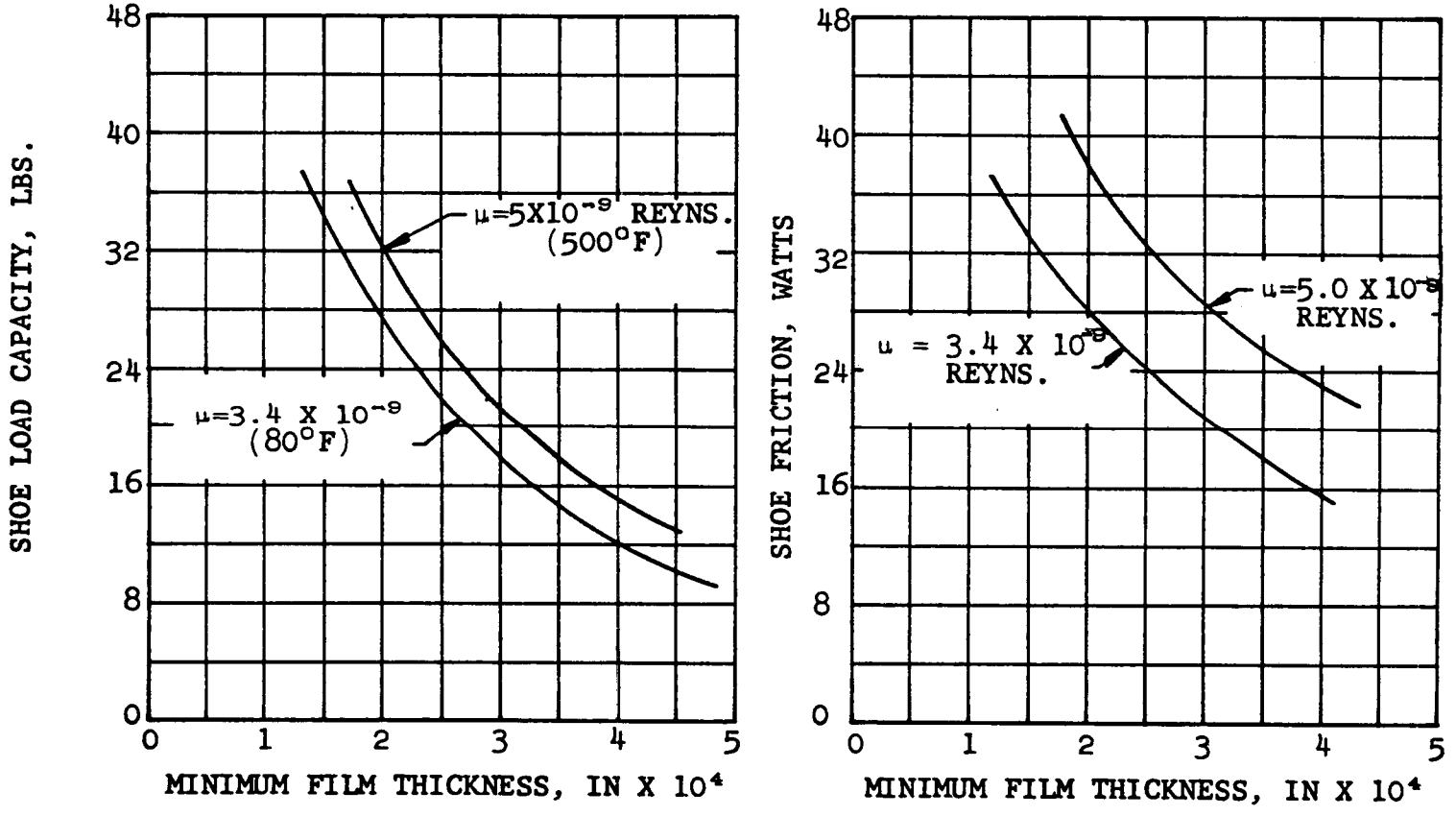

PREDICTION OF GAS GENERATOR JOURNAL BEARING PERFORMANCE AT DESIGN SPEED

FIGURE 16

(d) The bearing is to use argon as the lubricant, with the temperature in the range of 200°F to 800°F.

(e) Ambient pressure range in the bearing cavity is assumed to vary from 5 psia to 12.0 psia.

Figure 17 shows the double-sided thrust bearing design. The rotor slider is enclosed by two elements; the hydrodynamic bearing is on the compressor side, and the hydrostatic bearing is on the turbine side. The two thrust stators are tied together and supported by a gimbal that allows rotation of the stators in the plane of the slider. Figures 18 and 19 schematically show the hydrostatic and hydrodynamic thrust stators. The hydrostatic stator incorporates six orifices for the hydrostatic lift-off and operation during "reverse" thrust conditions (prior to self-sustained speeds). To facilitate start-up, four hydrostatic orificed pads have been incorporated in the hydrodynamic bearing surface to ensure an adequate operating clearance between the slider and the hydrodynamic bearing, thus precluding rubbing of these bearing surfaces.

By use of a computer program, studies were conducted on the normal thrust bearing to determine an optimum hydrodynamic bearing size based on load capacity and thrust bearing friction at the design operating conditions. Results of this analysis indicated that the thrust bearing surfaces should have an outside radius of 1.62 inches and an inside radius of 0.95 inch. Figures 20, 21, and 22 show the hydrostatic and hydrodynamic performance of the thrust bearings.

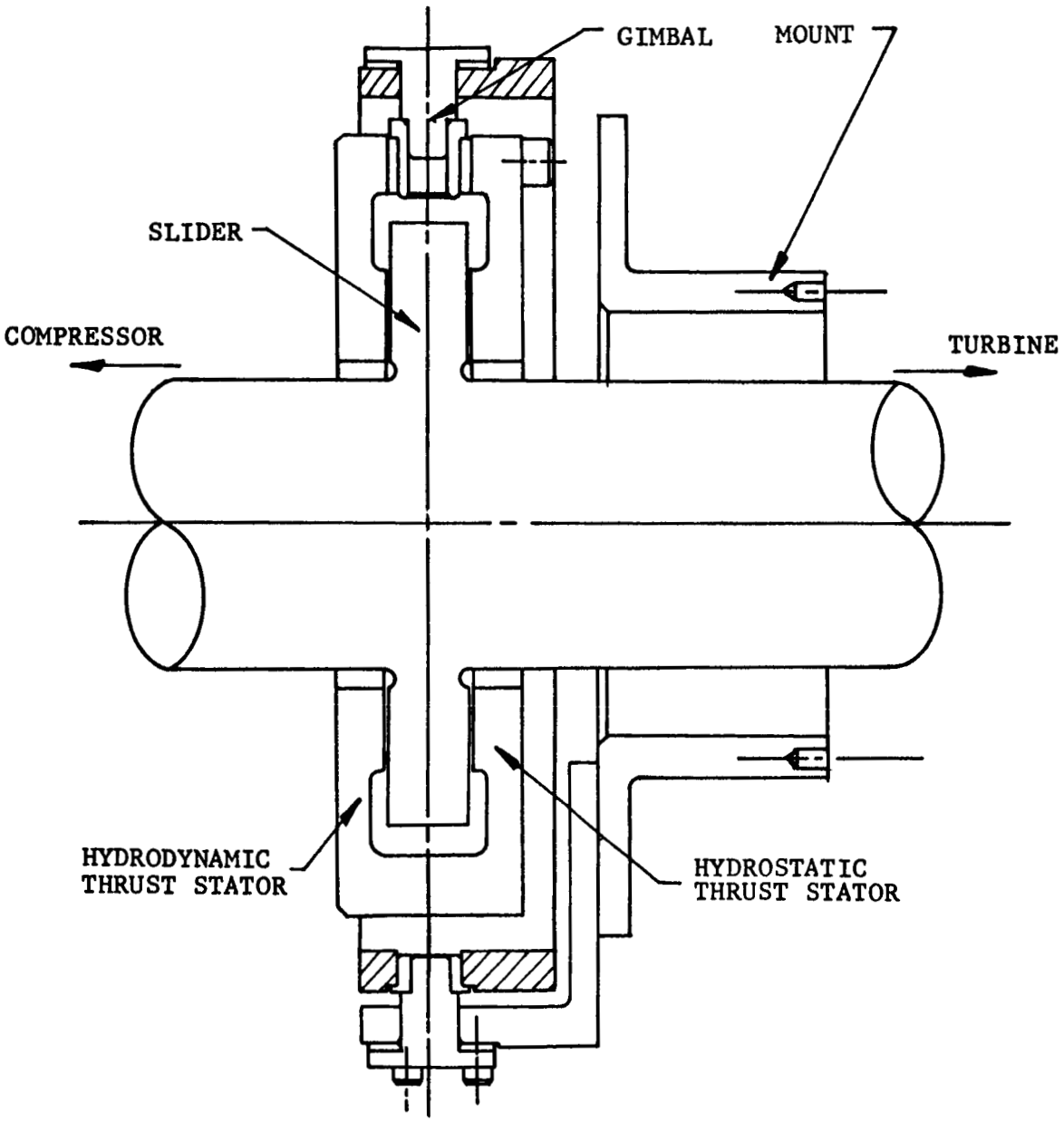

THRUST BEARING AND GIMBAL ASSEMBLY

FIGURE 17

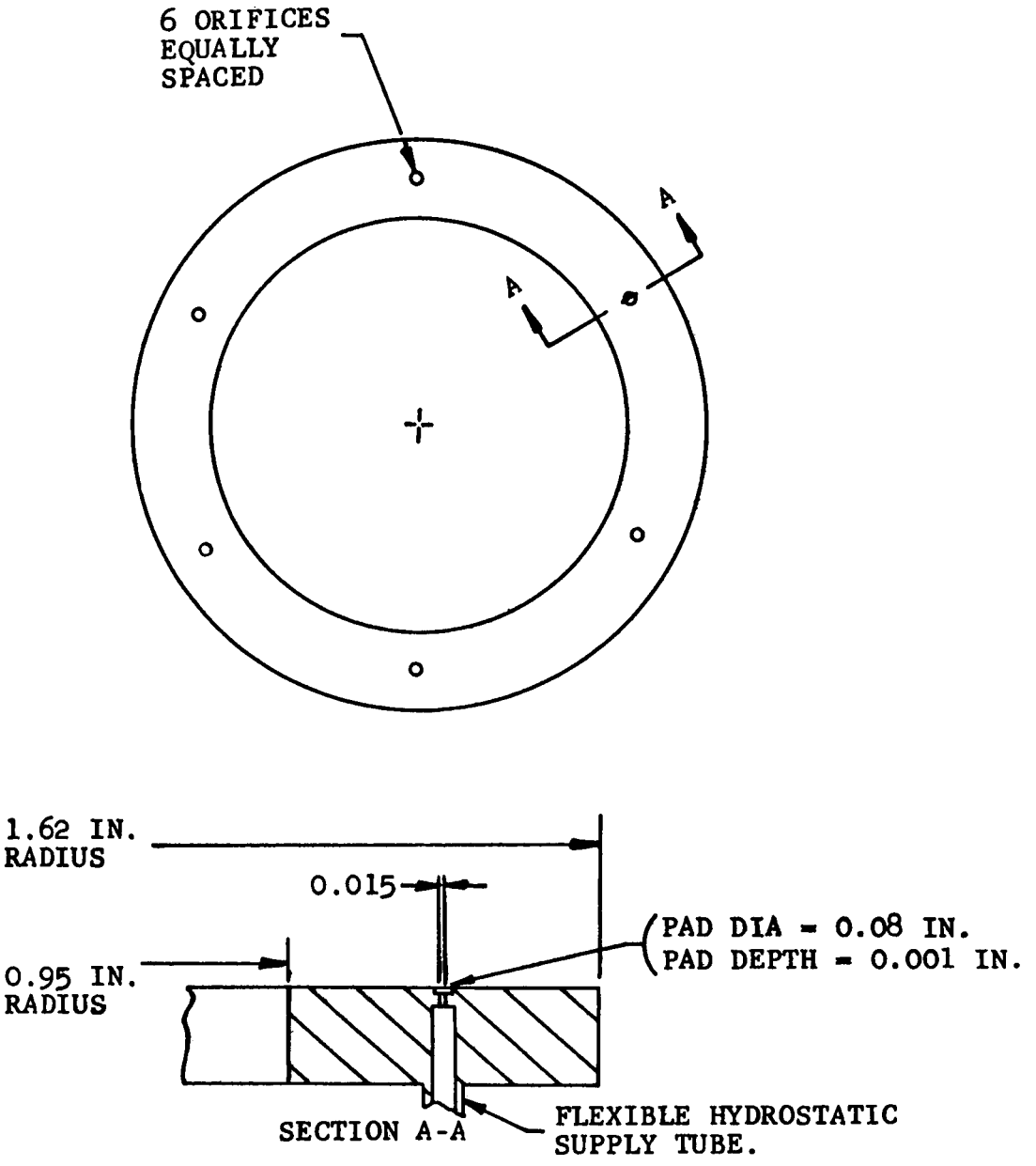

HYDROSTATIC THRUST BEARING FOR
NASA GAS GENERATOR

FIGURE 18

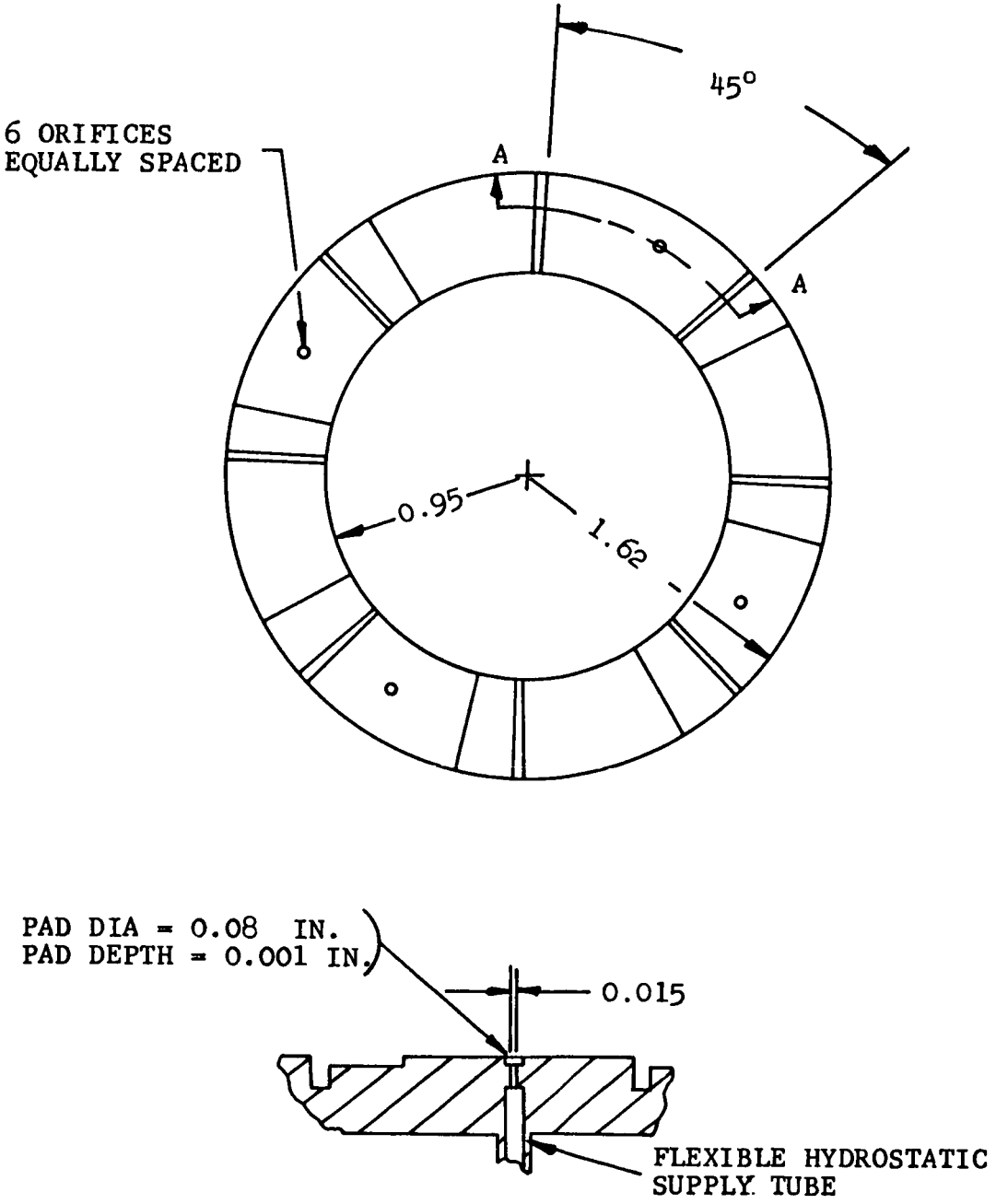

HYDRODYNAMIC THRUST BEARING FOR NASA GAS GENERATOR

FIGURE 19

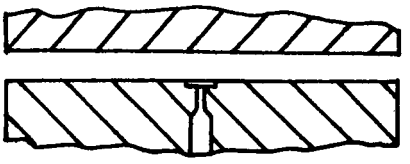

HYDROSTATIC STATOR CROSS-SECTION

BEARING CONFIGURATION

1. OUTER RADIUS = 1.62 INCHES
2. INNER RADIUS = 0.95 INCH
3. AMBIENT PRESSURE = 12 PSIA
4. ARGON LUBRICANT

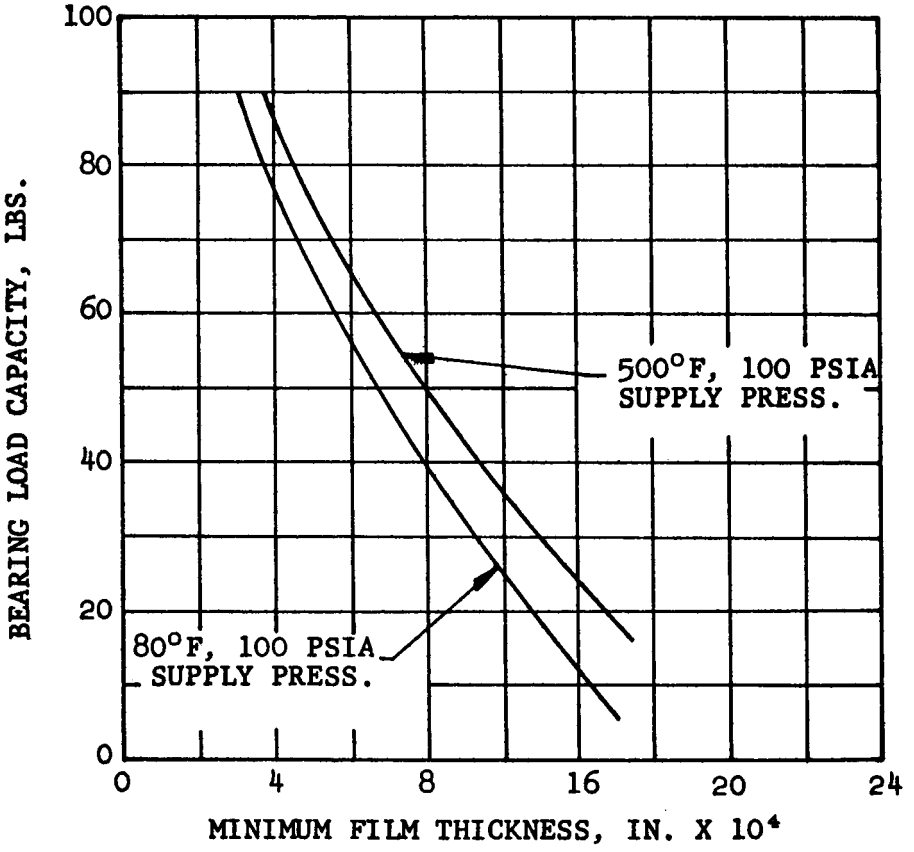

HYDROSTATIC THRUST BEARING LOAD CAPACITY

FIGURE 20

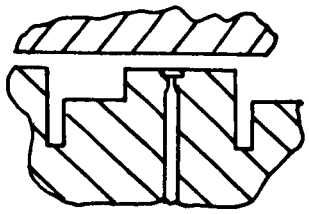

HYDRODYNAMIC THRUST BEARING CROSS-SECTION

BEARING CONFIGURATION

1. OUTER BEARING RADIUS = 1.62 INCHES
2. INNER BEARING RADIUS = 0.95 INCHES
3. AMBIENT PRESSURE = 12 PSIA
4. FOUR OF 8 PADS PROVIDED WITH EXTERNAL PRESSURIZATION ORIFICES
5. ARGON LUBRICANT

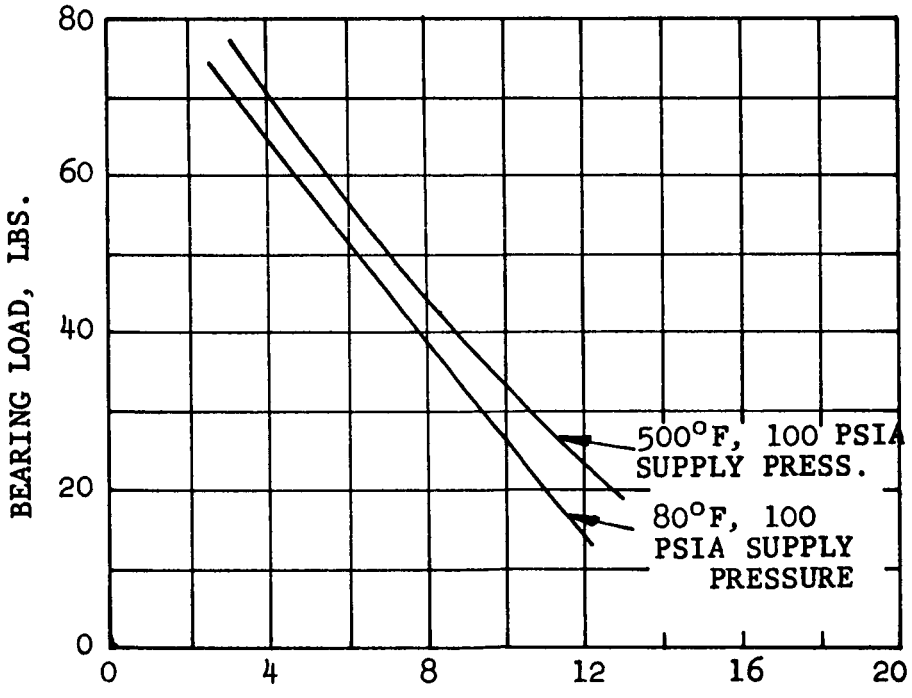

HYDRODYNAMIC THRUST BEARING,
HYDROSTATIC LOAD CAPACITY

FIGURE 21

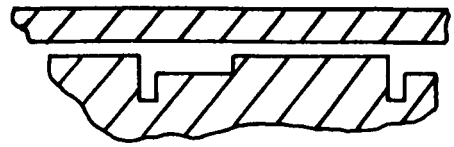

HYDRODYNAMIC STATOR CROSS-SECTION

BEARING CONFIGURATION

1. ARGON LUBRICANT, 500°F, $\mu=5X10^{-8}$
2. SHAFT SPEED = 38,500 RPM
3. THRUST SURFACES ASSUMED PLANE, NO THERMAL DISTORTION CONSIDERED
4. OUTSIDE PAD RADIUS = 1.62 INCHES
   INSIDE PAD RADIUS = 0.95 INCH
5. FRICTION POWER GENERATED IS INSENSITIVE TO SMALL CHANGES IN AMBIENT PRESSURE

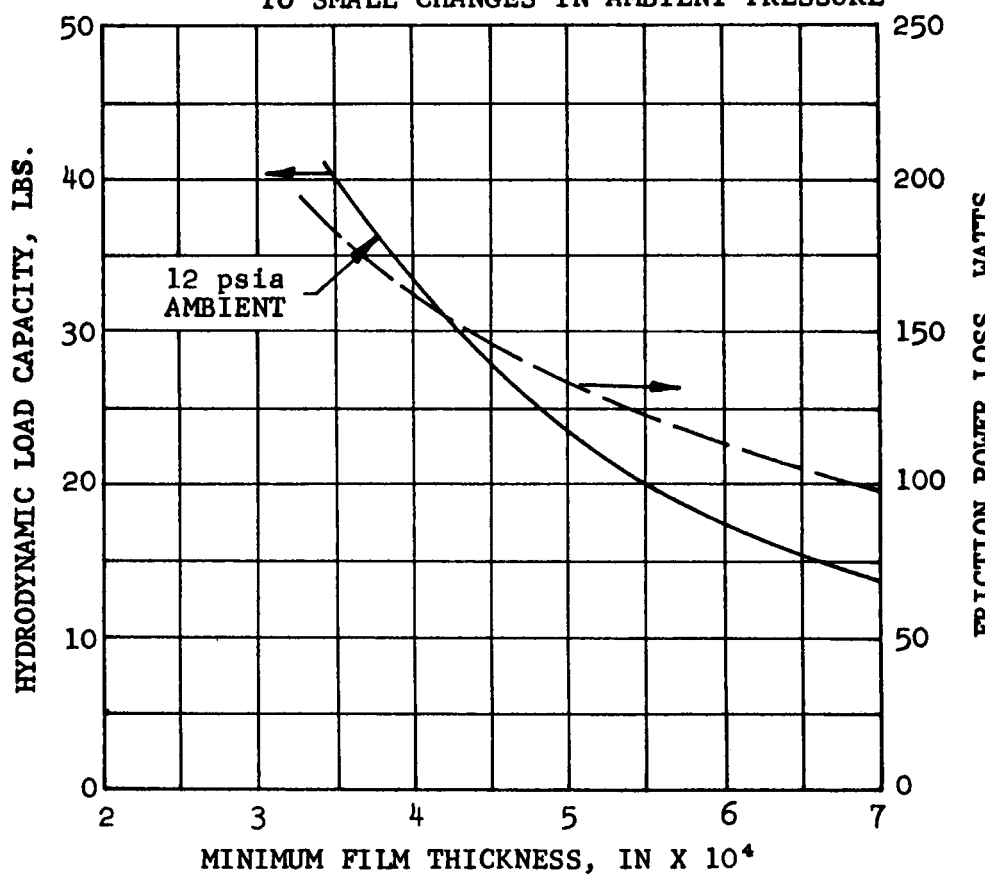

NASA GAS GENERATOR HYDRODYNAMIC
THRUST BEARING PERFORMANCE

FIGURE 22

3.5.2 Thrust Bearing Tests

3.5.2.1 Thrust Bearing Integration Test Rig

The integration of the thrust-bearing/gimbal-mount assembly and journal bearings was accomplished on a bearing test rig that very closely simulates the final gas generator design. The rig consists of a housing, bearing carriers, journal gas bearings, and shaft that exactly duplicate the final gas generator configurations. Dummy masses are included on the shaft to simulate the masses of the journal and turbine wheels. An air turbine motor is utilized to drive the shaft. Loading of the thrust bearing can be varied by introducing a positive or negative pressure in a cavity under the shaft. The test-rig instrumentation is similar to the final gas-generator instrumentation. Figure 23 shows the bearing test rig as installed in the bearing test facility.

3.5.2.2 Thrust Bearing Integration Tests

Various gimbal configurations were tested with varying degrees of success. The configuration that ultimately proved to be the most successful -- and the one which was incorporated into the gas generator -- utilized two pairs of pin-in-socket pivots, each pair located in the mean plane of the thrust surfaces.

Stable operation was obtained on both thrust surfaces, and thrust transfers between the thrust surfaces were very satisfactory. Loads up to 80 pounds were achieved on the reverse thrust bearing (hydrostatically). Loads from 0 to 35 pounds and 5 to 28 pounds were achieved on the normal thrust surface operating hydrostatically and hydrodynamically, respectively. These tests, undertaken on the frame test rig, were considered to have demonstrated that integration of the journal and thrust bearings had been achieved.

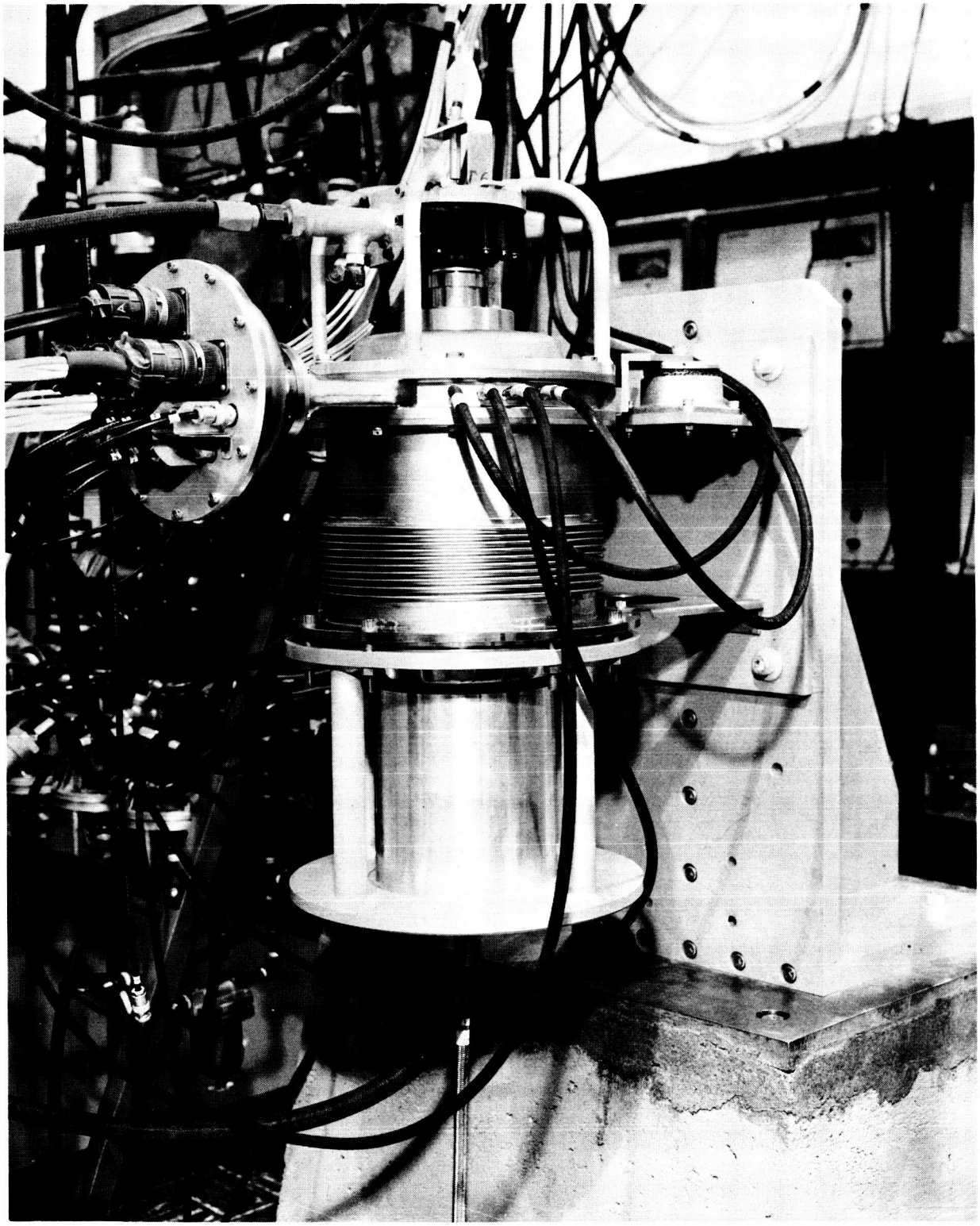

COMPANY-SPONSORED BEARING TEST RIG
FIGURE 23

3.6 Thermal Analysis

A digital computer thermal analysis program is the only economical means by which an integrated housing, rotating group/bearing assembly can be analyzed from a thermal standpoint to determine:

(a) Operating temperatures throughout the machine

(b) Relative parts movements

(c) Thermally induced stresses

(d) Material requirements

(e) Cooling flows if required

(f) Bearing operating requirements

Thermal analyses are conducted at AiResearch with digital computer programs by mathematically defining the complete turbomachine together with the inlet and discharge design conditions, bearing frictional power losses, bearing hydrostatic gas supply flow, and various cooling flow rates, etc. Information necessary for the thermal analyses is the basic machine configuration as defined by the preliminary layout; the wheel configuration as defined by the stress and aerodynamic analyses; and the bearing spacing, bearing initial configuration, and power losses as defined by the dynamic and bearing analyses.

Materials for the various component parts are selected from an initial thermal analysis, and cooling flows are selected, if required. The analysis is then performed again with the configuration

modifications until bearing temperatures and thermal gradients are reduced to within acceptable bearing design, stress, and growth limitations.

A thermal analysis by use of the method discussed above was conducted on the basic gas generator and the steady-state temperature results are shown in Figure 24.

Figure 25 illustrates the heat flow paths and the quantities of heat energy being transferred through the rotor and associated parts in the gas generator. It may be noted that approximately 50 percent of the heat input to the shaft is convected away by the cooling gas. The remaining 50 percent is conducted to the impeller where it is convected to the compressor through-flow. Figure 26 presents the gas generator's shaft temperature distribution at steady state and at three values of time during the start-up transient.

Figure 27 presents the transient and steady-state compressor and turbine axial shroud clearances. With initial shroud clearance settings of 0.012 and 0.014 inch for the compressor and turbine, respectively, steady-state running clearances of approximately 0.010 inch will be achieved. During transient operation the shroud clearances open up to a maximum of 0.017 and 0.020 inch for the compressor and turbine, respectively.

Figure 28 presents the temperature distribution at the bearing shoe and the adjacent journal area, for the compressor and turbine bearings, respectively, at steady state and at three time points during the transient. These illustrate how closely in temperature level the shoes and the journals follow each other and that they are relatively free from coning and crowning.

1. .25%-100°F COOLING FLOW AT COMPRESSOR JOURNAL BEARING
   .25%-100°F COOLING FLOW AT TURBINE JOURNAL BEARING

2. BEARING POWER LOSS
   a. 20 WATTS PER SHOE AT JOURNALS
   b. 100 WATTS AT NORMAL THRUST BEARING
   c. 20 WATTS AT REVERSE THRUST BEARING

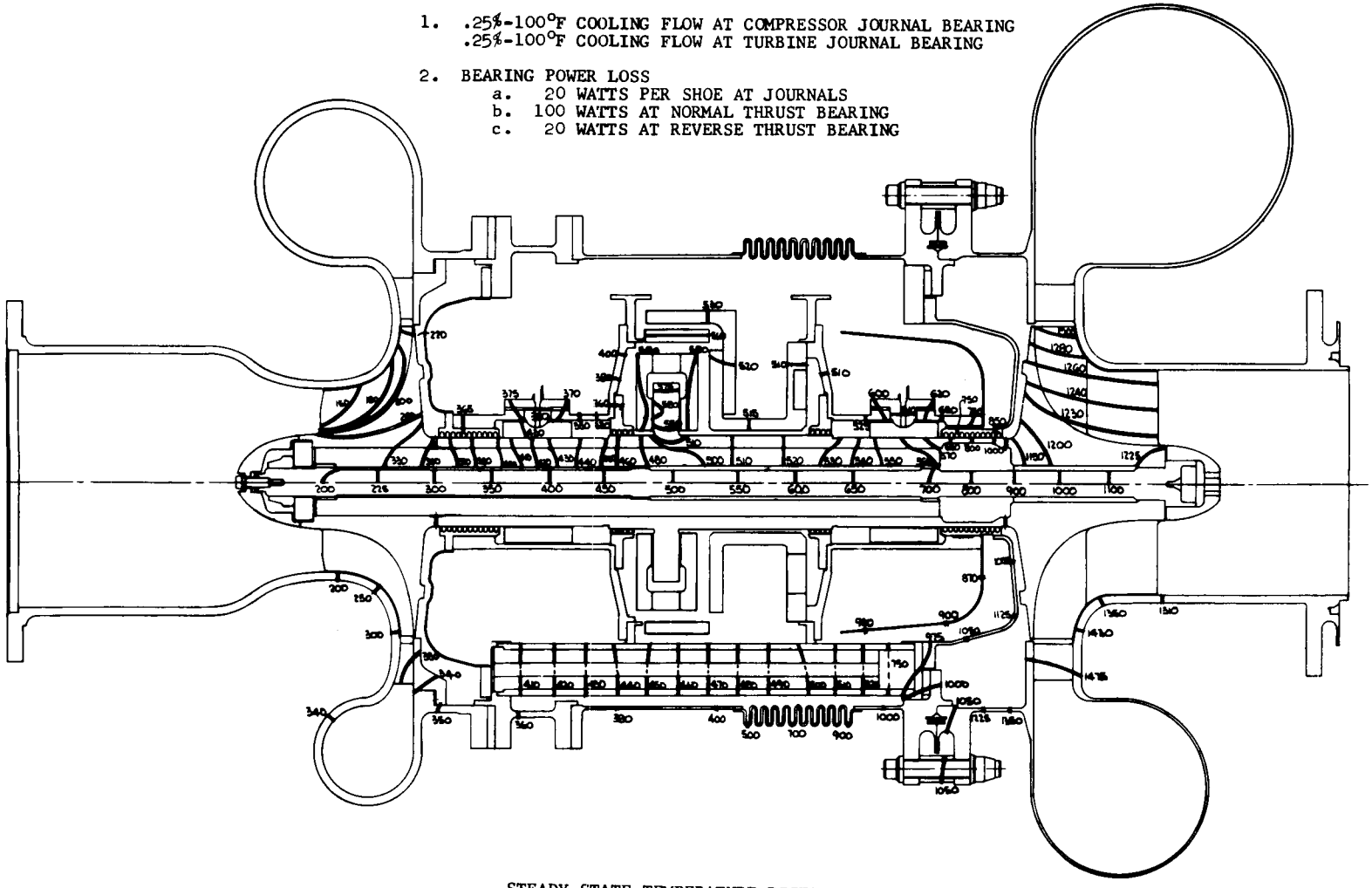

STEADY STATE TEMPERATURE DISTRIBUTION

FIGURE 24

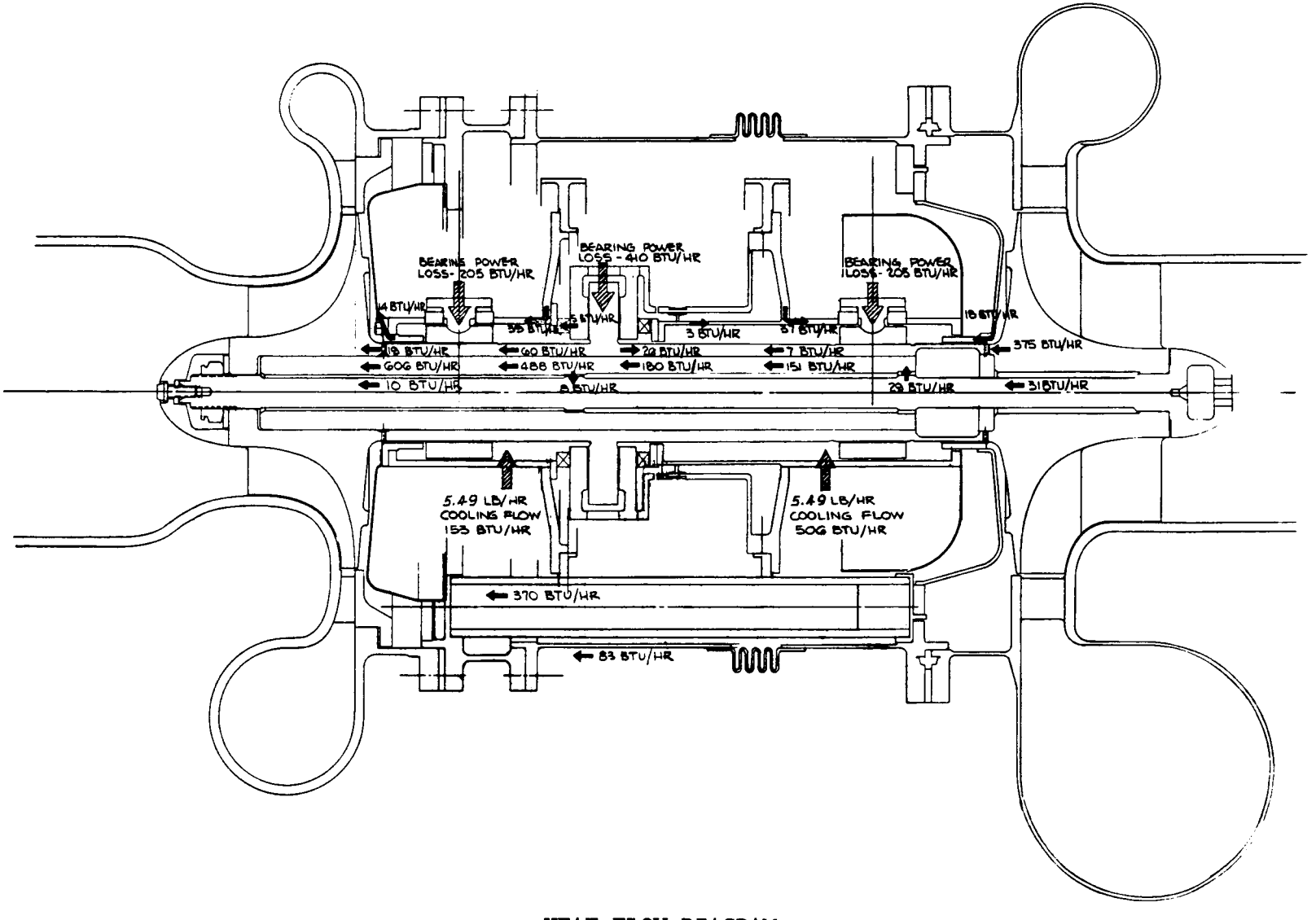

HEAT FLOW DIAGRAM
FIGURE 25

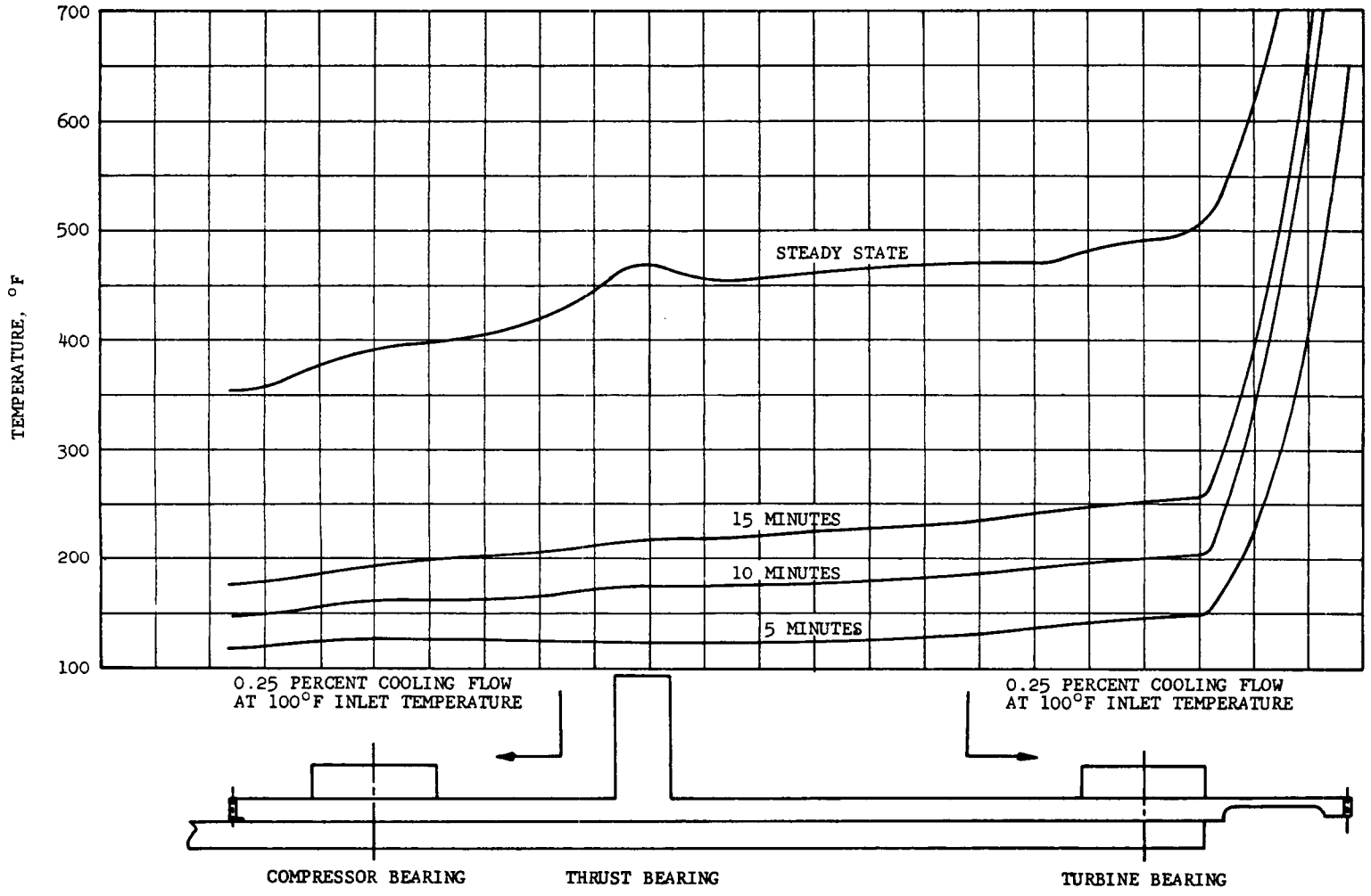

SHAFT TEMPERATURES AT DIFFERENT VALUES OF TIME

FIGURE 26

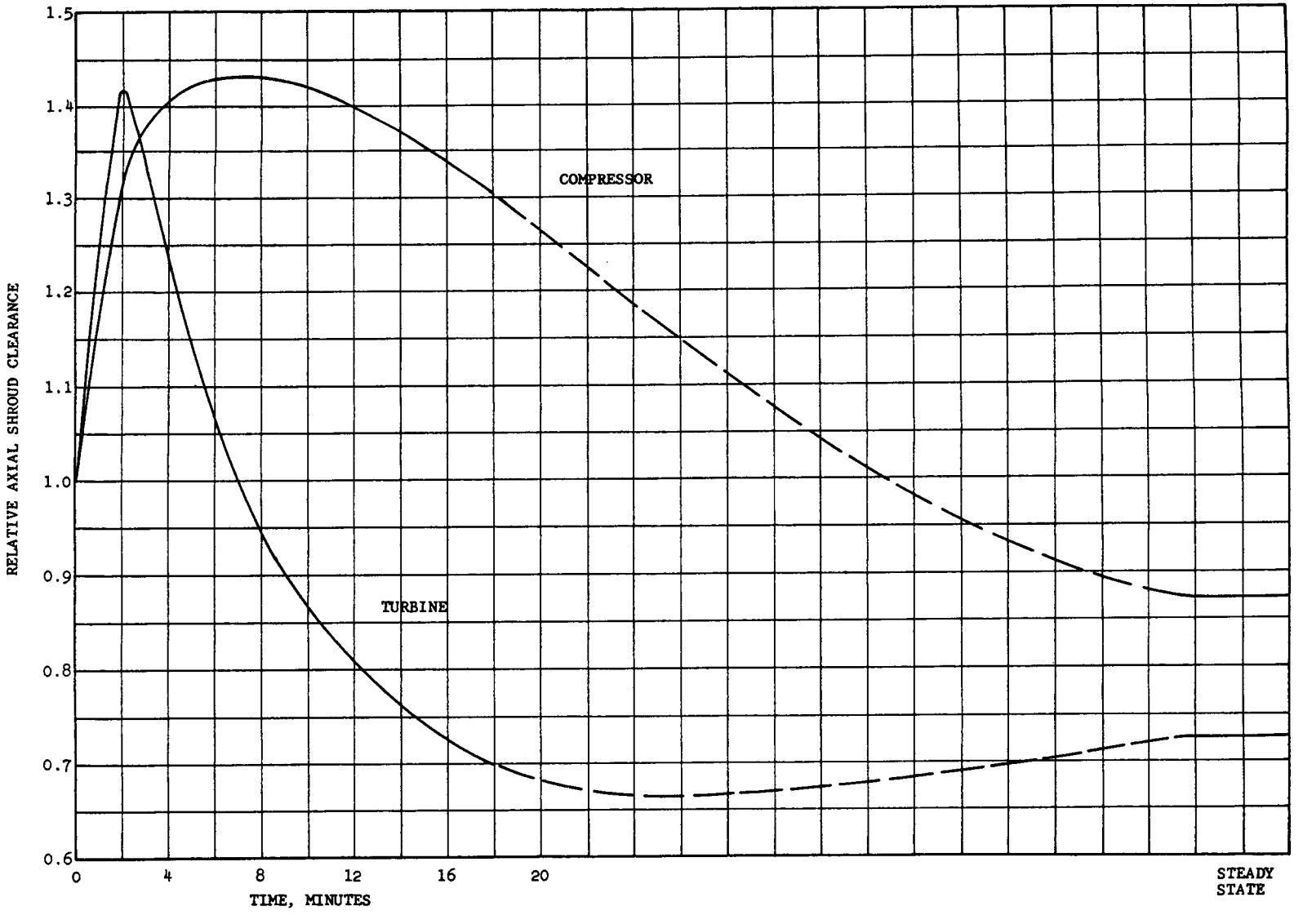

TRANSIENT AND STEADY-STATE COMPRESSOR AND TURBINE SHROUD CLEARANCE

FIGURE 27

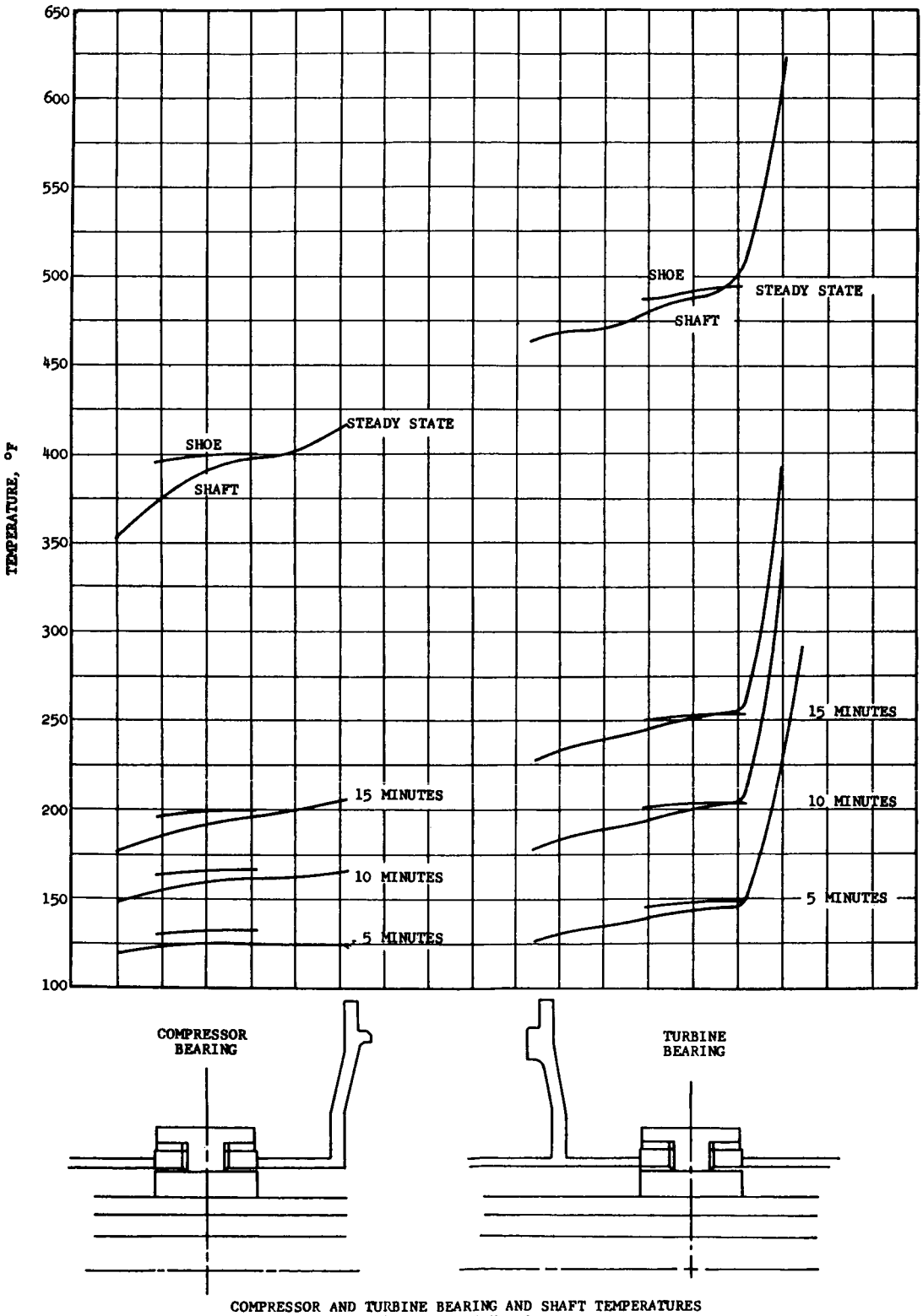

COMPRESSOR AND TURBINE BEARING AND SHAFT TEMPERATURES AT DIFFERENT VALUES OF TIME

FIGURE 28

Figure 29 presents the transient and steady-state relative movement between the bearing journals and the bearing carriers. Relative parts movement for the gas generator is in the order of 0.001 inch and must be accommodated by the resiliently mounted gas bearings.

Figure 30 presents the transient and steady-state position of the mass center lines of the journals relative to the geometric center lines of the scroll shrouds. The geometric center line of the shaft was initially displaced 0.002 inch relative to the geometric center line of the shrouds. Hence, the gas generator must be assembled with the shaft intentionally displaced approximately 0.002 inch, relative to the shrouds, in the direction opposite to the spring mount. This will give, as Figure 30 indicates, a maximum shift of centers of 0.002 and a steady-state running position that is nearly centered in the shrouds.

Figure 31 shows the transient and steady-state loads imposed on the compressor and turbine journal bearings. Effects considered in the load analysis were centrifugal growth, unbalance, relative thermal growth, and film thickness variation with load and ambient temperatures. An initial preload of 10 pounds and a rotor unbalance of 0.0002 c.g. eccentricity were assumed, and a spring rate of 1,500 pounds per inch was selected for the single, flexibly mounted bearing. For the thermally induced changes predicted by the gas generator thermal analysis, reasonable bearing loads and load transients exist with the gas generator design.

Figure 32 presents transient and steady-state temperatures for several representative points located throughout the gas generator. Points such as the turbine nozzle, the turbine wheel hub, and the diffuser vane react rather quickly, reaching their steady-state temperatures in a matter of a few minutes. Other

NOTE: NEGATIVE ORDINATE INDICATES GROWTH OF JOURNAL INTO CARRIER.

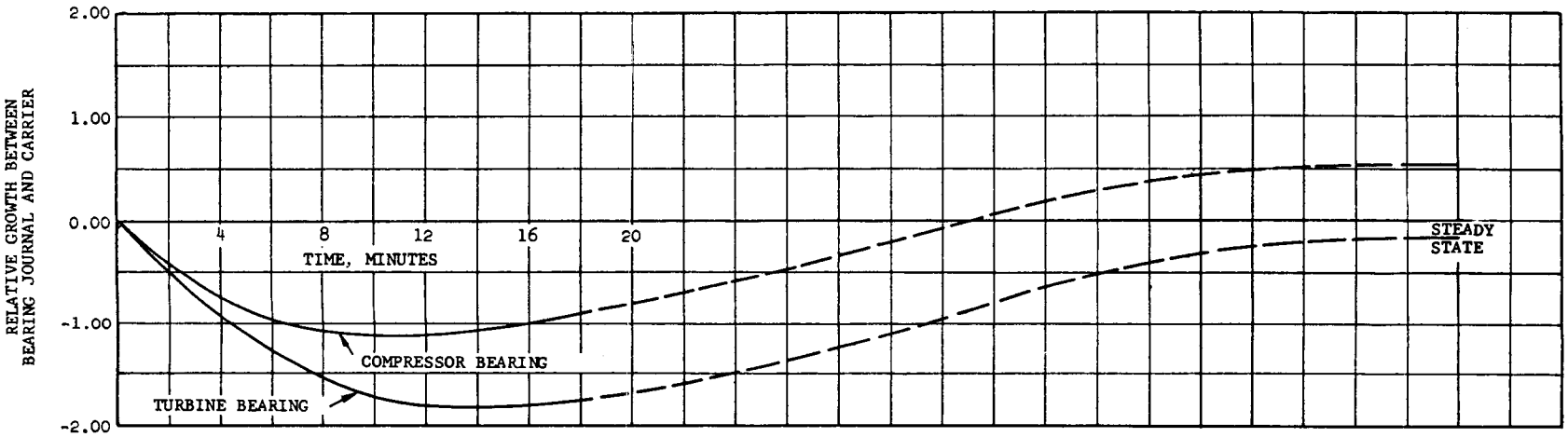

TRANSIENT AND STEADY-STATE BEARING JOURNAL
TO CARRIER RELATIVE EXPANSION

FIGURE 29

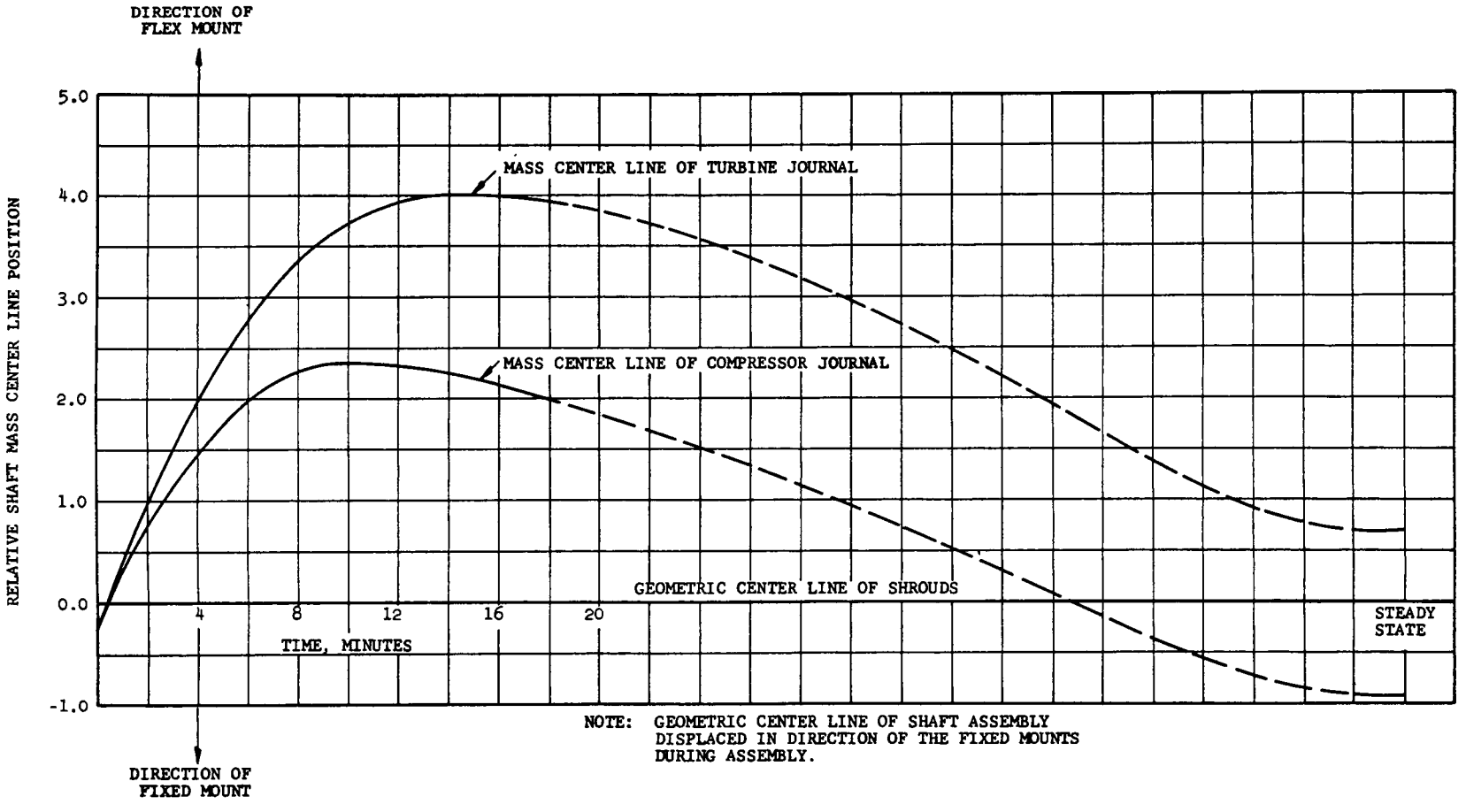

TRANSIENT AND STEADY STATE OF THE MASS CENTER LINE OF THE SHAFT

FIGURE 30

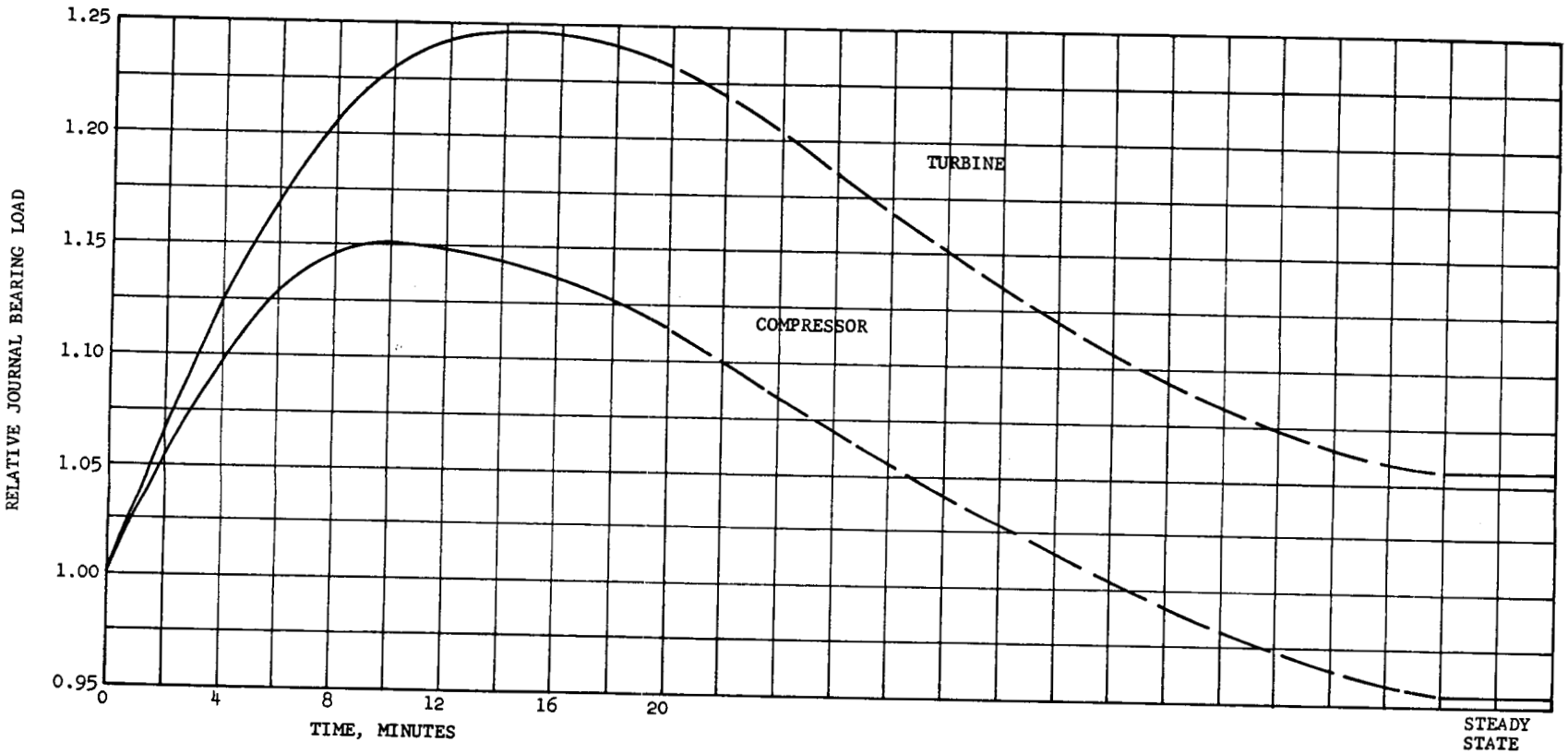

TRANSIENT AND STEADY-STATE JOURNAL BEARING LOADS

FIGURE 31

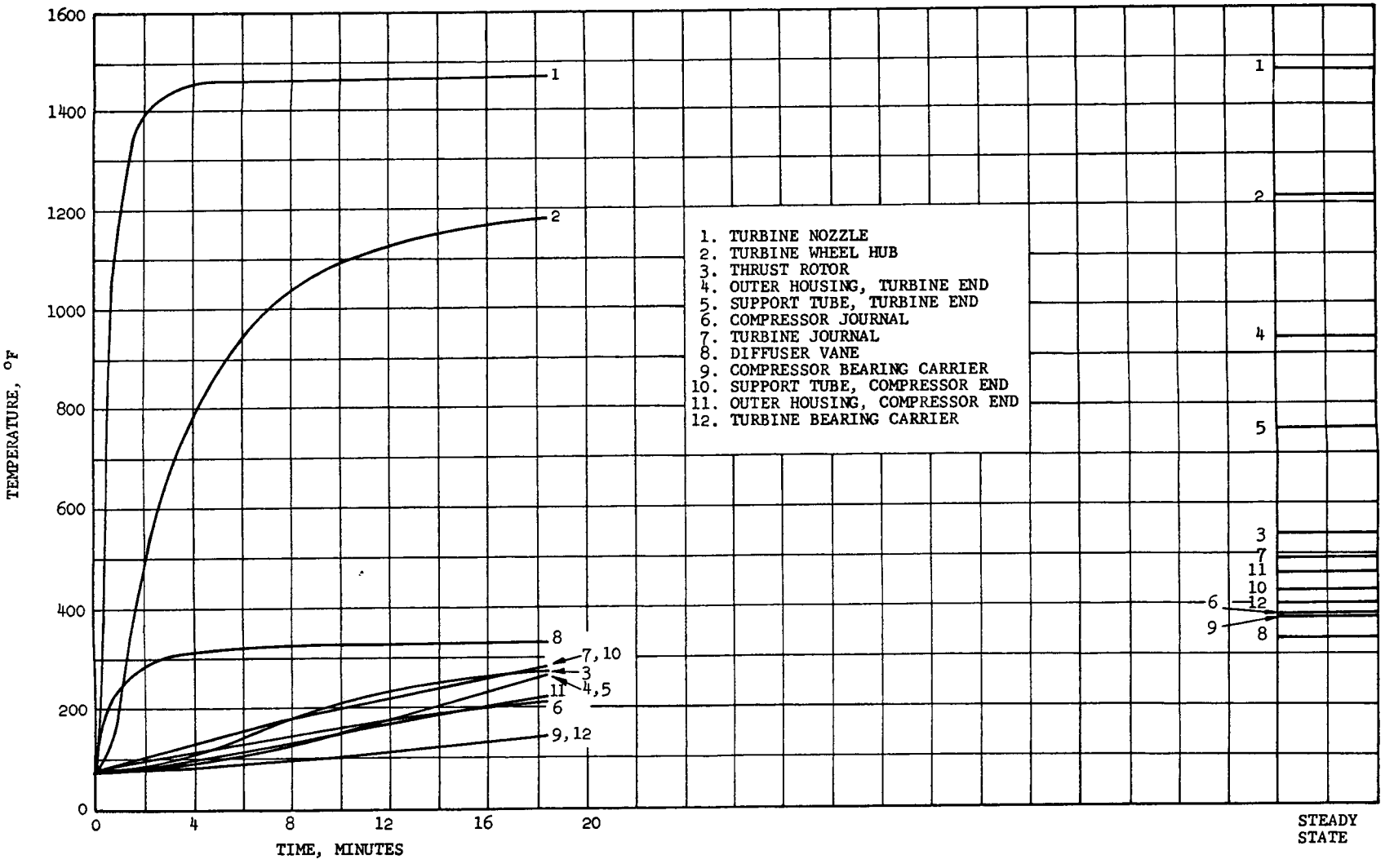

TRANSIENT AND STEADY-STATE TEMPERATURES OF REPRESENTATIVE POINTS IN THE GAS GENERATOR

FIGURE 32

points such as those in the support structure and bearing carrier take an unpredictably long time to reach steady state.

During the course of the thermal analysis, several combinations of coolant flow rates and coolant initial temperatures were investigated in an attempt to determine if there were any optimum combination. Figure 33 presents four of the many schemes investigated. These four, shown in dashed lines, are compared to the final design, indicated by the solid line, all using identical hardware. The accompanying table lists all the particulars of each scheme and presents the steady-state values of relative expansion between the bearing carrier and the journals for each scheme. In all instances the relative expansions are well within the capability limits of the gas generator final design. It appears that there should be no concern about choosing a cooling arrangement for its own sake, because of the relative freedom to base the selection on overall system performance and/or complexity.

Cooling scheme "A" was therefore selected, since,with the labyrinth seals at their minimum clearance, the seals could be opened up to increase the cooling flow during evaluation testing by the NASA.

3.7 Shock and Vibration Analysis

For the shock and vibration analysis of the gas generator, the system analyzed consisted of three bodies defined as follows:

Body 1 - Large mass representative of the launch vehicle structure

Body 2 - Gas-generator housing

Body 3 - Gas-generator rotating assembly

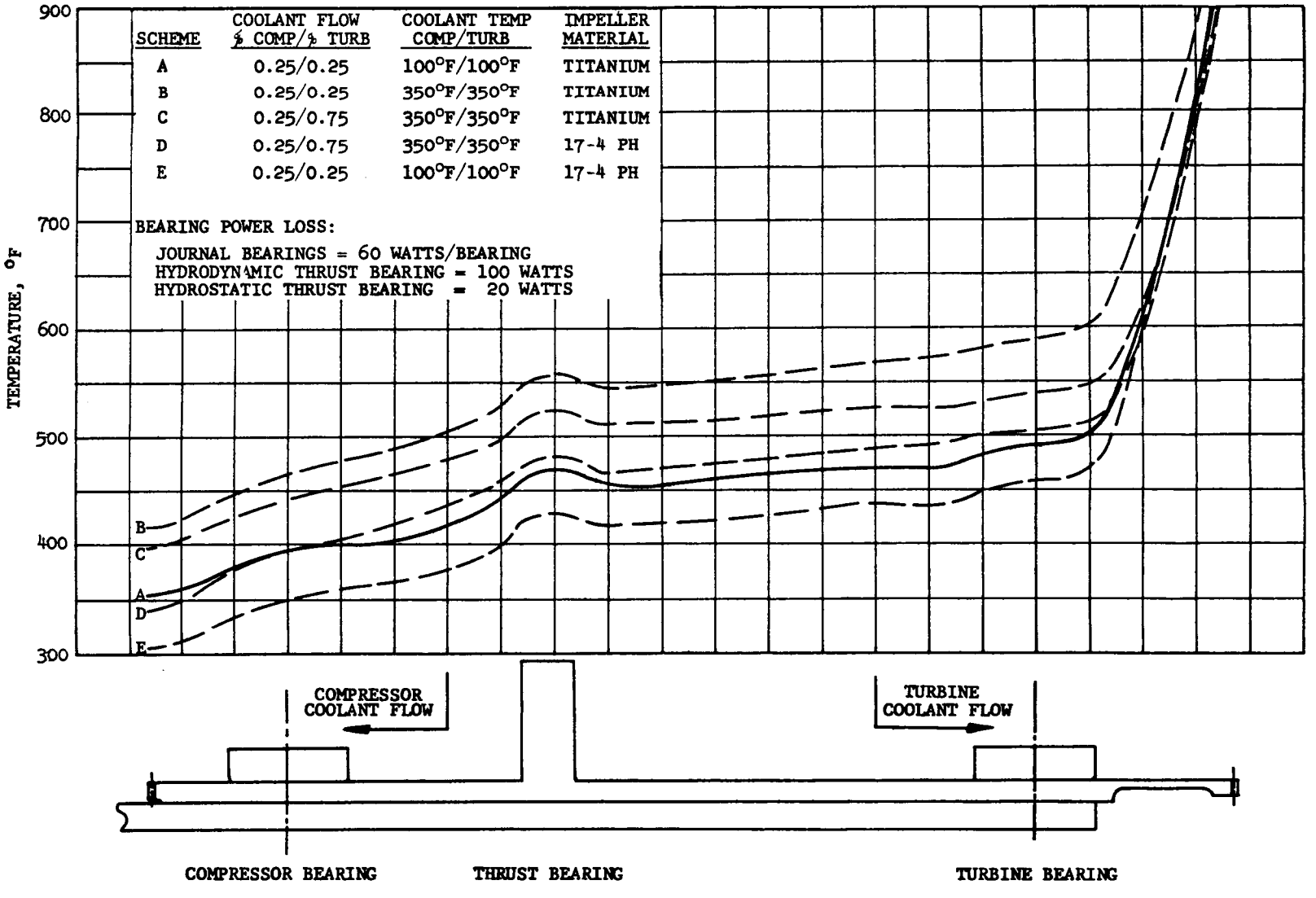

STEADY-STATE SHAFT TEMPERATURES FOR VARIOUS COOLING SCHEMES
FIGURE 33

The gas generator is isolated from the launch vehicle so that the acceleration and displacement imposed are within acceptable limits.

Figures 34 and 35 are schematics of the mount locations used in the design analysis, and Table 2 shows the spring rates of the mounts for each body during launch. It should be noted that, to have a complete analysis of the system, additional information would be required concerning the ducts to be attached to the gas generator. During launch the minimum vibratory frequency to be isolated is 61 cps. The gas-generator mounts should be designed to have a spring rate that will provide a natural frequency below 16 cps. This places the system resonant condition in a region of impressed frequency of relatively low input acceleration. By using the spring rates listed in Table 2, the natural frequency of the system is found to be 13.7 cps. This result is for an impressed acceleration in the Z direction shown below.

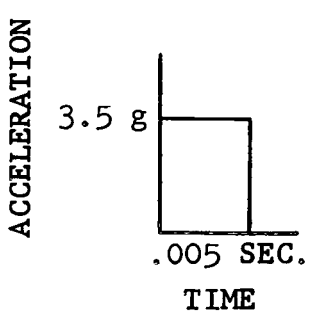

With the same impressed acceleration in both the X and the Z directions, the resulting loads are as shown in Tables 3 and 4. Note that the loads for Body 2 (97 pounds in weight) and Body 3 (15.5 pounds in weight) show that the 3.5-g impressed acceleration is effectively isolated. Figure 36 shows a shear and bending moment diagram for the Z direction shock application.

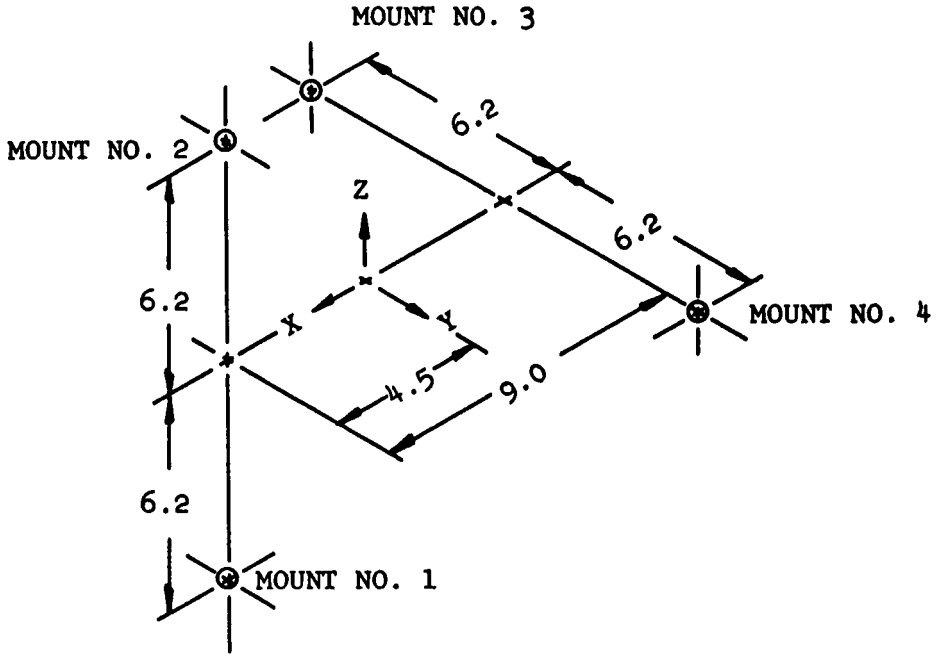

SCHEMATIC OF GAS GENERATOR FRAME
MOUNT POINTS (BODY 2)

FIGURE 34

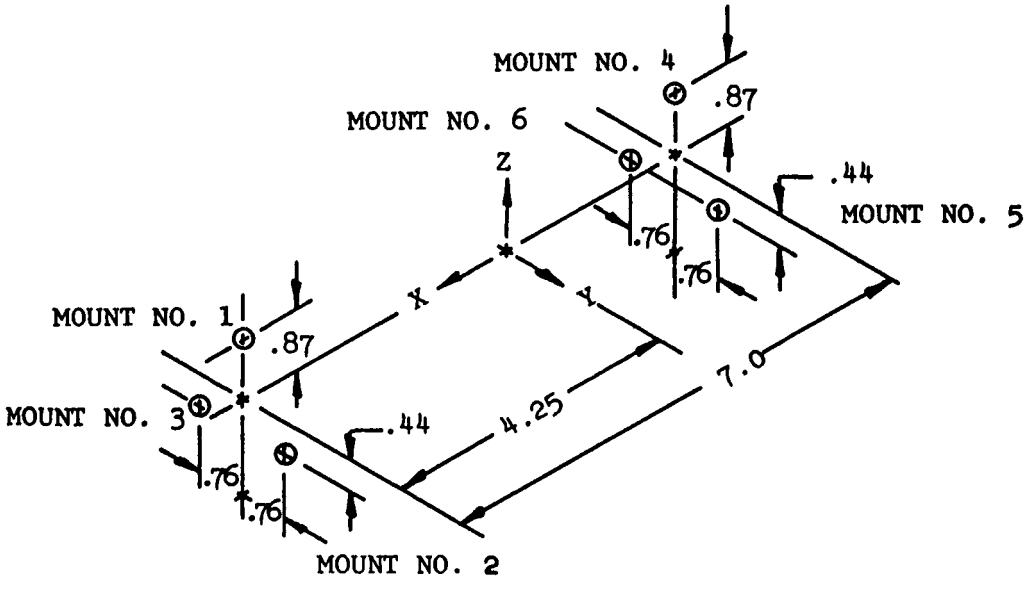

SCHEMATIC OF GAS GENERATOR SHAFT
MOUNT POINTS (BODY 3)

FIGURE 35

TABLE 2

SUMMARY OF SPRING RATES FOR LAUNCH CONDITION

K = LBS/INCH	BODY 2				BODY 3					
MOUNT / SPRING RATE	1	2	3	4	1	2	3	4	5	6
K_x	65.0	65.0	650.0	650.0	10^6	0	0	10^6	0	0
K_y	650.0	65.0	65.0	650.0	0	$5(10)^5$	$5(10)^5$	0	$5(10)^5$	$5(10)^5$
K_z	65.0	650.0	650.0	650.0	$3(10)^3$	$5(10)^5$	$5(10)^5$	$3(10)^3$	$5(10)^5$	$5(10)^5$

TABLE 3

SUMMARY OF MAXIMUM FORCES AT MOUNTS
FOR RECTANGULAR SHOCK PULSE IN
X DIRECTION DURING LAUNCH CONDITION

F = LBS	BODY 2				BODY 3					
MOUNT / FORCE	1	2	3	4	1	2	3	4	5	6
F_x	-48.6	-48.6	-485.6	-485.6	-92.2	0	0	-92.2	0	0
F_y	0	0	0	0	0	0	0	0	0	0
F_z	0	0	0	0	.1	10.9	10.9	0	-10.6	-10.6

TABLE 4

SUMMARY OF MAXIMUM FORCES AT MOUNTS
FOR RECTANGULAR SHOCK PULSE IN
Z DIRECTION DURING LAUNCH CONDITION

F = LBS	BODY 2				BODY 3					
MOUNT / FORCE	1	2	3	4	1	2	3	4	5	6
F_x	9.9	-9.9	0	0	-.3	0	0	-.3	0	0
F_y	0	0	0	0	0	0	0	0	0	0
F_z	-46.4	-466	-324.4	-324.4	-.2	-36.5	-36.5	-.4	-64.4	-64.4

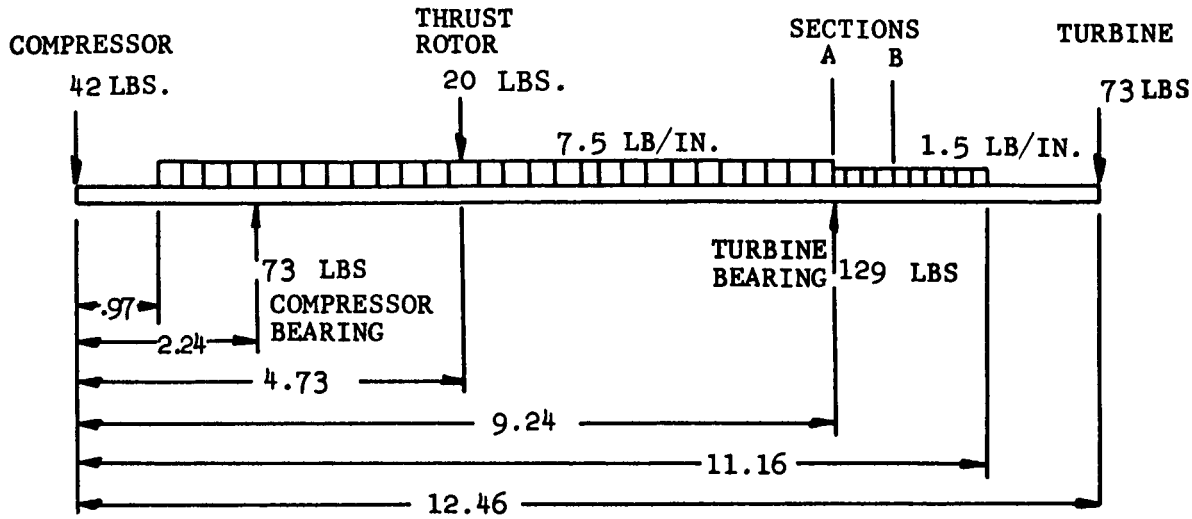

ALL DIMENSIONS IN INCHES

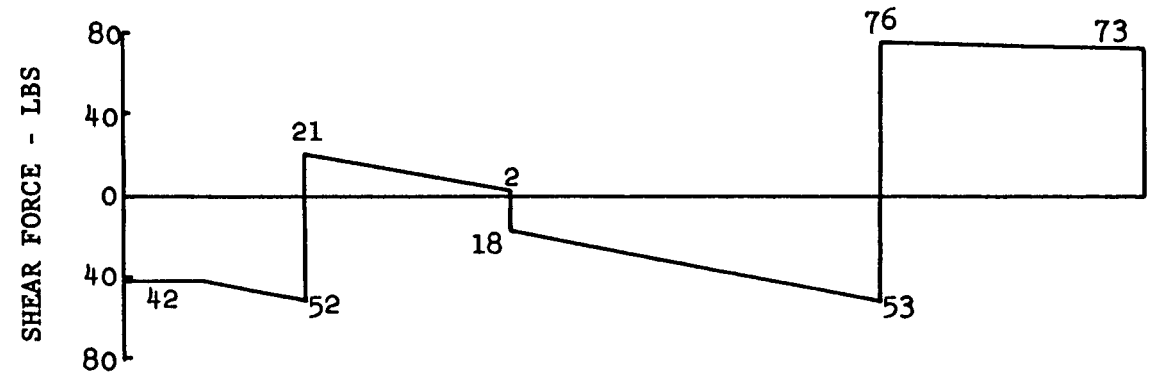

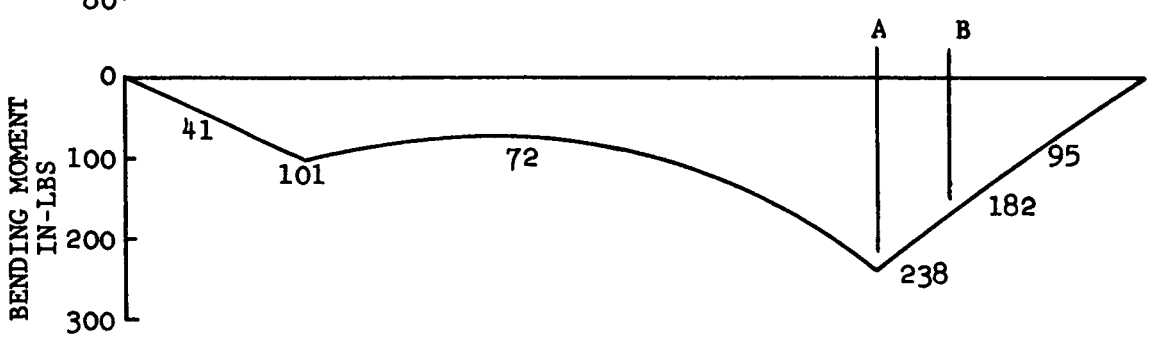

SECTION A
(MAXIMUM BENDING MOMENT)

$$\sigma = \frac{Mc}{I} = \frac{238\ (0.87)}{\frac{\pi}{64}\ (0.87^4 - 0.61^4)} = 9625 \text{ PSI}$$

SECTION B
(MINIMUM SHAFT SECTION)

$$\sigma = \frac{182\ (0.87)}{\frac{\pi}{64}\ (0.87^4 - 0.79^4)} = 17{,}700 \text{ PSI}$$

LOAD, SHEAR, AND BENDING MOMENT DIAGRAM
FOR RECTANGULAR SHOCK PULSE IN
Z DIRECTION DURING LAUNCH CONDITION

FIGURE 36

With the mount system that has been designed, the vibration frequencies that can cause the most damage have been isolated. The mount system also effectively reduces the acceleration transmitted through the mounts to the gas generator housing and rotating assembly.

3.8 Instrumentation

During the journal and thrust bearing testing, the instrumentation incorporated in the bearing test rigs (described in Section 3.4) was found to be very useful for setting up the bearings and determining the bearing performance. Bearing and shaft stability was monitored with capacitance probes. Bearing loads were determined and monitored with strain gauges. Thermocouples were utilized to determine bearing temperatures as well as the other instrumentation component temperatures for calibration purposes.

Based on the instrumentation utilized during the bearing testing, the instrumentation required to monitor the operation of the gas generator was analyzed and the requirements were determined as follows:

(a) Rotor shaft position at both the turbine and compressor journals, with proximity probes in quadrature (four probes required).

(b) Thrust bearing gas film thickness, with the use of proximity probes on the hydrostatic and hydrodynamic thrust faces (two probes required).

(c) Journal bearing shoe loads, with strain gauges used on the two flexible diaphragm mounts (eight gauges required).

(d) Thrust bearing loads, with strain gauges used on the bearing mount (four strain gauges required).

(e) Thermocouples monitoring temperatures within the machine (54 thermocouples required).

(f) Shaft speed, with three electronic speed pickups used in the same shaft plane (three required).

(g) Static pressure taps on the turbine scroll assembly (two required).

(h) Static pressure taps within the machine (two required for bearing labyrinths and one required for the cavity).

3.8.1 Capacitance Probes

Since commercially available proximity probes were not available, the required probes were purchased from the AiResearch Instrumentation Laboratory.

Tests on the completed gas-generator capacitance probes were performed and the results are summarized below:

(a) Structural integrity is more than adequate for the operating range of temperatures within the gas generator.

(b) Insulation resistance is fully compatible with the equipment to be used for readout purposes.

(c) Calibration of the probes showed good linearity with acceptable temperature characteristics. Representative data is shown in Figure 37 for a flat-plate calibration.

A complete probe assembly is shown in Figure 38.

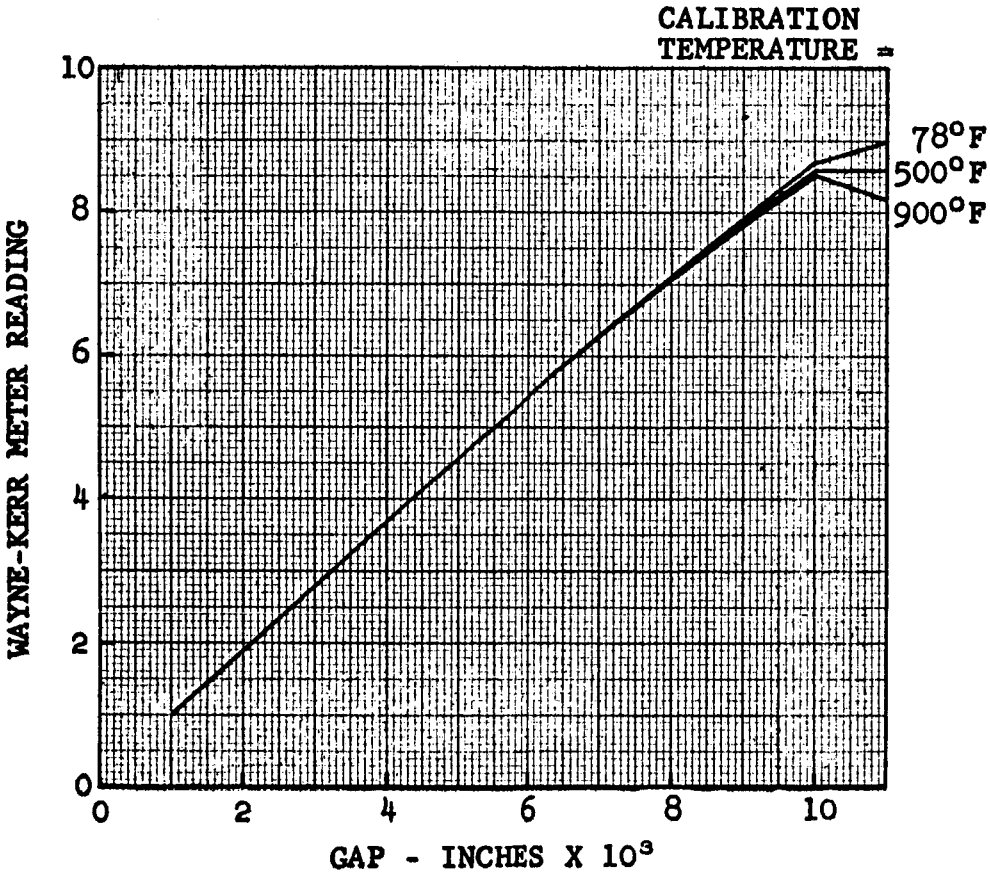

TEST RESULTS ON PROXIMITY PROBE CALIBRATIONS

FIGURE 37

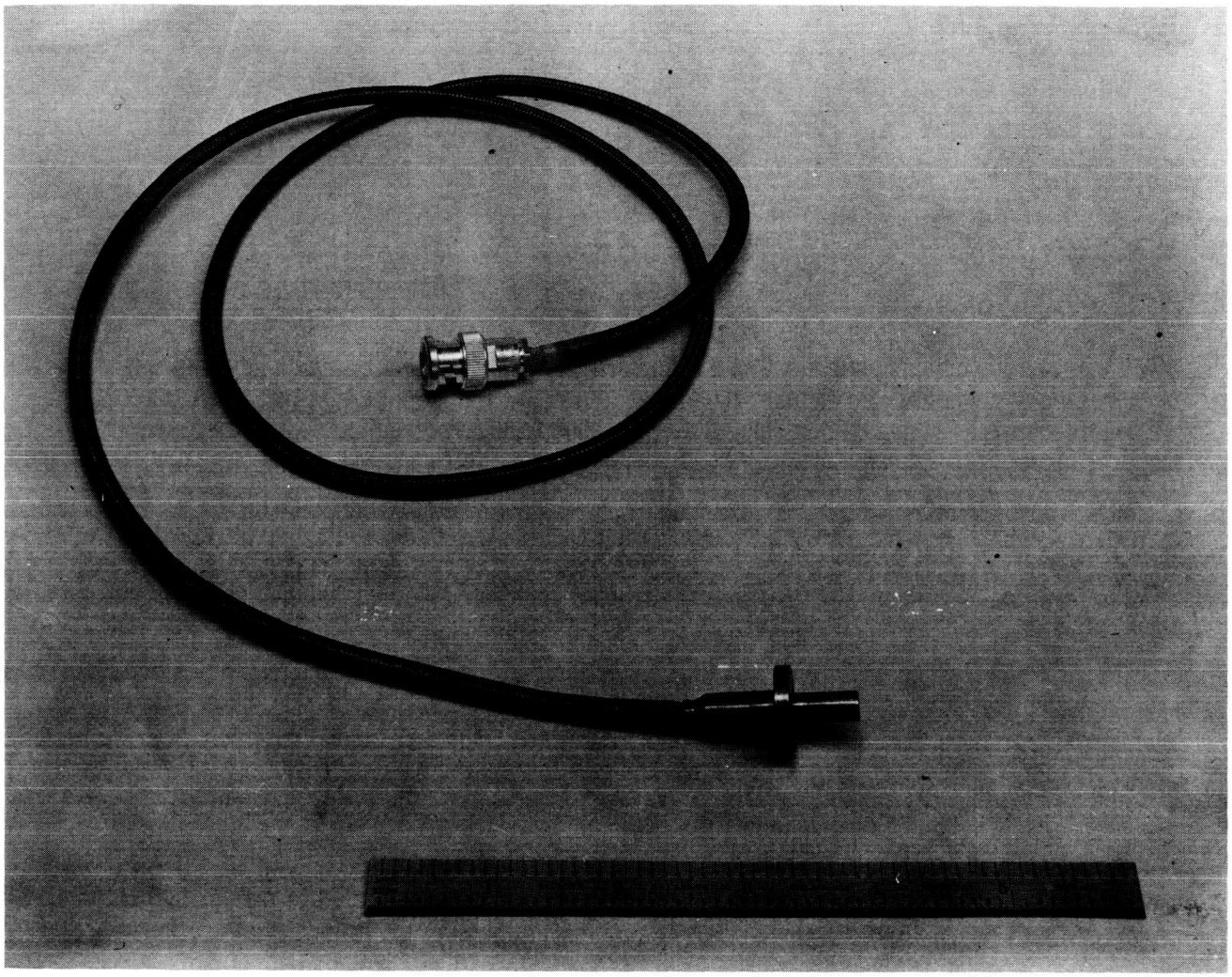

SHAFT CAPACITANCE PROBE

FIGURE 38

The test to determine the effect of a curved surface upon the calibration of a proximity probe showed that excellent correlation is obtainable between actual test results and Wayne-Kerr's predictions for similar probes. Figure 39 shows the test results obtained under normal ambient test conditions. The total variation between actual and predicted values is within ±1/2 percent of full scale. Wayne-Kerr's correction factor can therefore be applied to the flat-plate probe calibration for shaft diameters of the order of 2.00 inches. Figure 40 shows the test probe mounted in the calibration fixture, the curved surface representative of a 2.00-inch-diameter shaft, and the use of gauge-blocks to accurately set the probe gaps.

3.8.2 Strain Gauges

An experimental investigation was performed early in the program to establish whether or not four SR-4 strain gauges, mounted in quadrature on the plate surface, had sufficient sensitivity to indicate bearing load, bearing misalignment, and direction of bearing misalignment. Two prototype diaphragm mounts were instrumented, the diaphragms loaded in 5-pound increments, and the deflection recorded as a function of load. The angular stiffness of the diaphragm was determined by applying a moment at the plate center and measuring the angular deflection of the plate center.

The test results indicated that the strain gauge method for measuring bearing shoe load and angular misalignment has adequate sensitivity and provides a powerful tool for assisting in the aligning of the bearings, setting bearing preload, and measuring bearing loads during transient and steady-state operation.

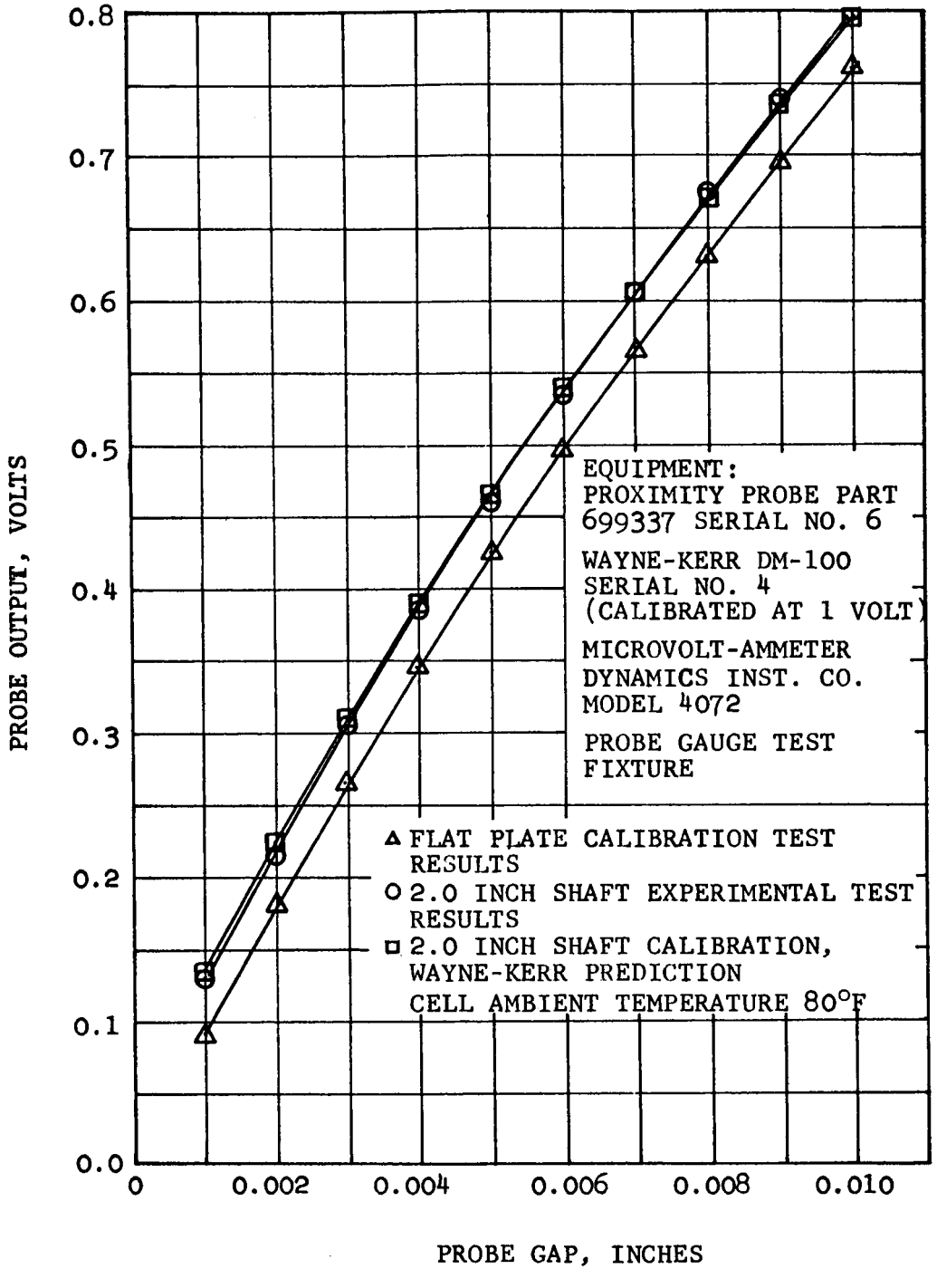

PREDICTED AND ACTUAL TEST RESULTS OF EFFECT OF CURVED SURFACE ON FLAT-PLATE CALIBRATION OF WAYNE-PERR PROXIMITY PROBE SYSTEM

FIGURE 39

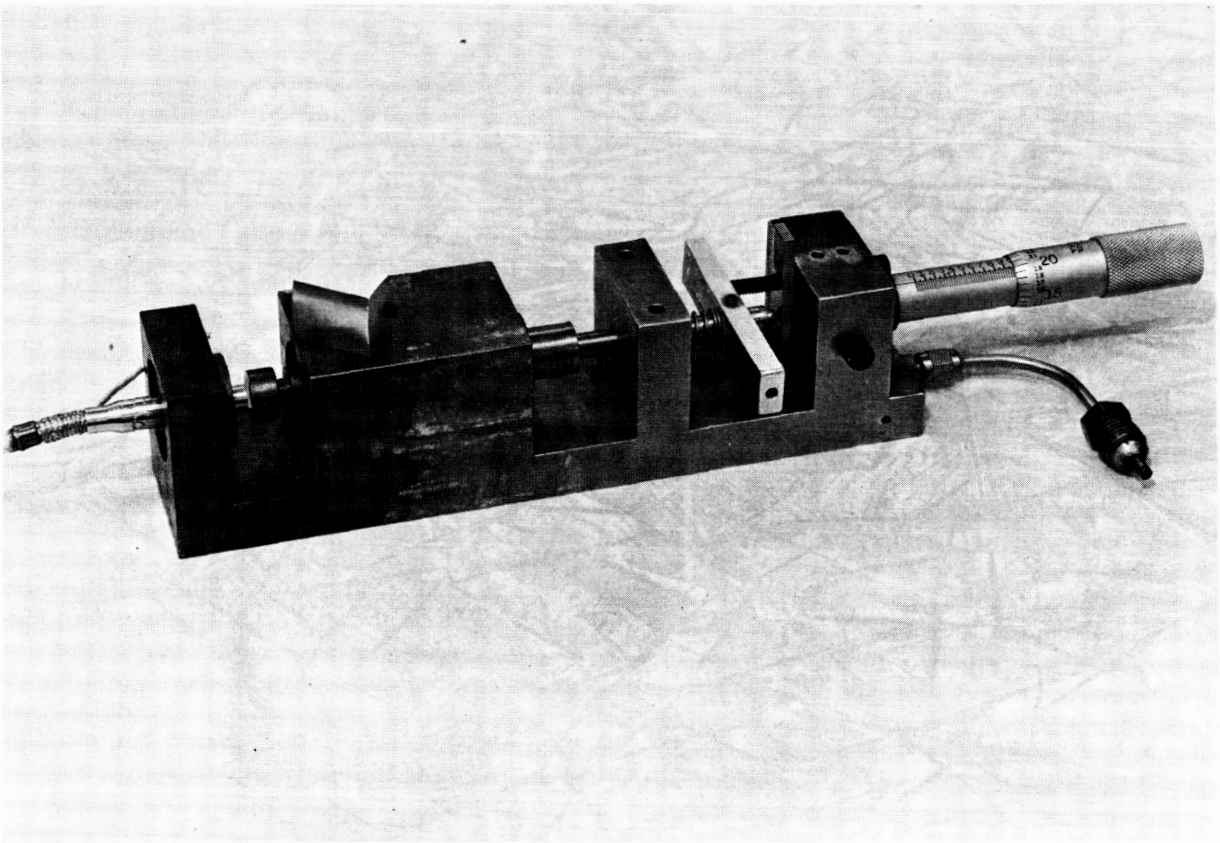

PROXIMITY PROBE IN CALIBRATION FIXTURE

FIGURE 40

The utilization of strain gauges on the thrust bearing mount to determine thrust loading is similar to journal bearing use.

The three strain-gauge circuits comprise the conventional four-arm bridge network, with two opposite arms of the bridge being subjected to the readout system's excitation signal and the two remaining arms reading the output signal. A representation of the turbine-end shoe diaphragm circuit is shown in Figure 41.

The compressor-end shoe diaphragm circuit and thrust bearing load-sensing circuit are to be handled in a like manner. Calibrations of the strain gauges were provided with the final gas generator.

3.8.3 Thermocouples

A total of 54 points were instrumented on the basis of the thermal analysis undertaken during the design phase of the program. However, 23 thermocouples were hooked up to the instrumentation receptacle plate for readout during the acceptance tests, as discussed in Section 5.0. The remaining 31 thermocouples were included since the incorporation of additional thermocouples would necessitate the complete disassembly of the gas generator at the NASA, thus resulting in possible delays during the subsequent testing program.

3.8.4 Additional Instrumentation

Figure 42 shows one of the magnetic speed pickups, three of which are incorporated into the gas generator. Figures 43, 44, 45, and 46 show the installation of the instrumentation prior to the acceptance test. The instrumentation leads are hooked to the instrumentation receptacle plate shown in Figure 47.

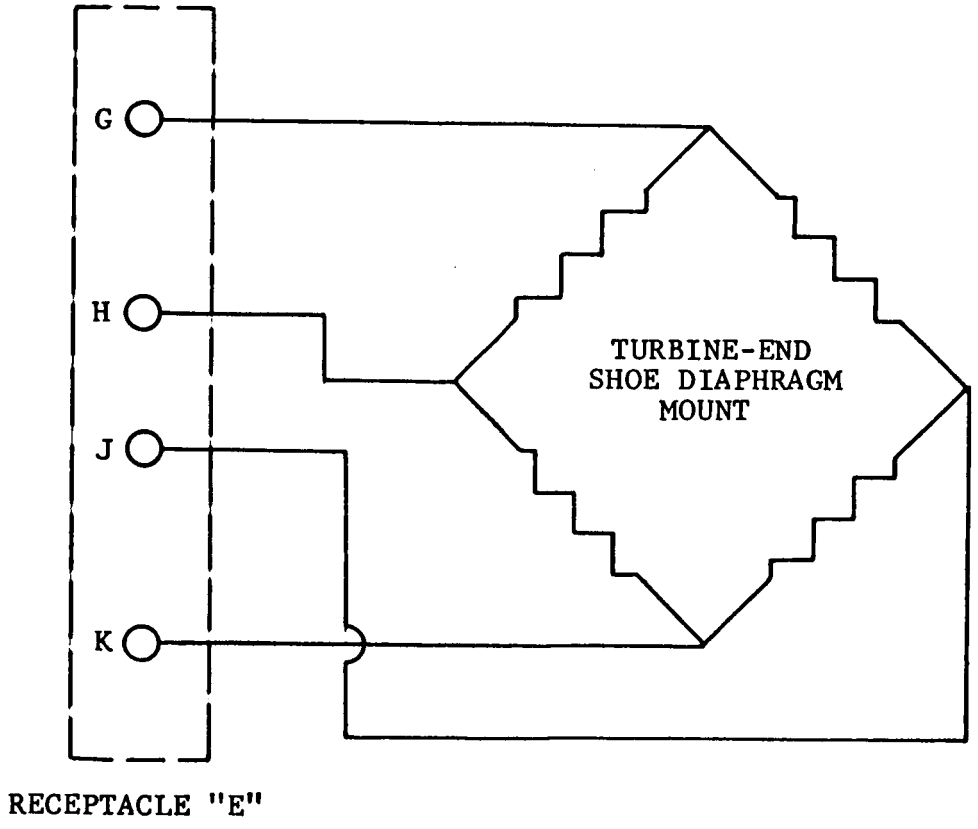

REPRESENTATIVE STRAIN-GAUGE CIRCUIT

FIGURE 41

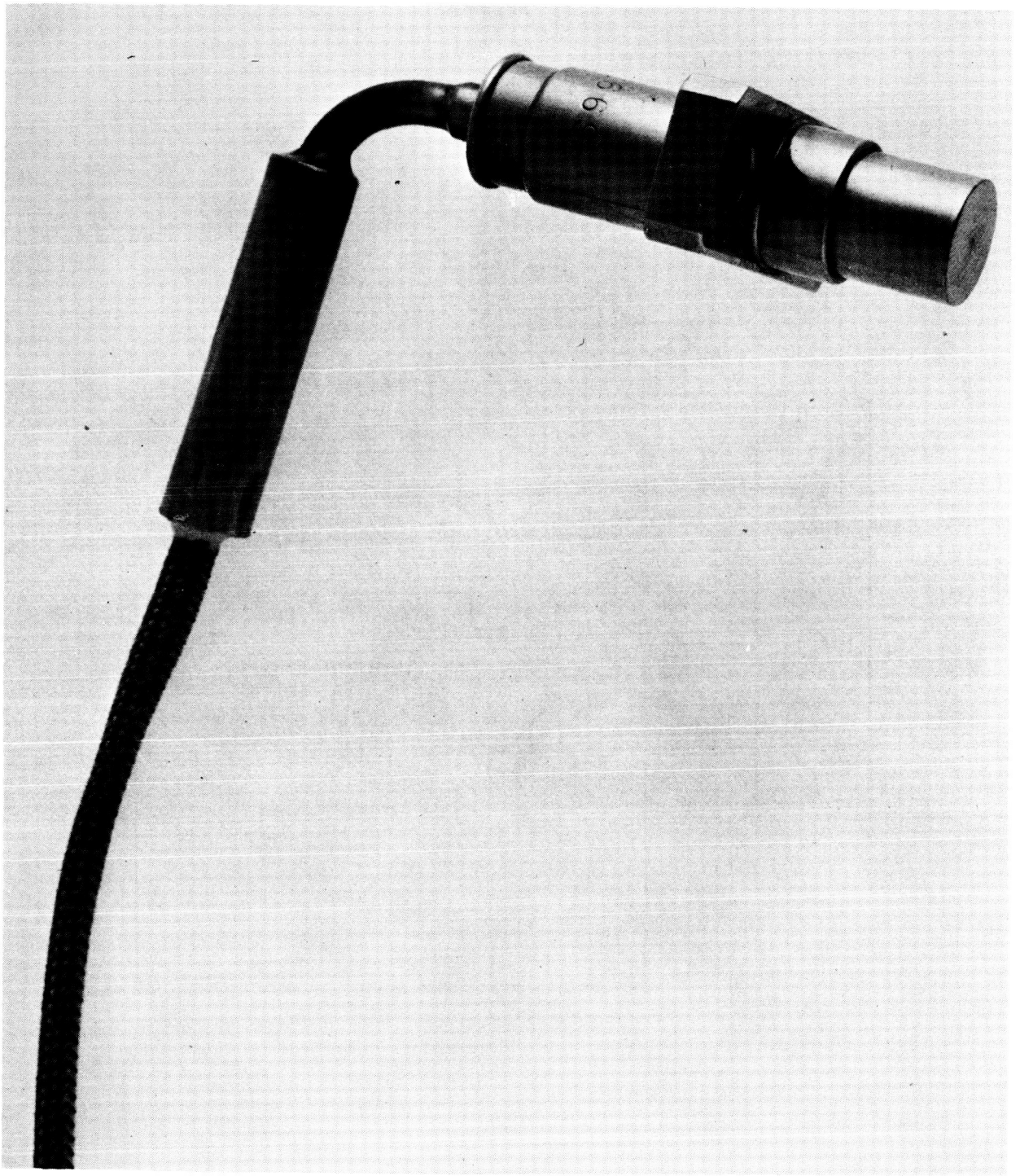

MAGNETIC SPEED PICKUP

FIGURE 42

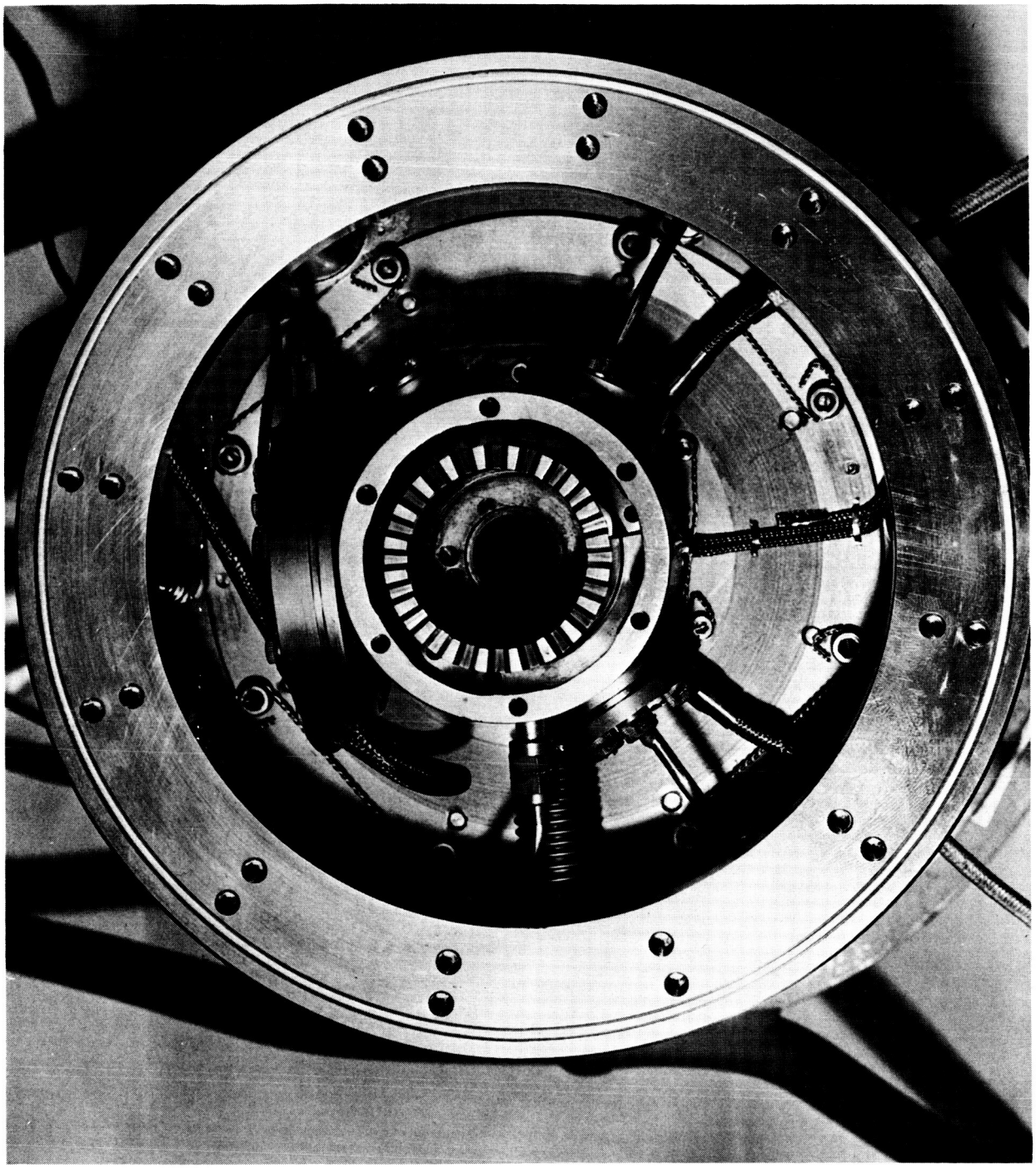

INSTRUMENTATION INSTALLATION, PARTIAL ASSEMBLY
NASA GAS GENERATOR

FIGURE 43

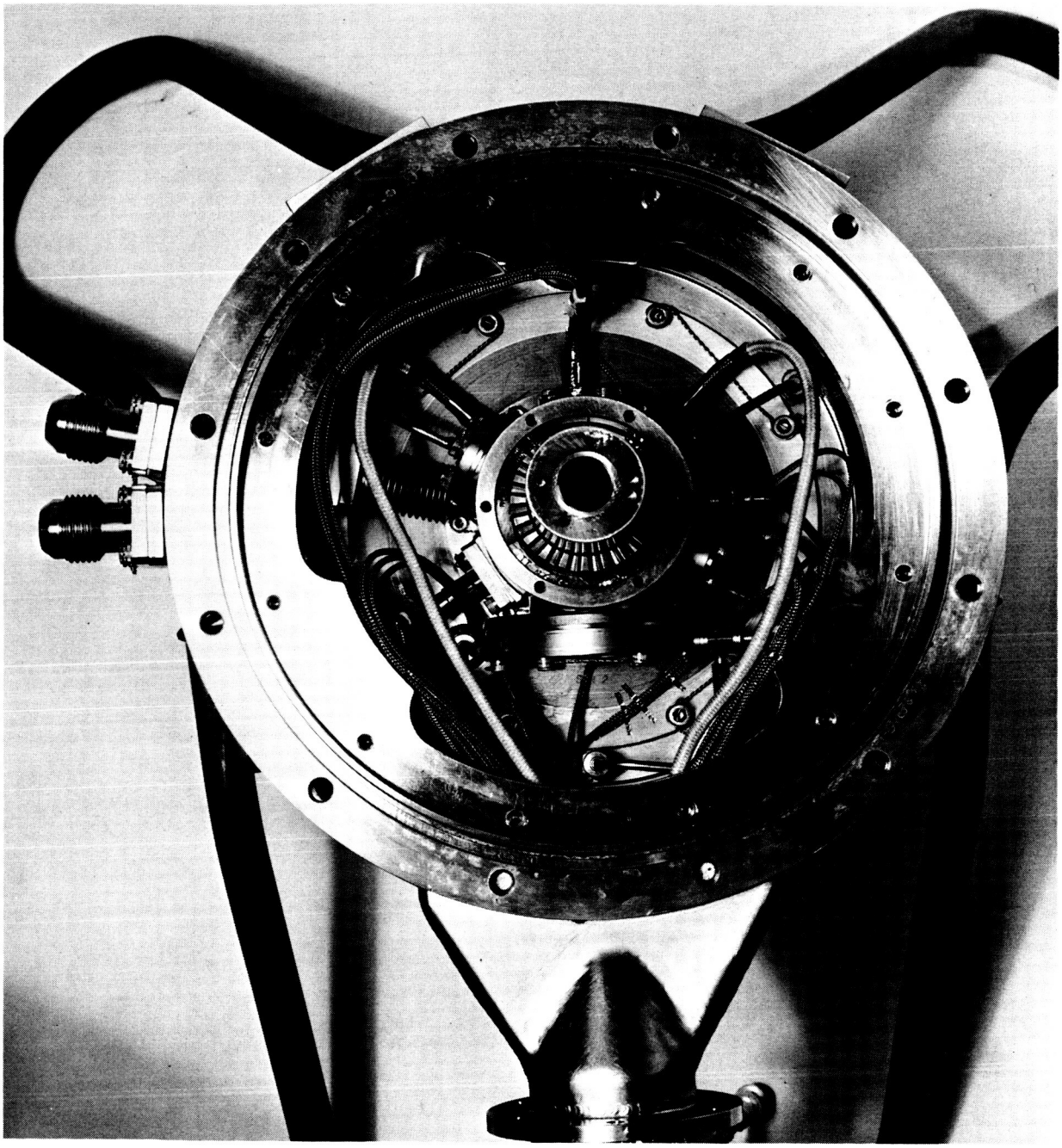

INSTRUMENTATION INSTALLATION, FINAL WIRING
NASA GAS GENERATOR

FIGURE 44

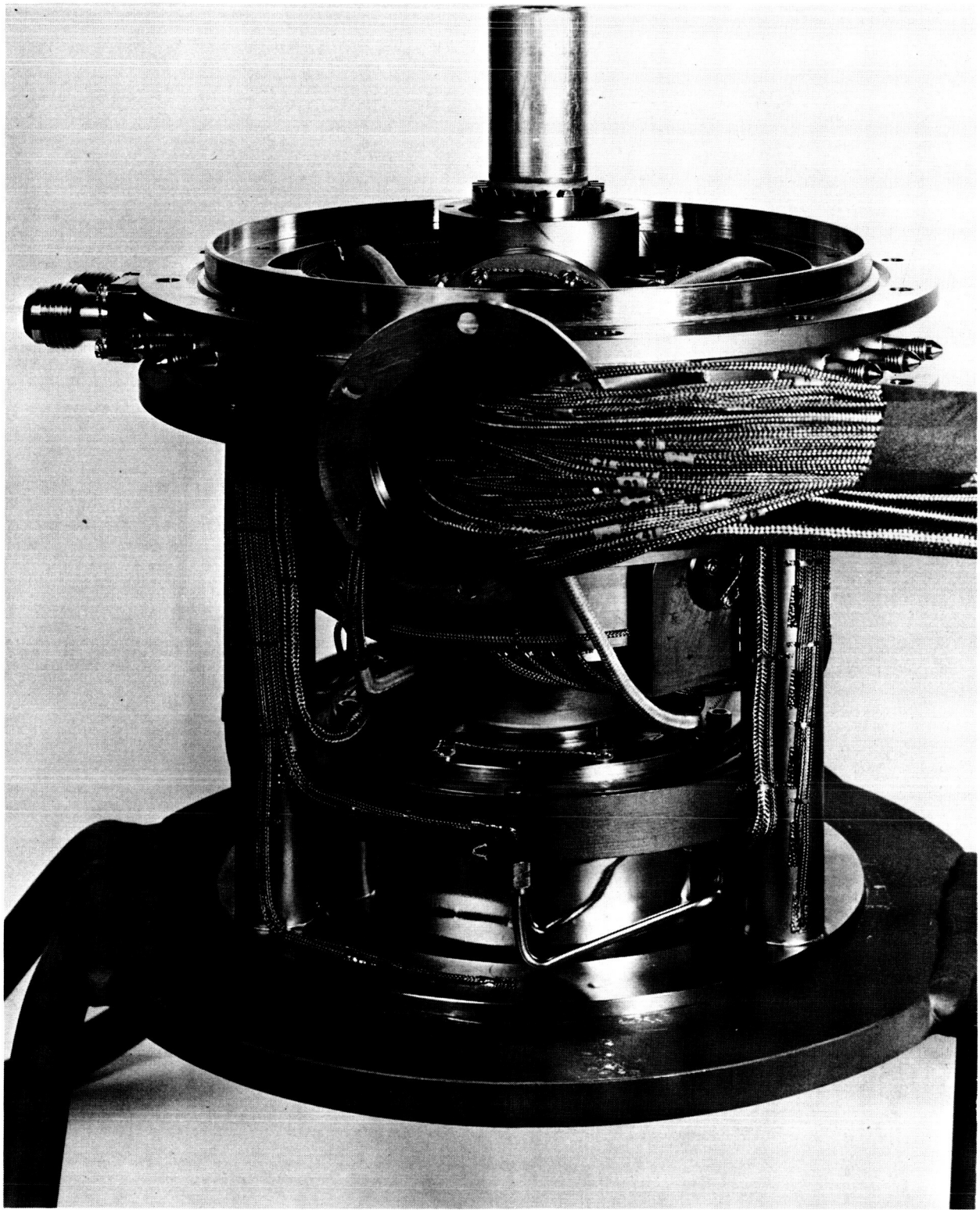

INSTRUMENTATION INSTALLATION, FINAL WIRING
NASA GAS GENERATOR

FIGURE 45

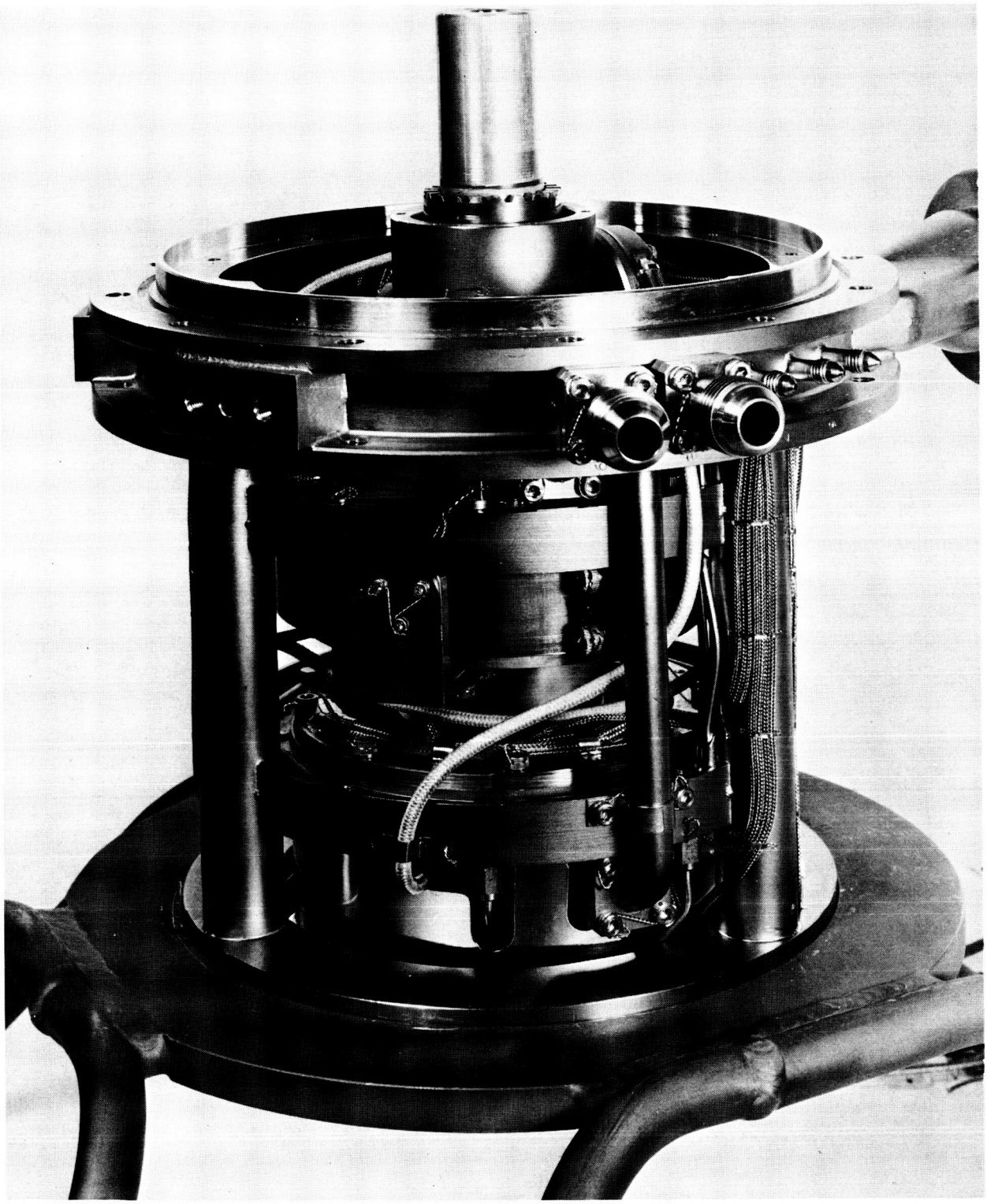

INSTRUMENTATION INSTALLATION, FINAL WIRING
NASA GAS GENERATOR

FIGURE 46

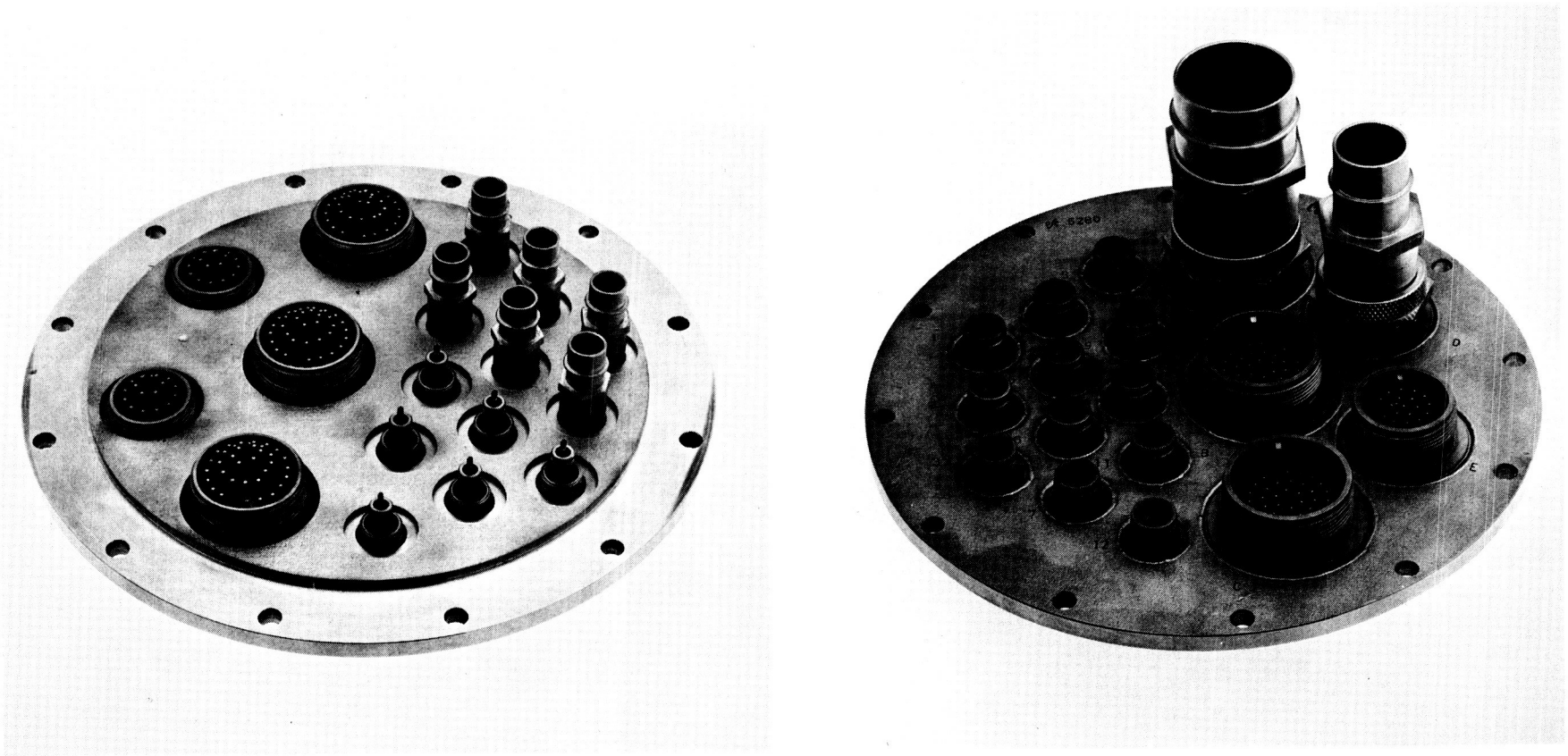

INSTRUMENTATION RECEPTACLE PLATE

FIGURE 47

In addition, the gas generator has been designed to accept gas bearing shoes with the following incorporated instrumentation:

(a) Capacitance probes located in the bearing housing and situated such that they can monitor the bearing shoe leading edge of the first trailing shoe behind the resiliently mounted shoe on each bearing to determine pitch and roll characteristics of the bearings (four probes).

(b) Capacitance probes built into the same shoes described above to determine the bearing shoe-to-shaft film thickness. The probe position will be on the pivot pitch axis as close to the pivot as possible (two probes).

This instrumentation would be utilized to determine gas bearing performance.

4.0 FINAL GAS GENERATOR CONFIGURATION

4.1 Gas Generator Description

Figure 48 presents a simplified cross section of the final gas generator. For purposes of clarity, the unit may be considered to consist of eight groups of parts. These are (1) the rotating assembly, (2) the compressor-journal bearing assembly, (3) the turbine-journal bearing assembly, (4) the gimbal and thrust bearing assembly, (5) the compressor scroll and diffuser assembly, (6) the turbine scroll and nozzle assembly, (7) the main frame assembly, and (8) the mount assembly. In the following paragraphs, each of the above subassemblies is described. A list of the individual parts is presented in Table 5.

4.1.1 Rotating Assembly

The rotating assembly consists of the shaft, the compressor wheel, and the turbine wheel. The compressor wheel and the turbine wheel are positioned on the shaft with curvic couplings. A tension bolt, drawn up by the self-locking shaft nut and washer, provides the axial force required to hold the assembly together as a rigid body. The compressor wheel spinner completes the rotating assembly and is attached to the end of the tension bolt with a self-locking screw.

4.1.2 Compressor/Turbine Journal Bearing Assembly

The compressor/turbine journal bearing assembly consists of the compressor/turbine journal bearing carrier, two shoe-and-fixed-mount assemblies, and one shoe-and-flexible-mount assembly.

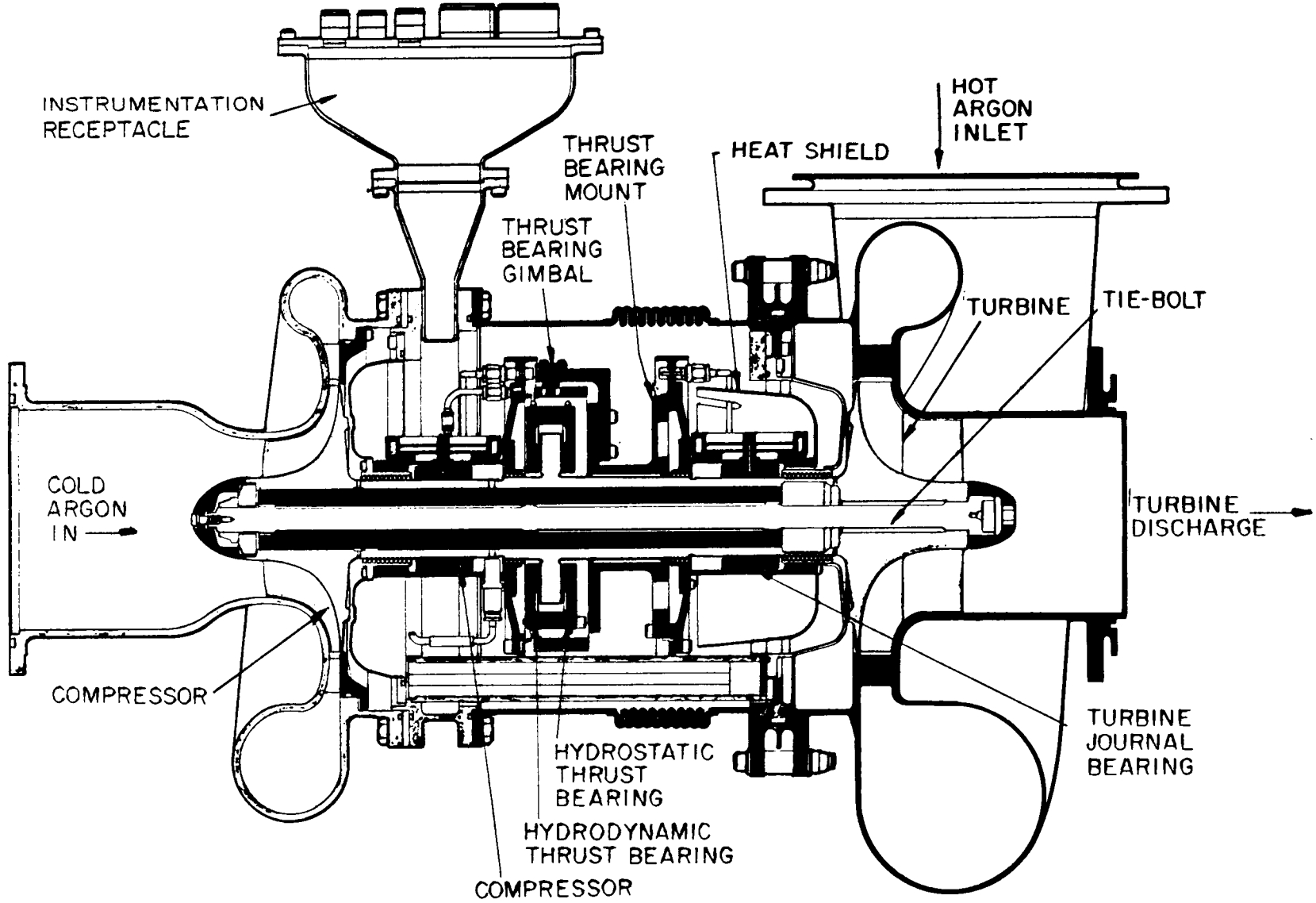

NASA BRAYTON-CYCLE RADIAL GAS GENERATOR
FIGURE 48

TABLE 5

NASA GAS GENERATOR PARTS LIST

DRAWING NO.	TITLE	USED ON	NO. REQD.
699301-1	GAS GENERATOR ASSEMBLY		
699302-1	Scroll Assembly, Turbine	699301-1	1
699303-1	Wheel, Turbine	699301-1	1
699304-1	Impeller, Compressor	699301-1	1
699307-1	Seal, Static	699301-1	1
699307-2	Seal, Static	**	1
699307-3	Seal, Static	**	1
699308-1	Scroll Assembly, Compressor	699301-1	1
699309-1	Diffuser Assembly Compressor	699301-1	1
699310-1	Shaft Assembly, Gas Generator	699301-1	1
699311-1	Bolt, Tension	699301-1	1
699312-1	Frame Assembly, Main	699301-1	1
699313-1	Carrier Assembly, Turbine Bearing	699312-1	1
699314-1	Carrier Assembly, Compressor Bearing	699312-1	1
699315-1	Mount Assembly, Bearing	699363-1	1
699317-1	Mount Assembly, Bearing	699364-1	1
699318-1	Tube Assembly, Thrust Bearing	699301-1	2
699320-1	Stator, Hydrostatic Thrust Bearing	699301-1	1
699321-1	Stator, Hydrodynamic Thrust Bearing	699301-1	1
699324-1	Seal Assembly, Turbine	699301-1	1
699325-1	Seal Assembly, Compressor	699301-1	1
699326-1	Shield, Turbine Radiation	699301-1	1
699327-1	Housing Assembly, Outer	699301-1	1
699328-1	Housing Assembly, Instrumentation	699301-1	1
699329-1	Plate Assembly, Connector	699301-1	1
699330-1	Shoe Assembly, Bearing	699363-1	1
699330-1	Shoe Assembly, Bearing	699364-1	1
699333-1	Tube Assembly, Metal Pressure Tap	699301-1	2
699334-1	Spinner, Impeller	699301-1	1
699335-1	Washer, Thrust	699301-1	1
699337-1	Probe, Capacitance (Shaft)	699301-1	4
699338-1	Probe, Capacitance (Thrust Bearing)	699301-1	2
699339-1	Pickup Assembly, Magnetic	699301-1	3
699340-1	Bellows, Duct	699313-1	1
699340-1	Bellows, Duct	699314-1	1
699342-1	Bellows, Outer Housing	699327-1	1
699343-1	Flange, Turbine Inlet	**	1
699344-1	Flange, Turbine Outlet	**	1
699345-1	Spacer, Sleeve	699301-1	12
699345-1	Spacer, Sleeve	**	16
699346-1	Shim, Bearing Mount	699301-1	2
699348-1	Shim, Bearing Mount	699301-1	4
699349-1	Shim, Turbine Scroll	699301-1	1
699354-1	Shim, Capacitance Probe	699301-1	4
699354-3	Shim, Capacitance Probe	699301-1	2
699355-1	Shim, Magnetic Pickup	699301-1	3
699356-1	Base, Mounting	699301-1	1
699357-1	Bracket Assembly, Support	699301-1	1
699358-1	Adapter, Fitting	699301-1	3
699359-1	Bracket Assembly, Mounting	699301-1	2
699360-1	Mount, Flexible Metal	699301-1	2
699363-1	Bearing, Matched Set	699301-1	4
699364-1	Bearing, Matched Set	699301-1	2
699365-1	Nut, Self Locking	699301-1	1
699366-1	Tube Assembly, Diaphragm Mount	699301-1	1
699368-1	Cover, Capacitance Probe Boss	699301-1	4
699376-1	Tube Assembly	699301-1	1
699410-1	Probe Assembly, Electrical Ground	699301-1	1
699411-1	Housing, Probe Support	699410-1	1
699412-1	Stem Assembly, Probe	699410-1	1
699413-1	Guide, Stem	699410-1	1
699424-1	Seal, Shaft	699301-1	2
699434-1	Pivot, Thrust Bearing Mount	699452-1	4
699435-1	Insert Pivot	699440-1	2
699436-1	Shim, Pivot	699452-1	4
699440-1	Ring Assembly, Thrust Bearing Mount	699452-1	1
699441-1	Spacer Assembly, Thrust Bearing	699452-1	1
699443-1	Bushing, Pivot	699441-1	2
699451-1	Mount Assembly, Thrust Bearing	699452-1	1
699452-1	Gimbal, Matched Set	699301-1	1

DRAWING NO.	TITLE	USED ON	NO. REQD.
369745	Shim, Sealing Spacer	699301	1
369778	Flange, Compressor Outlet	**	1
369779	Flange, Compressor Inlet	**	1
369813	Seal, "O"-Ring	699301	3
362-506-9013	Gasket	699301	1
362-506-9014	Gasket	699301	1
362-506-9015	Gasket	699301	1
362-522-9006	Gasket	699301	2
362-542-9002	Gasket	699301	16
473-010-9001	Lubricant	699301	AR
525-578-9003	Nut	699301	12
655-601-9208	Screw	699301	1
S8171AP5	"O"-Ring	699301	1
S8171AP16	"O"-Ring	**	1
S8171AP30	"O"-Ring	**	1
S8171AP30	"O"-Ring	699301	1
S8171AP37	"O"-Ring	699301	1
S8152BC46-0-240	Pin	699312-1	4
S8152BC46-0-240	Pin	699451-1	4

COMMERCIAL PARTS

AN4CH4A	Bolt	699301	4
AN5CH4A	Bolt	699301	12
AN5CH5A	Bolt	699301	12
AN929-10S	Cap Assembly	699301	1
AN960C416L	Washer	699301	16
AN960C516	Washer	699301	14
AN906C516L	Washer	699301	12
MS9068-015	"O"-Ring	699301	2
MS20995C32	Lockwire	699301	AR
MS21045C4	Nut	699301	8
MS21281-25	Screw	699301	12
MS21288-06	Screw	699301	12
MS21288-07	Screw	699301	12
MS24585C51	Spring	699410-1	1
MS24673-1	Screw	699301	24
MS24673-1	Screw	699312-1	16
MS24673-2	Screw	699301	18
MS24673-2	Screw	699451-1	8
MS24673-3	Screw	699301	8
MS24673-9	Screw	699301	2
MS24673-9	Screw	699440-1	4
MS24673-11	Screw	699301	4
MS24673-12	Screw	699301	8
MS24673-22	Screw	699301	2
MS24674-1	Screw	699301	18
MS24674-2	Screw	699301	6
MS24674-3	Screw	699301	18
MS24674-6	Screw	699312-1	4
MS24674-7	Screw	699301	32
MS24674-22	Screw	699301	2
MS24677-1	Screw	699301	18
MS24677-2	Screw	699301	12
MS24677-2	Screw	699452-1	12
MS24678-15	Screw	699301	8
MS29513-004	"O"-Ring	699410-1	1

**Shipped with unit

A shim provides radial adjustment capability in each fixed-mount assembly. The axial center line of the rotating assembly is positioned by adjusting the two fixed mounts relative to the bearing carrier. A shim provides for bearing preload adjustment through the flexibly mounted shoe. Hydrostatic bearing gas is supplied to each fixed-mount bearing shoe by supply lines incorporated into the fixed mount and to the flexibly mounted bearing shoe by a tube assembly.

Two orthogonal capacitance probes, for monitoring shaft position, are provided at each bearing and adjusted by shims.

Three speed pickups are provided on the compressor journal bearing carrier and adjusted by shims.

4.1.3 Gimbal and Thrust Bearing Assembly

A gimbal assembly is provided to give the two thrust bearing stators alignment capability. Hydrostatic bearing gas is supplied individually to each thrust stator through tube assemblies.

A film-thickness capacitance probe and shim on each stator allow the bearing film thicknesses to be monitored during operation.

Attachment of the thrust bearing and gimbal assembly to the main frame is accomplished with the thrust bearing mount assembly into which are incorporated strain gauges for determining the thrust loads.

4.1.4 Compressor Scroll and Diffuser Assembly

The diffuser is attached by screws to the compressor scroll and sealed by an elastomer O-ring. The compressor discharge cooling-flow bleed fitting is located on the scroll discharge from which the cooling flow is ducted to the cooling inlet lines on the unit.

Axial face clearance between the wheel and the scroll is determined by sizing a shim located at the scroll mounting flange. The axial clearance was set at 0.012 inch during the design of the gas generator. From an aerodynamic consideration, a zero clearance would be optimum; however, a clearance of 0.002 inch per inch of wheel diameter can be utilized without serious performance penalty. From a mechanical consideration, it is advantageous to maintain large clearances so that, with rotor radial and axial displacements due to tolerance stackup, thermal growth, and flexible bearing displacements, the rotor does not rub the shroud.

For the acceptance test gas generator, the axial shroud clearance(for the turbine and the compressor) was increased over the design requirements to allow for test experience to be gained on the unit prior to extracting final efficiency figures.

4.1.5 Turbine Scroll and Nozzle Assembly

The turbine scroll and nozzle assembly is an integral one-piece assembly fabricated from an investment casting and several sheet-metal stampings. The axial face clearance between the turbine wheel and the scroll assembly is determined by sizing a shim located adjacent to the scroll mounting flange.

The axial clearance was set at 0.014 inch during the design. However, this clearance was increased for the acceptance test, as discussed above.

4.1.6 Main Frame Assembly

The main frame assembly serves two functions. First and foremost, it provides a framework to which all major components or subassemblies are attached. This assures extreme accuracy in aligning those parts that have critical running clearances, such as the turbine scroll, the compressor scroll, the turbine labyrinth seal, and the compressor labyrinth seal.

Secondly, it contains all of the hydrostatic bearing gas supply lines, the cooling flow ducts and static pressure tap plumbing and provisions for routing and leading out all the electrical instrumentation lines.

4.1.7 Mount Assembly

An assembly is provided for mounting the unit in a vertical position with the turbine end down. The mount assembly consists of a base, a bracket, two flexible mounts, and two flexible mount brackets. The flexibility in the brackets and the two flexible mounts is intended to accommodate thermal expansions that occur during elevated-temperature operation of the unit.

4.2 Component Configurations and Fabrication

The compressor and turbine aerodynamic components utilized in the final gas generator are described in detail in NASA Reports CR-54368 and CR-54367, respectively. The journal gas bearing configuration is described in Section 3.4.4 of this report, and the thrust bearing configuration is described in Section 3.5.1. Figure 49 shows a simplified cross-section of the gas generator with the materials of more pertinent parts noted.

Fabrication of the gas generator components was initiated as the design of the components was finalized. Figures 50 and 51 show the major components after fabrication prior to the acceptance test. Details of some of the major components are shown in Figures 52 through 64, and Figure 65 shows the assembled gas generator.

4.3 Inspection

Inspection of the components of the delivery gas generators and final assembly were in accordance with the quality-assurance program established at the start of the program. Figures 66 and 67 show the Critical Parts Inspection and Serialization record for the turbine and compressor wheels of both delivery units. Figure 68 shows both sides of the Assembly Inspection and Laboratory Traveler for the gas generator, Serial No. P-A, assembled and operated for an acceptance test. The second gas generator, Serial No. P-B, was shipped as "component parts" at the request of the NASA; therefore, an Assembly Inspection and Laboratory Traveler is not available for this unit.

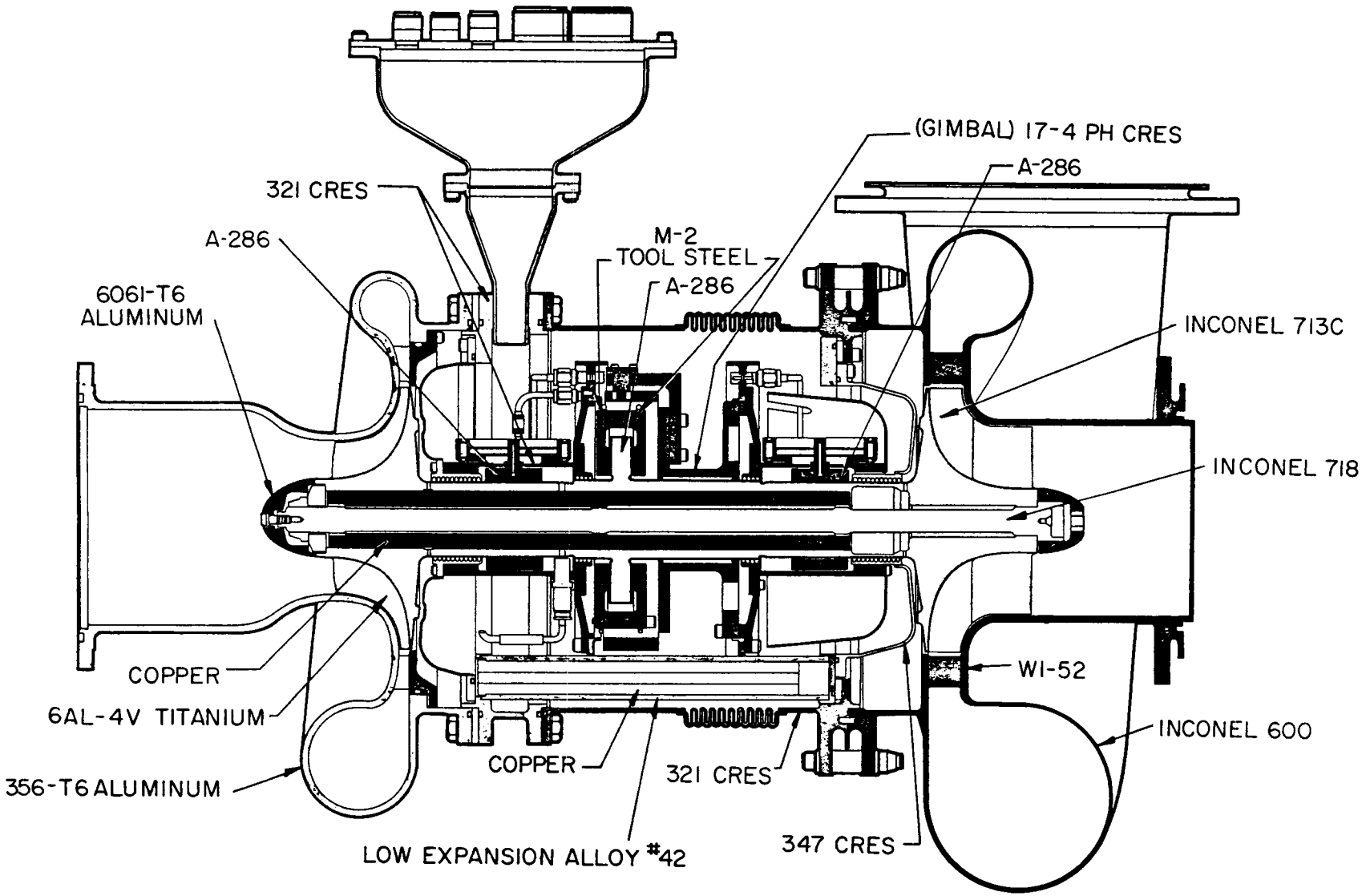

NASA BRAYTON-CYCLE RADIAL GAS GENERATOR
WITH MATERIALS OF PERTINENT PARTS NOTED
FIGURE 49

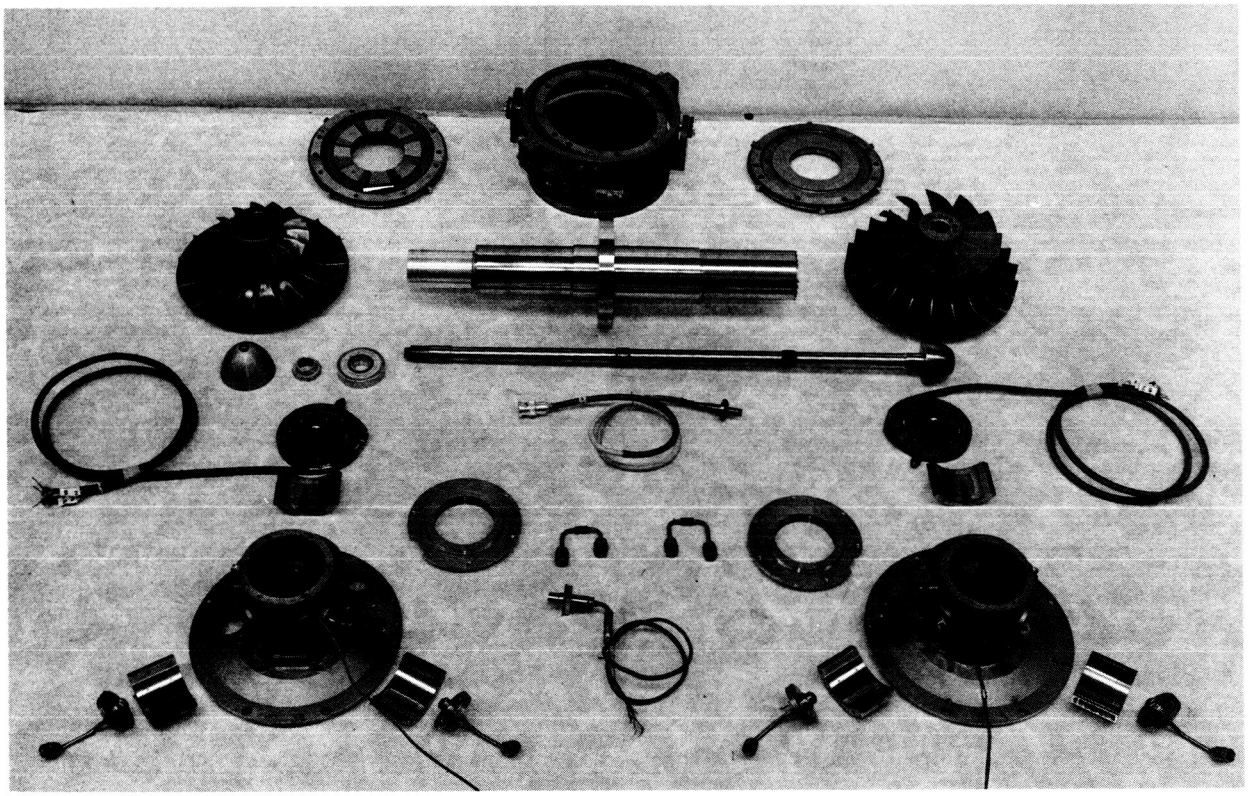

NASA GAS GENERATOR PART 699300
COMPONENT DISASSEMBLY

FIGURE 50

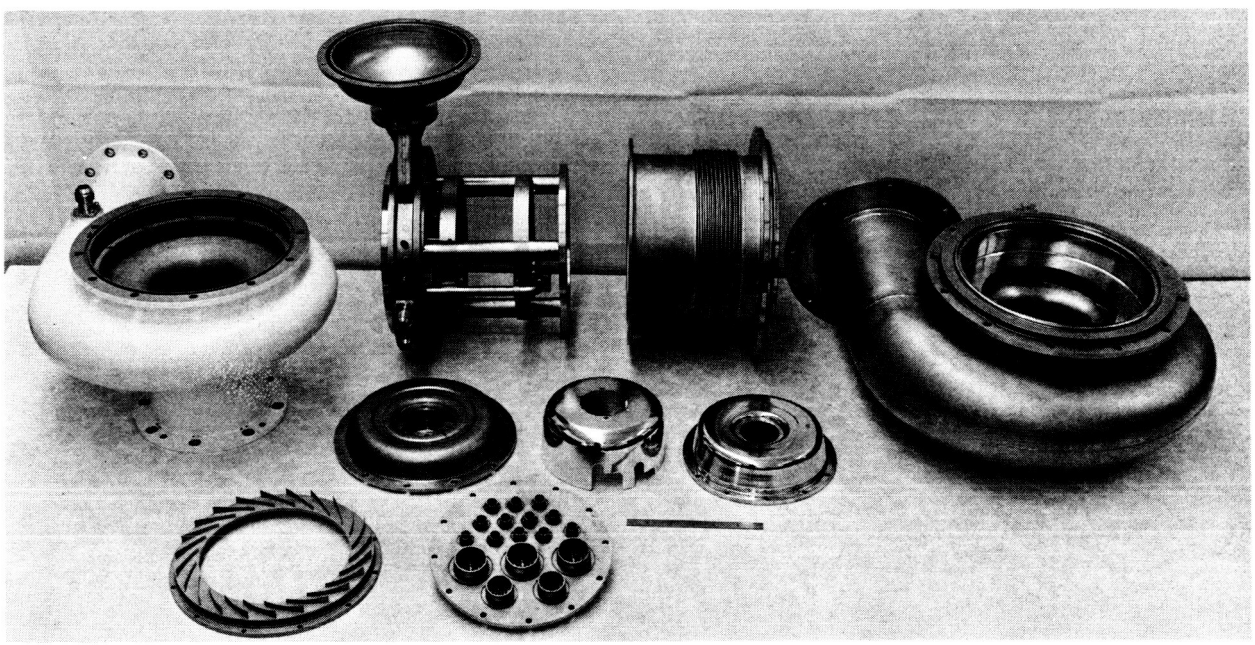

NASA GAS GENERATOR PART 699300
COMPONENT DISASSEMBLY

FIGURE 51

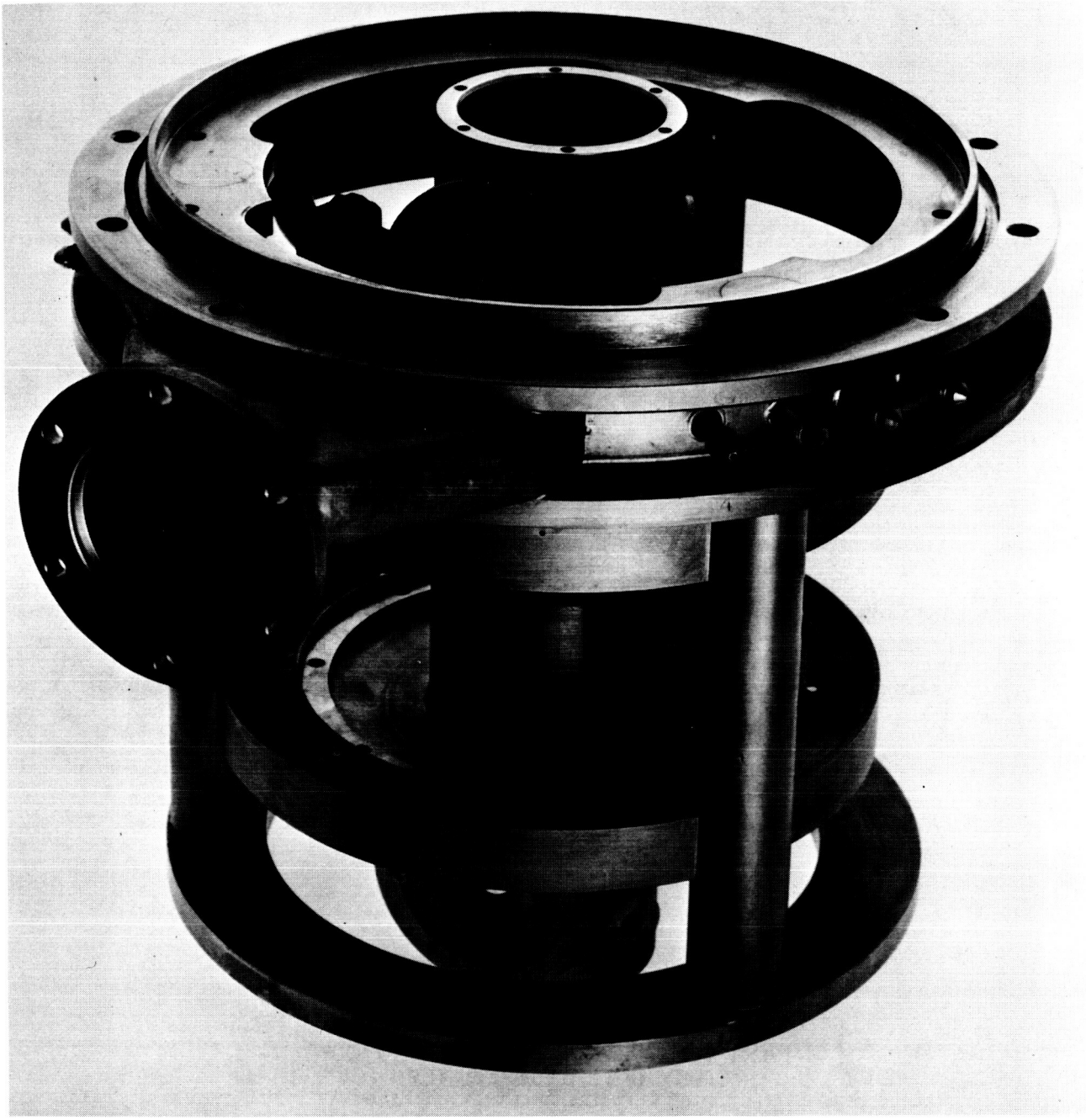

BEARING CARRIER AND FRAME ASSEMBLY

FIGURE 52

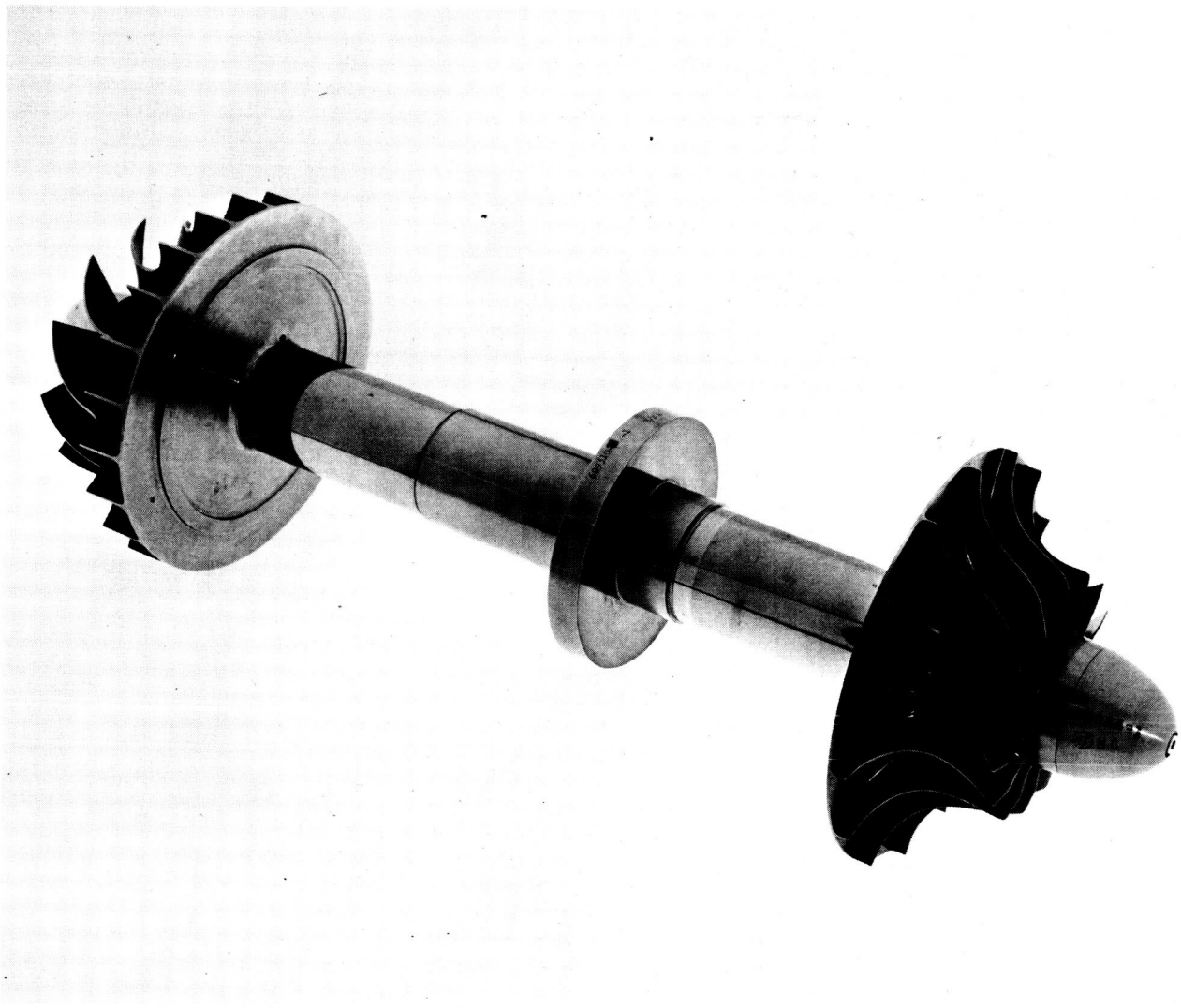

ROTATING COMPONENT GROUP ASSEMBLY

FIGURE 53

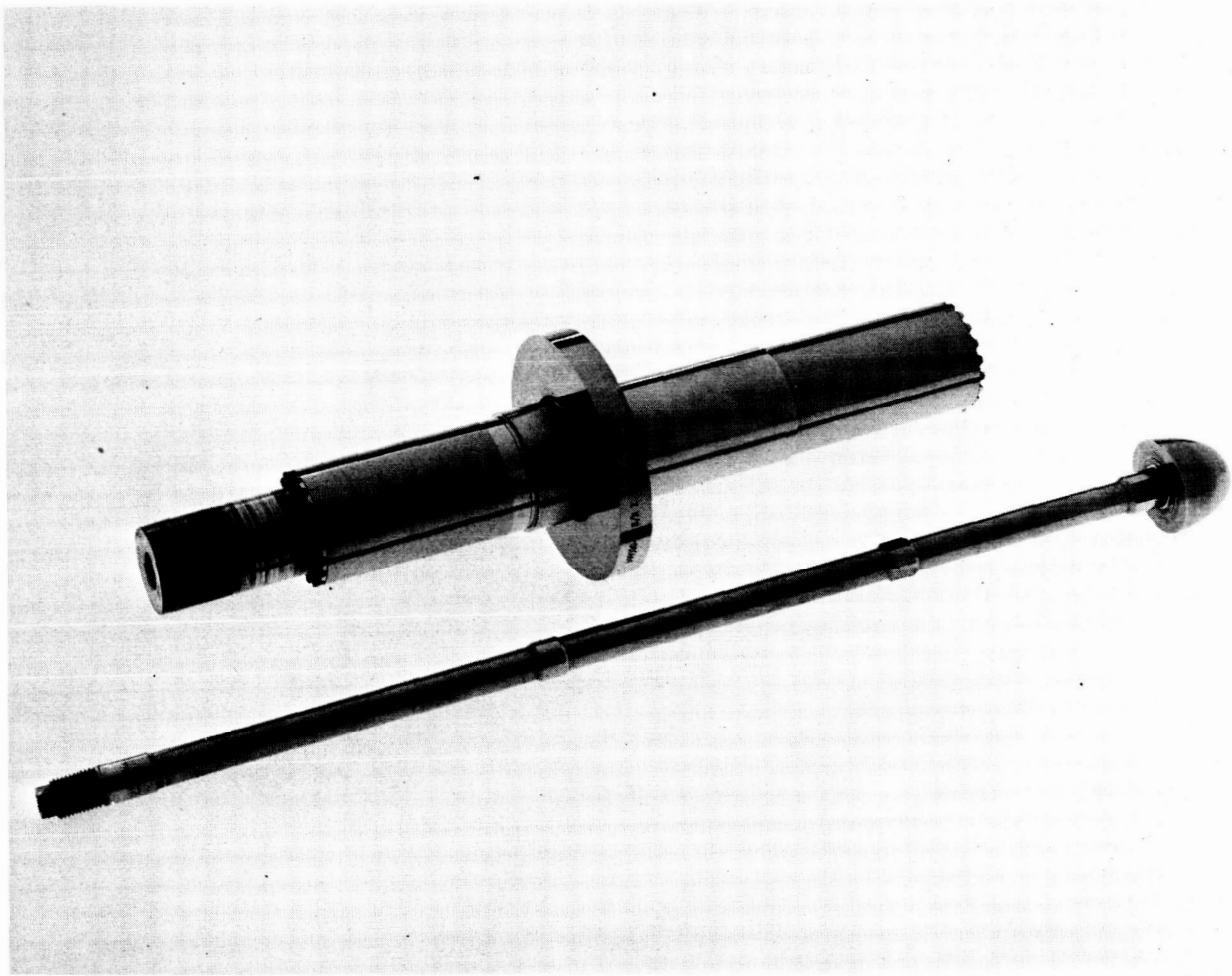

SHAFT ASSEMBLY AND TENSION BOLT

FIGURE 54

TURBINE SCROLL AND NOZZLE ASSEMBLY

FIGURE 55

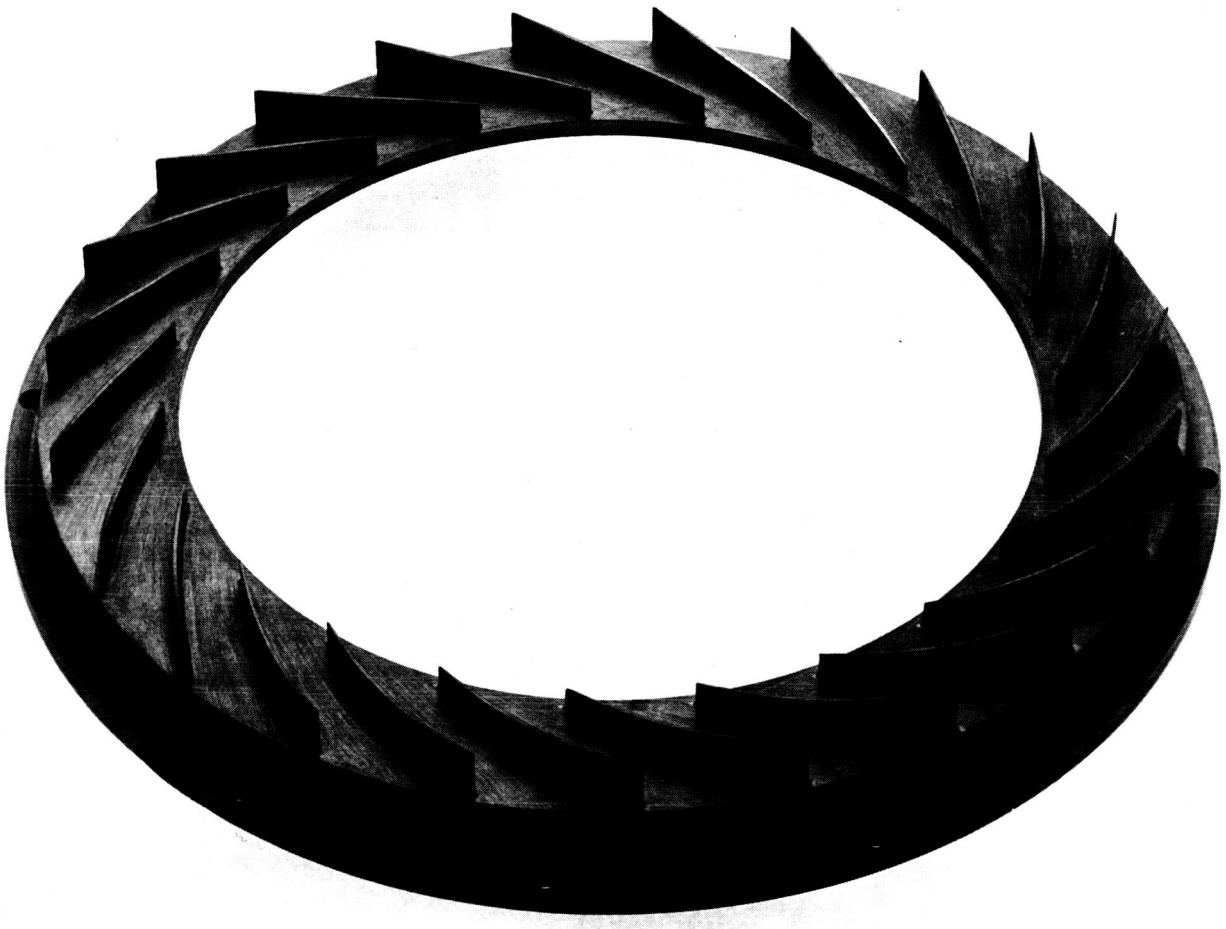

COMPRESSOR DIFFUSER ASSEMBLY

FIGURE 56

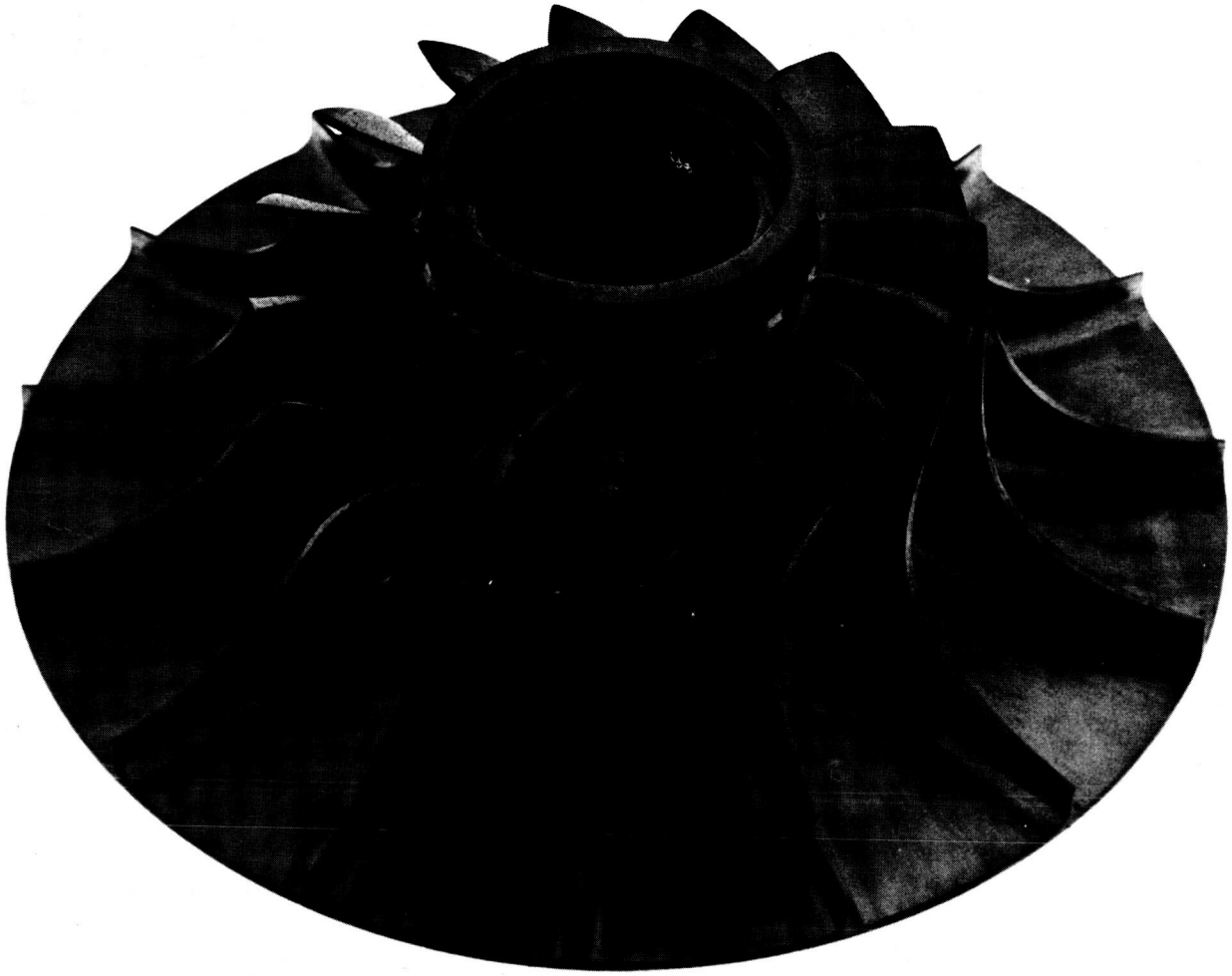

COMPRESSOR IMPELLER

FIGURE 57

COMPRESSOR SCROLL ASSEMBLY

FIGURE 58

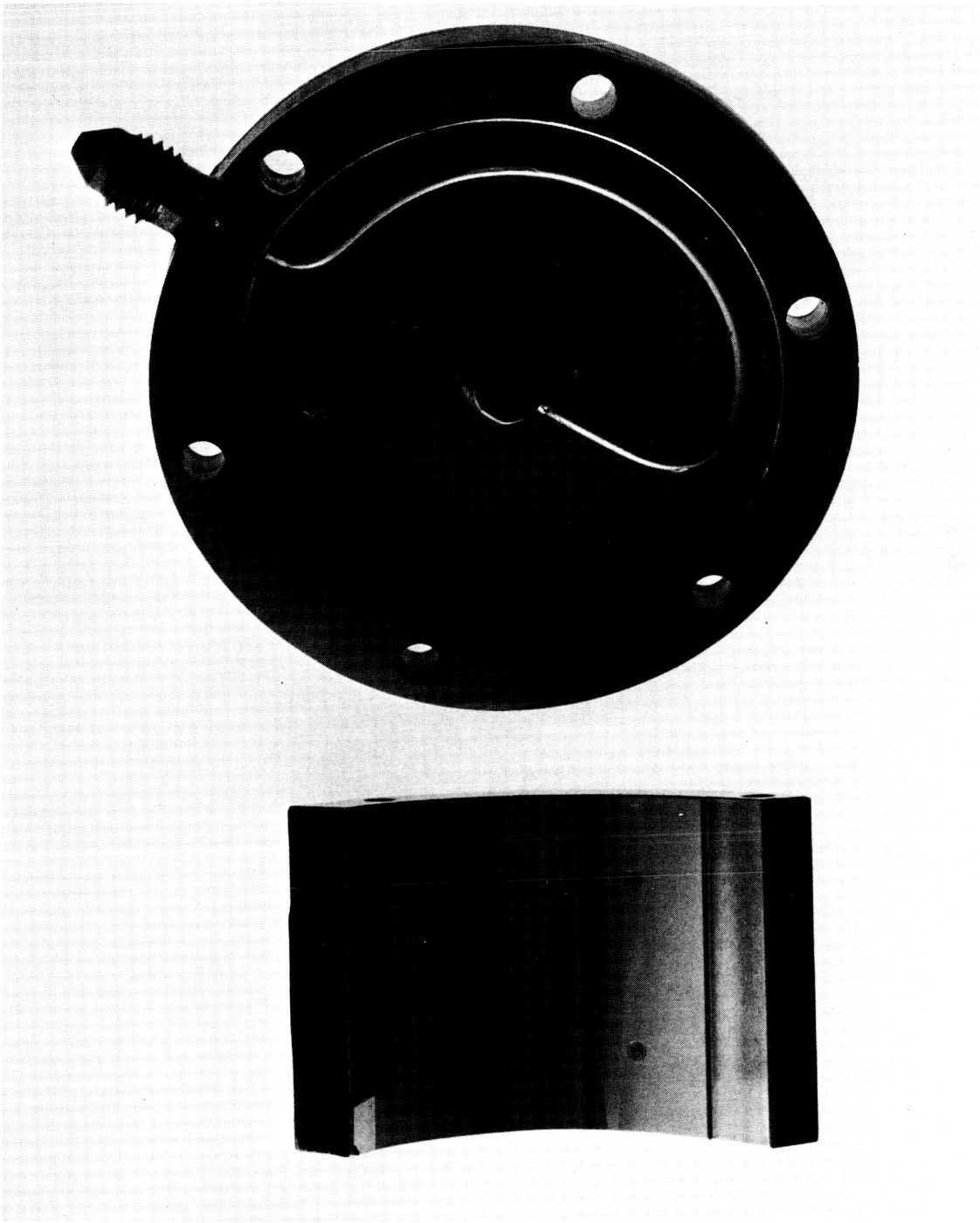

SHOE AND DIAPHRAGM ASSEMBLY, MATCHED SET

FIGURE 59

SHOE AND SOLID MOUNT, MATCHED SET

FIGURE 60

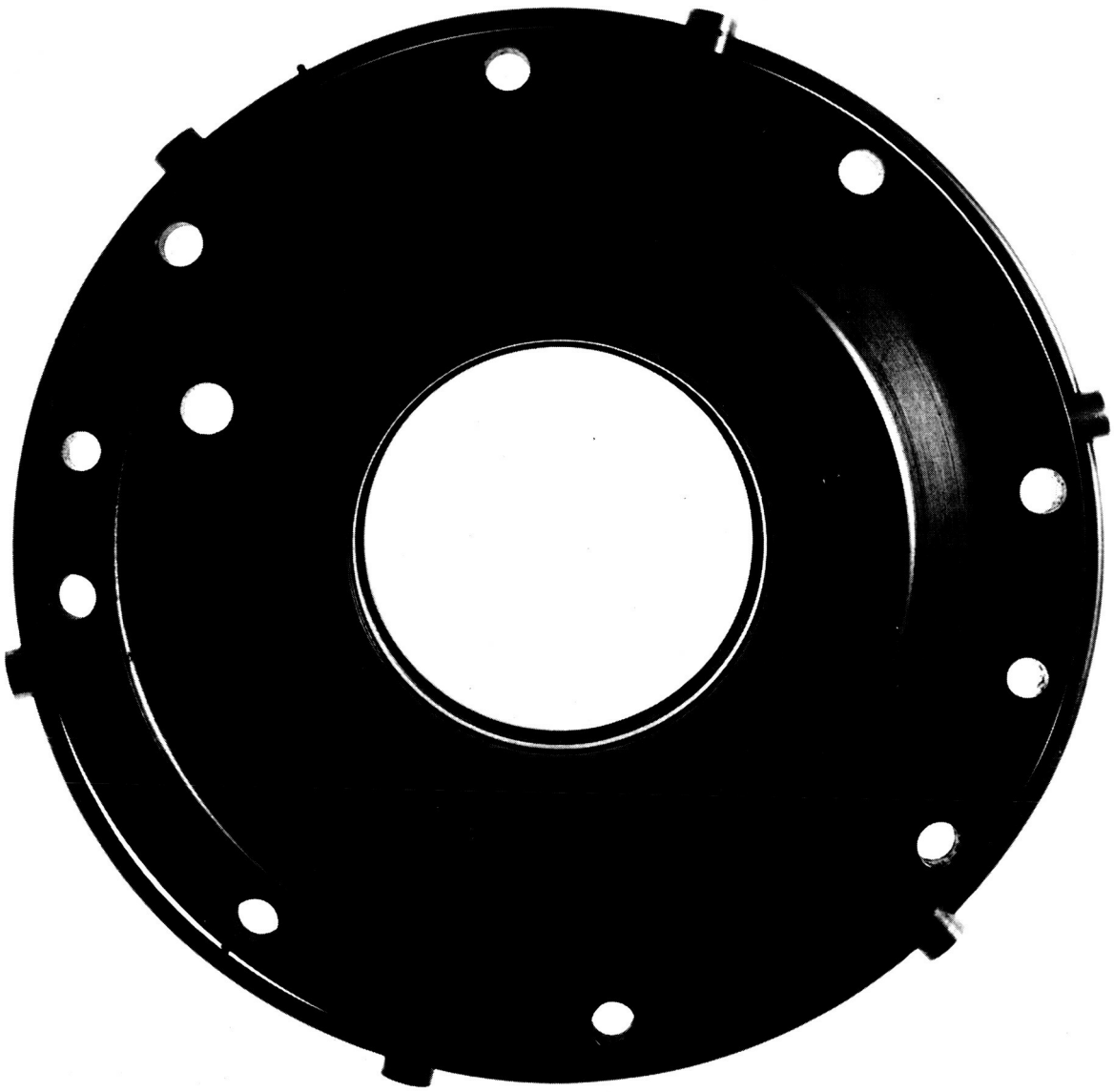

HYDROSTATIC THRUST BEARING STATOR

FIGURE 61

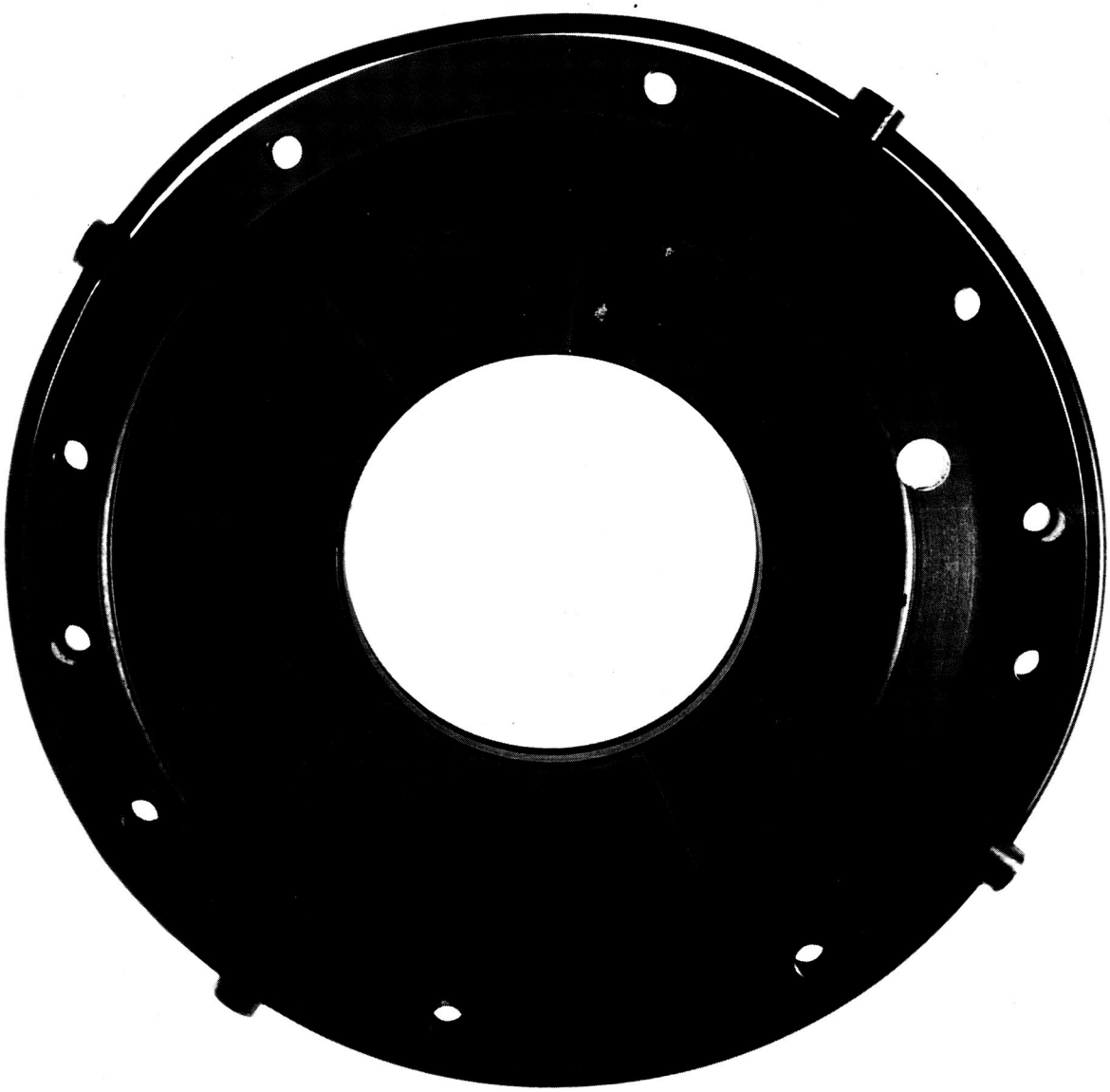

HYDRODYNAMIC THRUST BEARING STATOR

FIGURE 62

TURBINE AND COMPRESSOR BEARING CARRIERS

FIGURE 63

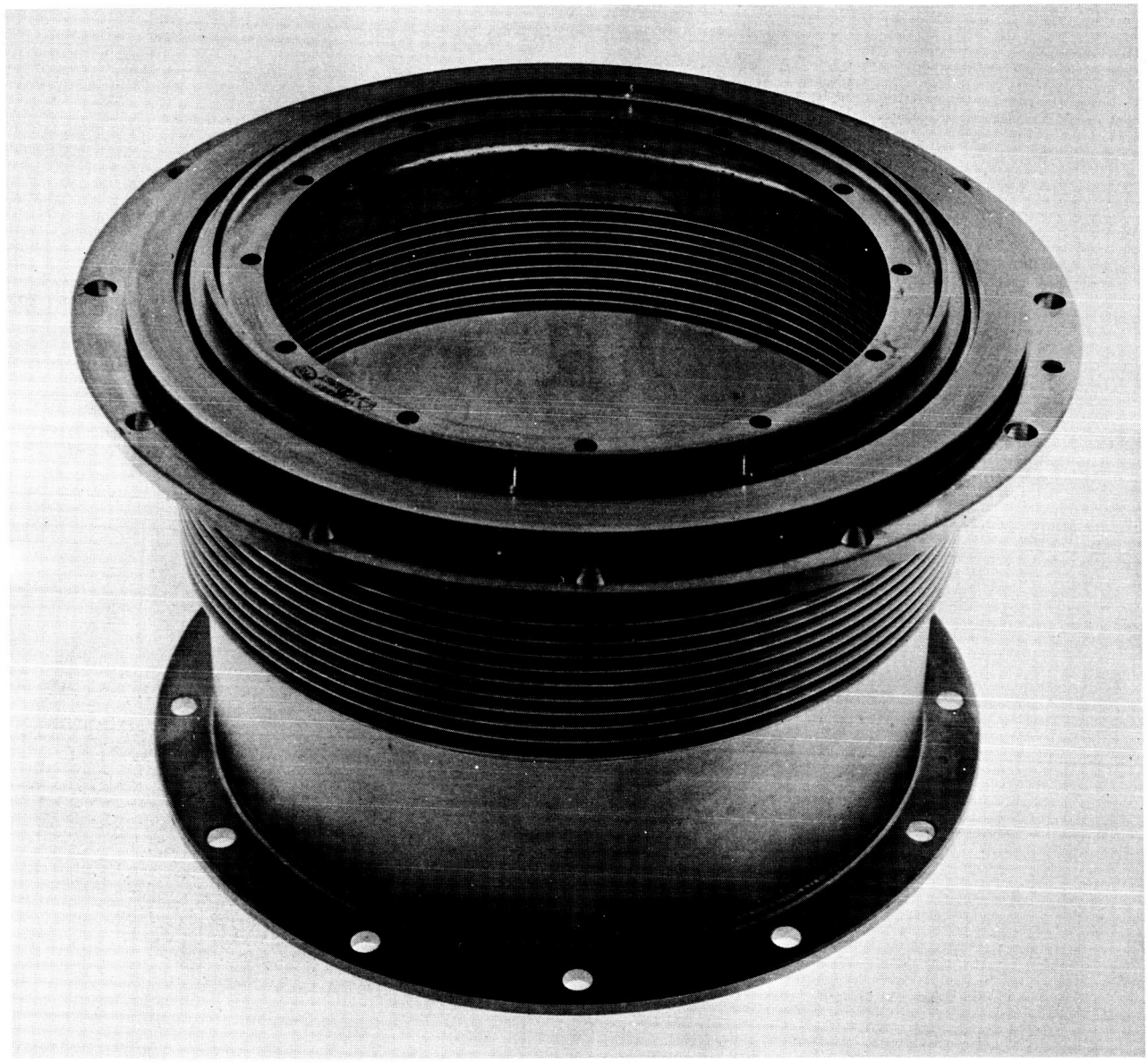

OUTER HOUSING ASSEMBLY

FIGURE 64

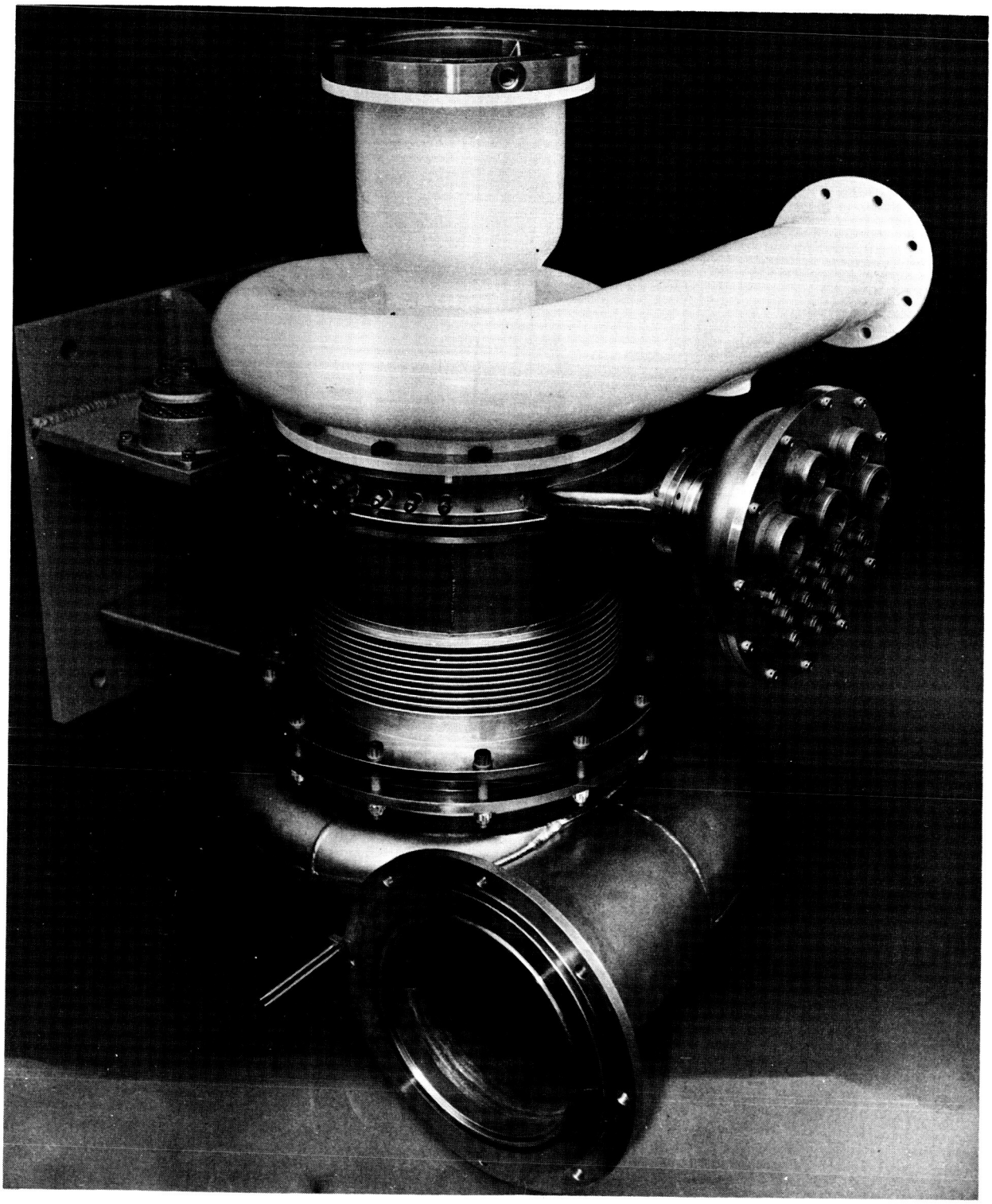

NASA BRAYTON-CYCLE GAS GENERATOR

FIGURE 65

TURBINE WHEEL FOR GAS GENERATOR P-A

FORM P2741-F RESEARCH — CRITICAL PART INSPECTION AND SERIALIZATION RECORD

Forging/Casting No.	C/L	Serial Number	O.S. GROWTH DATA	Machined Part No.	C/L
• 369726-3	B	4X107 (40-203)		• 699303-1	N/C

Oper. Raw Matl.	Date	Insp. Stamp	Oper. Mach. Part	Date	Insp. Stamp	Control Dim/Dia	After G.R.	After O.S.	Z/M After
Dim.	2-22-64		Dim.			6.0195		6.020	
Ultra			Ultra/Mch						
HT/Stress			HT/Stress						
Zyglo/Mag	2-22-64		Zyglo/Mag						
Radiogr.	2-22-64		Pull Test						
Heat No.	RW055		Balance		DAL 4				
2nd H.T.			Overspeed	MAY 1963 14	S				
Remarks:			Green Run						
			2nd O.S.						
			R.R. No. IPT # 134789			Part No. Changes			

MRB Disp. After	Final	Assy	R&O
USE			
RWK			
SCP			
RTV			

ITR NUMBER
~~53469~~ 23382

*Raw Matl. Mfg. Co.

*Mach. Part Mfg. No.

COMPRESSOR WHEEL FOR GAS GENERATOR P-A

CRITICAL PART INSPECTION AND SERIALIZATION RECORD

Forging/Casting No.	C/L	Serial Number	O.S. GROWTH DATA	Machined Part No.	C/L
• 379932-3	J	4L-5545		• 699304-1	"A"

Oper. Raw Matl.	Date	Insp. Stamp	Oper. Mach. Part	Date	Insp. Stamp	Control Dim/Dia	After G.R.	After O.S.	Z/M After
Dim.	10-14-64		Dim.			5.4761		5.4762	
Ultra	10-14-64		Ultra/Mch						
ANN HT/Stress	10-14-64		HT/Stress						
Zyglo/Mag			Zyglo/Mag						
Radiogr.			Pull Test						
Heat No.	D-7403		Balance		BAL 1				
2nd H.T.			Overspeed	JUN 1963 4	S				
Remarks: Duplicate card Original one lost			Green Run						
2.358 2.348 S.D is 2.354 LDA 5/7/65			2nd O.S.						
			R.R. No. 8221			Part No. Changes			

MRB Disp. After	Final	Assy	R&O
USE			
RWK			
SCP			
RTV			

ITR NUMBER
54060

*Raw Matl. Mfg. Co.

*Mach. Part Mfg. No.

FIGURE 66

TURBINE WHEEL FOR GAS GENERATOR P-B

FORM P2741-F — CRITICAL PART INSPECTION AND SERIALIZATION RECORD

Forging/Casting No.	C/L	Serial Number	O.S. GROWTH DATA	Machined Part No.	C/L
• 369726-3	B	4X105 (40-201)		• 699303-1	N/C

Oper. Raw Matl.	Date	Insp. Stamp	Oper. Mach. Part	Date	Insp. Stamp	Control Dim/Dia	After G.R.	After O.S.	Z/M After
Dim.	2-22-64		Dim.			6.0700		6.0702	
Ultra			Ultra/Mch						
HT/Stress			HT/Stress						
Zyglo/Mag	2-22-64		Zyglo/Mag						
Radiogr.	2-22-64		Pull Test						
Heat No. RW055			Balance		BAL 4 BAL 2				
2nd H.T.			Overspeed	MAY 6 1965	S				
Remarks:			Green Run						
			2nd O.S.						
			R.R. No. IIT # 134789			Part No. Changes			

MRB Disp. After	Final	Assy	R&O
USE			
RWK			
SCP			
RTV			

ITR NUMBER	
23382	

*Raw Matl. Mfg. Co.

*Mach. Part Mfg. No.

COMPRESSOR WHEEL FOR GAS GENERATOR P-B

CRITICAL PART INSPECTION AND SERIALIZATION RECORD

Forging/Casting No.	C/L	Serial Number	O.S. GROWTH DATA	Machined Part No.	C/L
• 379932-3	J	4L 5546		• 699304-1	A

Oper. Raw Matl.	Date	Insp. Stamp	Oper. Mach. Part	Date	Insp. Stamp	Control Dim/Dia	After G.R.	After O.S.	Z/M After
Dim.	10-6-64	G 224L	Dim.			5.9910		5.9910	
Ultra	10-6-64	G 224	Ultra/Mch						
HT/Stress ANN	10-6-64	G CC-4	HT/Stress						
Zyglo/Mag			Zyglo/Mag						S
Radiogr.			Pull Test						
Heat No. D-7403			Balance		BAL 4				
2nd H.T.			Overspeed	JUN 4 1965	S				
Remarks:			Green Run						
2.358 2-348 S.D.'s 2.3535			2nd O.S.						
			R.R. No. 8221			Part No. Changes			

MRB Disp. After	Final	Assy	R&O
USE			
RWK			
SCP			
RTV			

ITR NUMBER	
54061-50.	

*Raw Matl. Mfg. Co.

*Mach. Part Mfg. No.

FIGURE 67

AiResearch Manufacturing Company of Arizona — TRAVELER NO. ORIG.

PX 1372-2 — SUB UNIT — ASSEMBLY INSPECTION TRAVELER

OUTLINE	MODEL	SERIAL NUMBER
699300-1	CCGG 20-1	P-A

DESCRIPTION	CUSTOMER	SERIES	C/L
GAS GENERATOR	NASA		

START DATE	CURE DATE	RELEASE OR R. O. NUMBER
9-2-65	-	NAS3-2778 3409-27136-14-1000

PRODUCTION ☐ OVERHAUL ☐ REPAIR ☐ MILITARY ☐ COMMERCIAL ☐ R&D ☒

M. O. T. NUMBER	OPER NO	ASSY SIG.	RECORD DIMENSIONS	INSP STAMP	M. O. T. NUMBER	OPER NO	ASSY SIG.	RECORD DIMENSIONS	INSP STAMP
COMP PRELOAD	5		5.4/14.5		COMP CLEAR. ANGEL	39		.0208	
TURB PRELOAD	5		6.0/13.2		TURB CLEAR. ANGEL	39		.0155	
COMP SEAL CONCENT.	27		.0019						
TURB SEAL CONCENT.	28		.0018						
COMP. SMIN	39		.1358						
TURB SMIN	39		.1305						
H/D FILM @ 4"	TEST		.00054						
H/S FILM @ 6"	TEST		.00088						
H/S FILM @ 16"	TEST		.00165						

PART NUMBER	MODEL	SERIAL NO.		INSP
699303-1		4X-107		
699304-1		4L-5545		
SHIPPED	9-15-65			
ENGINEERING				

DATE	ASSEMBLY SIGNATURE	INSPECTION SIGNATURE	CUSTOMER SIGNATURE
8 Sept 65	J. Philip Spencer		

PX 1372-1 — S/N

AiResearch Manufacturing Company of Arizona — TRAVELER NO.

LABORATORY TRAVELER

PARTS REPLACED IN LABORATORY

PART NO.	SERIAL NO.	REASON REPLACED

LABORATORY REJECTION REASONS

LAB SIG.

ENGINEERING REWORK RECOMENDATIONS

ENG. SIG.

ASSEMBLY REWORK (LIST ALL PARTS EXCEPT AN 8 STD LINE PARTS)

ASSY. SIG.

DEVIATION

CUSTOMER — T. I.

	SINCE O'HAUL	TOTAL
STARTS		
HOURS		5HR 35 MIN
SAFETY WIRED		

UNIT PRESERVED: FUEL | OIL

T. I. NO.

OIL CONSUMPTION GRAMS

WT. FLOW

ACCEL. TIME SECS

ACCEPTED	REJECTED	DATE
✓	~~9-7-65~~	9-7-65

LAB SIGNATURE Frank C. Pender (QC2)

ASSEMBLY INSPECTION AND LABORATORY TRAVELER, GAS GENERATOR
FIGURE 68

As can be seen from Figure 68, the first gas generator was run for a total of 5.58 hours during the acceptance test. This test is discussed in Section 5.0.

5.0 ACCEPTANCE TEST

5.1 Test Installation

Operation of the gas generator for the acceptance test consisted of running the unit with plant air supplied to the turbine and with the compressor open to a clean air supply. Bearing and cavity pressurization was accomplished with filtered argon. Figure 6 schematically shows the acceptance test gas generator installation.

With the completion of the thrust bearing/gimbal assembly integration tests utilizing the gas generator frame test rig (see Section 3.5.2.2), the test frame rig was rebuilt with a set of wheels and scrolls to (a) determine the aerodynamic effects of the wheels upon the bearing system when subjected to cold-acceptance-test conditions and (b) check out the cold-acceptance-test installation prior to acceptance testing the delivery gas generator. The initial test-cell installation is shown in Figures 70 and 71. Other than an initial rotating-group balance problem in the unit, the main problem was one of cell piping modifications in order to eliminate extraneous random vibrations fed into the unit by pneumatic ducting forces. A total of 15 hours of test time was logged in the turbine test cell without incident. At the conclusion of these tests, it was considered that the facility was suitable for the cold acceptance test of the NASA delivery gas generator No. 1. Of significant importance was the fact that the behavior of the bearing system, as established in the frame test-rig configuration with dummy rotating masses, was not in any way disturbed by the aerodynamic effect of the added wheels and scrolls.

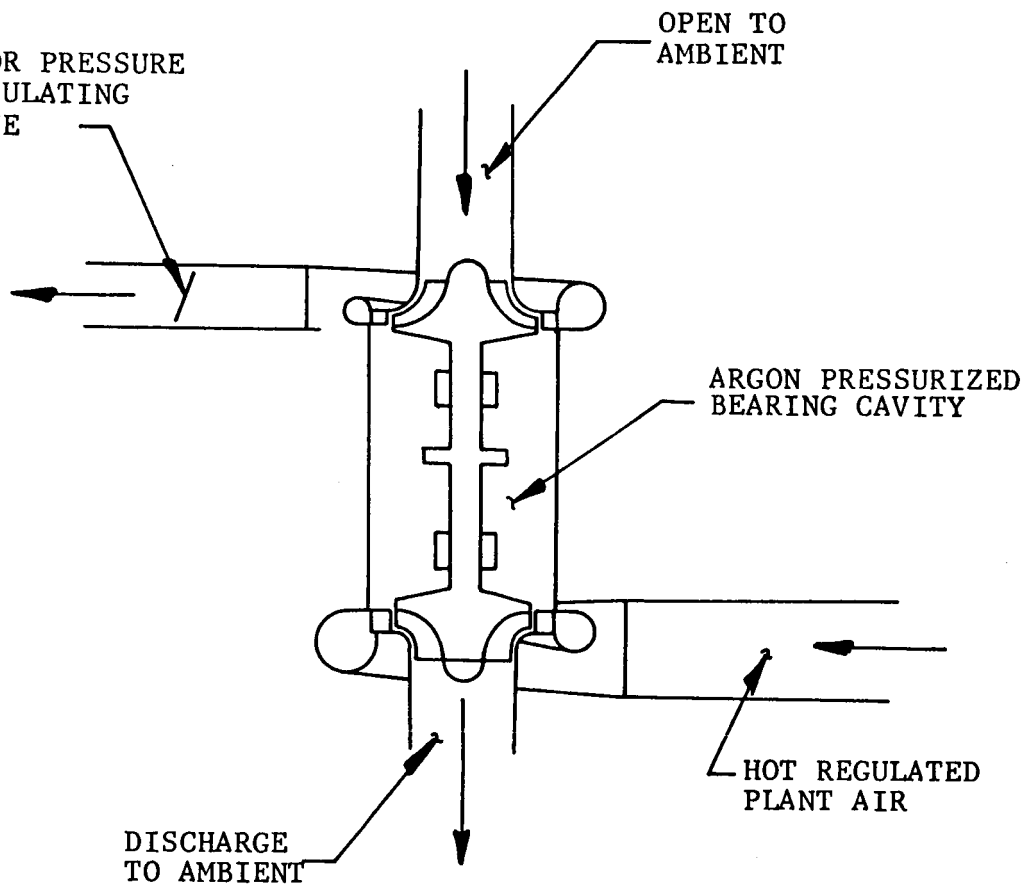

GAS GENERATOR ACCEPTANCE TEST INSTALLATION SCHEMATIC

FIGURE 69

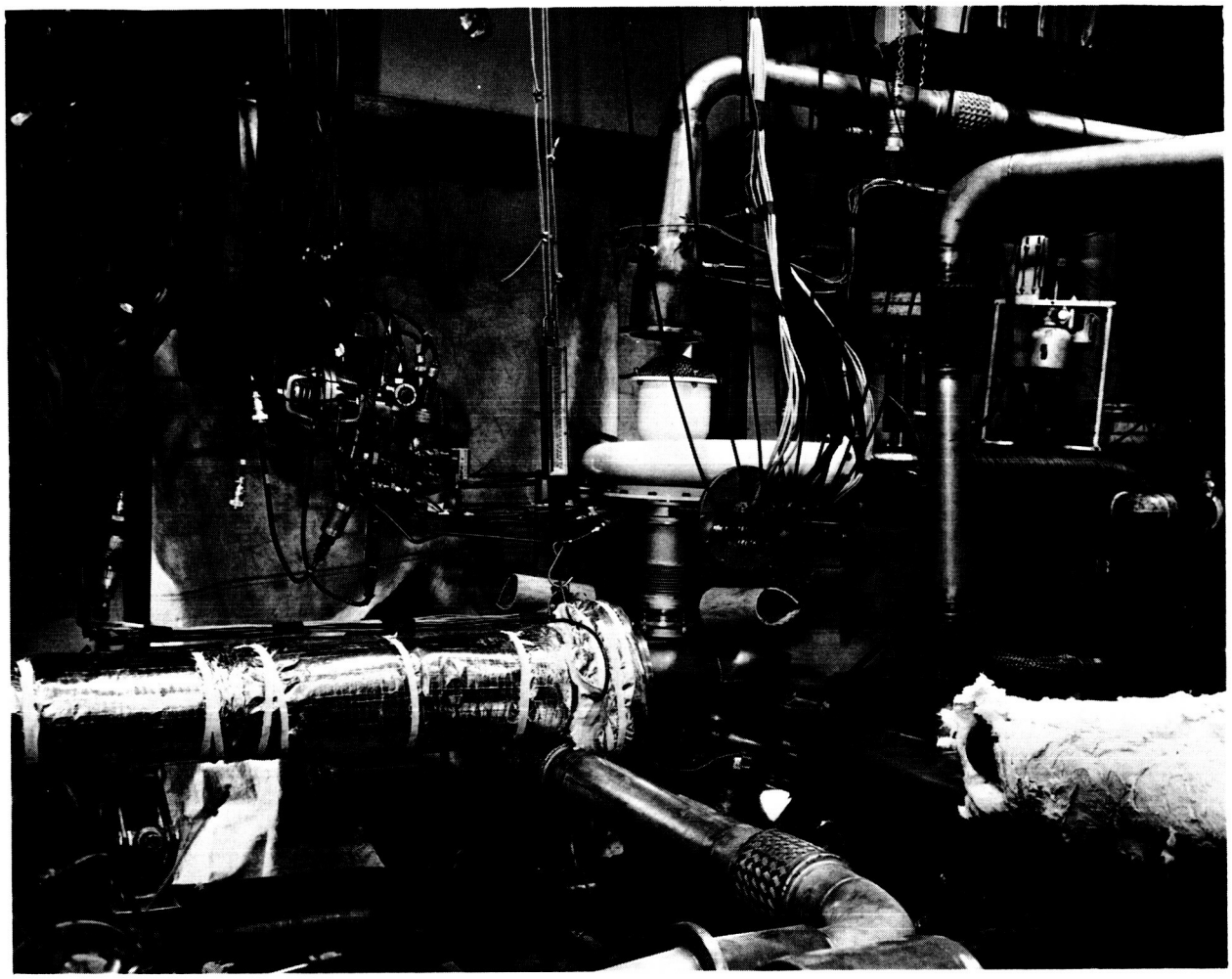

ACCEPTANCE TEST MOCK-UP OF GAS GENERATOR
INSTALLED IN TEST CELL

FIGURE 70

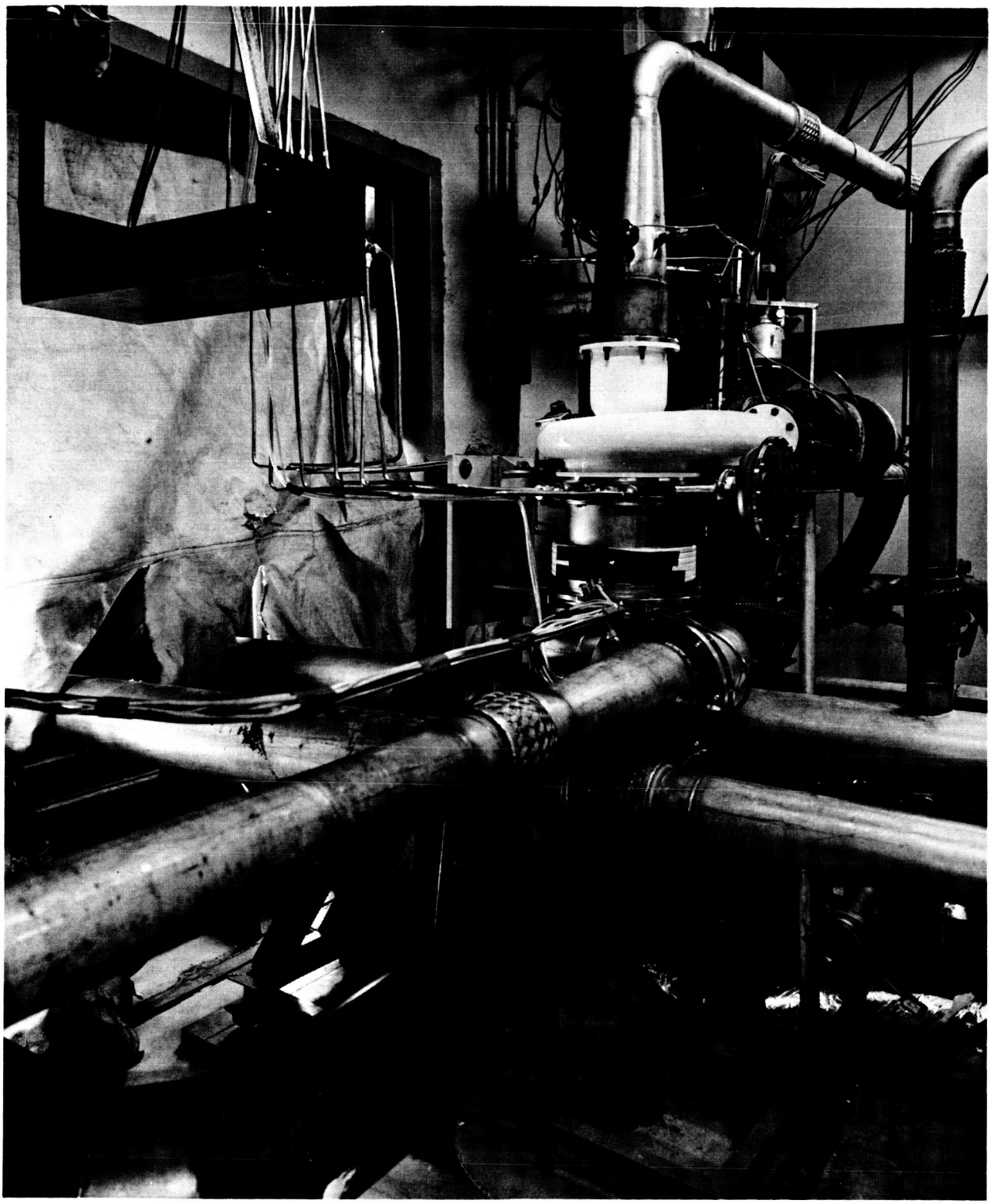

ACCEPTANCE TEST MOCK-UP OF GAS GENERATOR
INSTALLED IN TEST CELL

FIGURE 71.

Testing of the gas generator in the turbine test cell indicated that the net aerodynamic thrust of the two wheels was in the reverse-thrust direction and that at 20,000 rpm the addition of temperature to the turbine inlet air in the range of 450 to 500°F allowed speed to be increased to 100 percent without subjecting the unit to excessive reverse-thrust loads. At 100 percent design speed, the resultant thrust load was of the order of 20 pounds in the reverse direction, which indicated that a balance of aerodynamic forces had been achieved. Test-plan requirements for the acceptance test were thus established.

5.2 Assembly of Gas Generator, First Shipping Unit

The first shipping unit, Serial No. P-A, Outline 699300, was assembled, and the assembly data on this unit was collected and documented in AiResearch Report APS-5174-R and forwarded to the NASA when the unit was shipped. The data relevant to the assembly is as follows:

Shaft-to-shoe geometric clearances.

Bearing mount shimming log, including bearing preload settings, axial center shift, and seal concentricities.

Turbine and compressor axial shroud clearance data.

Capacitance probe and speed pickup shimming log.

Capacitance probe calibrations (6)

Gas generator thrust-mount load calibration.

Compressor and turbine journal bearing flexible-mount diaphragm calibrations (2).

Instrumentation pin call-out data.

Instrumentation location schematic

For safety considerations, the axial shroud clearances were increased over the design requirements to allow for test experience to be gained on the unit prior to extracting final efficiency figures. The data presented will allow the NASA to remove material from the shims in successive stages in achieving the end objective during closed-loop testing.

5.3 Initial Test and Calibration of First Shipping Unit

The shipping unit, after basic buildup, was equipped with the dummy masses and tie-bolt from the frame test rig. The rotating group was then subjected to gas bearing evaluation tests in order to determine unit performance and to check out the instrumentation, particularly the proximity probes and certain specific thermocouples. Checkout included operation of the bearing journals and thrust faces hydrostatically, with the reverse thrust bearing being calibrated for film thickness versus load. The normal thrust bearing was also calibrated in the same manner when in the hydrostatic regime. A single-point calibration was also established when the normal thrust bearing was run hydrodynamically. These calibrations have been reported in AiResearch Report APS-5174-R. The journal bearings were also operated in the hydrostatic regime. Additional thrust-transfer checks were performed in both directions with hydrostatic operation, between normal and reverse-thrust faces at 35,000, 30,000, 25,000, and 20,000 rpm. Overspeed was also checked in the hydrostatic mode to 42,000 rpm. All of the tests conducted in the bearing test cell were performed without any problems occurring. The unit proved to have even better performance than had been demonstrated previously on the company-sponsored test rig, particularly with respect to shaft balance and thrust stator face operating clearances.

5.4 Acceptance Test of First Shipping Unit

The test-plan procedure had been adequately established by the prior test series undertaken with the modified frame test rig. The installation configuration in the test cell was similar to Figures 70 and 71. Figures 72 and 73 show the test instrumentation setup of the Wayne-Kerr proximity meters in relation to the test unit and the visual recording data outputs, respectively.

After installation, the unit was subjected to a test run to full speed, hydrostatically, to determine that the rotational balance of the shaft components was acceptable. The balance was proven to be satisfactory.

The final instrumentation hook-up for recording purposes was arranged as follows:

Tape Recorder:	Seven channels, to record the four orthogonal and two thrust probes, with speed and voice combined on one channel.
Oscillograph Recorder:	20 channels, to record 16 thermocouples, 3 strain gauges, and speed.
Visual Readout:	The remaining thermocouples chosen for safety reasons. Shaft and thrust surface proximity probes, speed, temperature, and strain-gauge output on the thrust mount through an X-Y plotter.

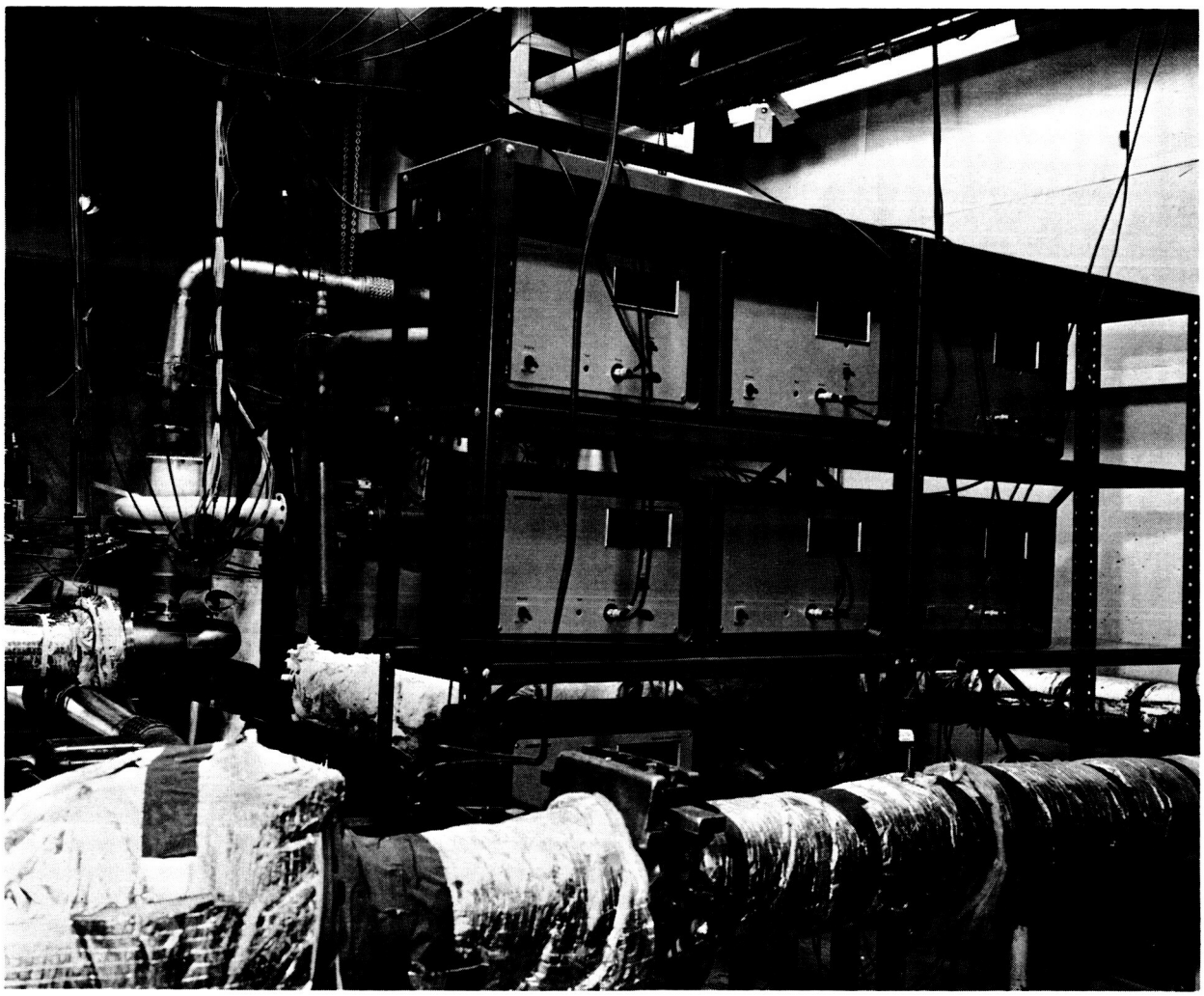

WAYNE-KERR PROXIMITY METERS
NASA GAS GENERATOR ACCEPTANCE TEST

FIGURE 72

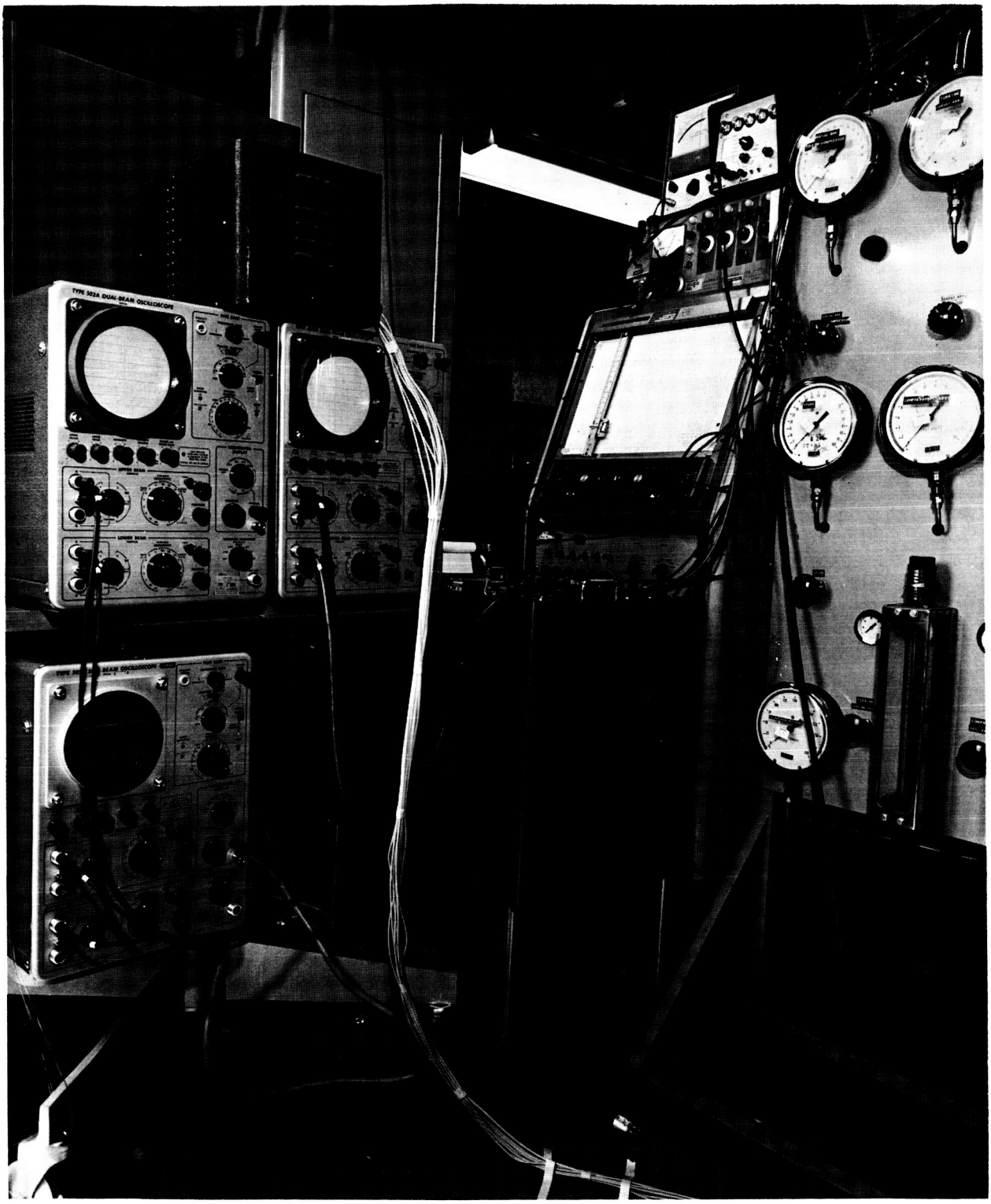

GAS BEARING CONTROL PANEL AND INSTRUMENTATION
NASA GAS GENERATOR ACCEPTANCE TEST

FIGURE 73

The acceptance test was run in accordance with the test plan and successfully demonstrated the requirements of the contract. This test was witnessed by the NASA representatives, and the unit was accepted.

Although performance demonstration was not required, measurements were required to establish steady-state operation and control during tests. Figure 74 shows the test-cell log sheet for the acceptance test on the Serial No. P-A gas generator, and Figures 75 and 76 show the data log sheets for the acceptance test. Figure 77 shows the tape and oscillograph log sheets.

QUALIFICATION TEST LOG

E.W.O. No. 2409-27136-16-1006	Date 9-9-65	Test Cell or Station No. D-107
Assembly No. 699301	Model No. CCGG-20-1	Unit Serial No. P-A
Development Engineer B HEATH	Technician BENDER	Grp. Ldr. TIMMER
Test Type DEV.	Test Schedule APS 5173-R	Modification —

TIME START	TIME STOP	Event	O.C.
		DAYS; CALIBRATED ALL INSTRUMENTATION	
		RUN #1 TAPE #800 (C-1400)	
10:20		TOOK STATIC DATA COLL. AA	
			G2
1025		BEGIN RUN, ACCEL. TO 20000 RPM & INCR TURB. INLET TO 400°F	
1030		ACCEL. TO 38,500 RPM	
1035		DATA; COLL. BB	
10.42		REMOVED TOWER, PRG. H.S. ARGON & INCR. TURB. INLET TO 475°F	G2
1045		DATA COLL. CC	
11:15		DATA COLL. DD	
11:45		DATA COLL. EE	
12:15		DATA COLL. FF	
12:45		DATA COLL GG	
1:3:15		DATA COLL HH	
13:45		DATA COLL II	
14:15		DATA COLL JJ	
1445		DATA COLL. KK	
15:15		DATA COLL LL	
1545		DATA COLL MM	
		RETURNED HYDROSTATIC ARGON TO TOWER. RLES (60 PSIG)	
15:50		REDUCED SPD TO 20000 RPM & TOOK DATA (TAPE) EVERY TWO MIN. FOR TEN MIN.	
15:54		INCR. COOLING ARGON FLOW TO 60 SCFM ON TURB & COMP.	G2
	1600	SHUT DOWN	
		REMOVED UNIT FROM CELL	

SUMMARY: Total Running Time 5 hrs. 35 min. Ref. Data Page
Total Manual Starts 1
Total Automatic Starts —
Engineering K B Bender

ORIGINAL

FIGURE 74

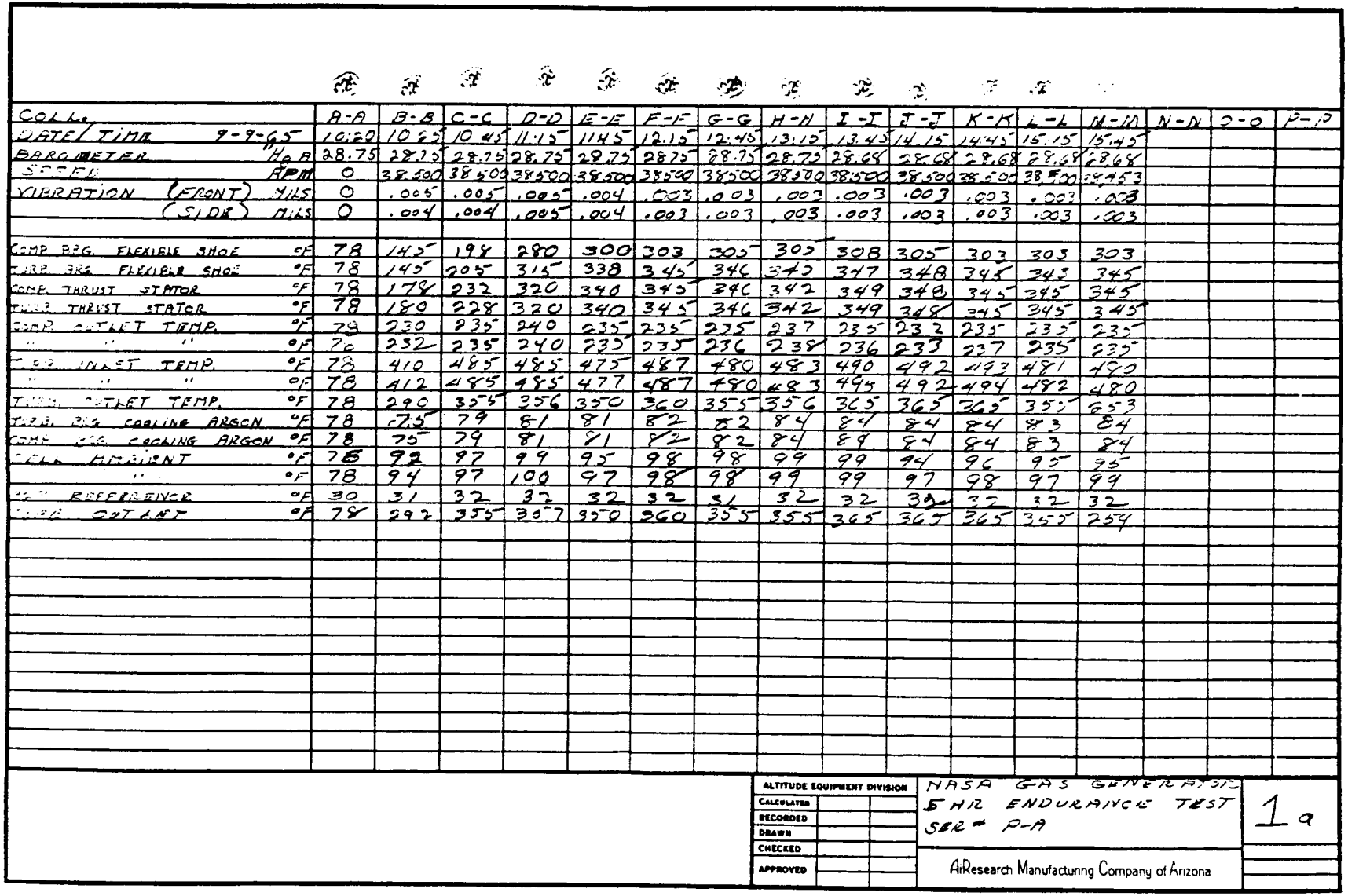

CALL		A-A	B-B	C-C	D-D	E-E	F-F	G-G	H-H	I-I	J-J	K-K	L-L	M-M	N-N	O-O	P-P
DATE/TIME 9-9-65		10:20	10 25	10 45	11:15	11:45	12:15	12:45	13:15	13:45	14:15	14:45	15:15	15:45			
BAROMETER	H_g A	28.75	28.75	28.75	28.75	28.75	28.75	28.75	28.75	28.68	28.68	28.68	28.68	28.68			
SPEED	RPM	0	38,500	38,500	38,500	38,500	38,500	38,500	38,500	38,500	38,500	38,500	38,500	38,453			
VIBRATION (FRONT)	MILS	0	.005	.005	.005	.004	.003	.003	.003	.003	.003	.003	.003	.003			
(SIDE)	MILS	0	.004	.004	.005	.004	.003	.003	.003	.003	.003	.003	.003	.003			
COMP BRG. FLEXIBLE SHOE	°F	78	142	198	280	300	303	305	307	308	305	303	303	303			
TURB BRG FLEXIBLE SHOE	°F	78	145	205	315	338	345	346	342	347	348	345	343	345			
COMP THRUST STATOR	°F	78	178	232	320	340	345	346	342	349	348	345	345	345			
TURB THRUST STATOR	°F	78	180	228	320	340	345	346	342	349	348	345	345	345			
COMP OUTLET TEMP.	°F	78	230	235	240	235	235	235	237	235	232	235	235	235			
" " "	°F	76	232	235	240	235	235	236	238	236	233	237	235	232			
TURB INLET TEMP.	°F	78	410	485	485	475	487	480	483	490	492	493	481	480			
" " "	°F	78	412	485	485	477	487	480	483	495	492	494	482	480			
TURB OUTLET TEMP.	°F	78	290	355	356	350	360	355	356	365	365	362	353	353			
TURB BRG COOLING ARGON	°F	78	75	79	81	81	82	82	84	84	84	84	83	84			
COMP BRG COOLING ARGON	°F	78	75	79	81	81	82	82	84	84	84	84	83	84			
CELL AMBIENT	°F	78	92	97	99	95	98	98	99	99	94	96	95	95			
" "	°F	78	94	97	100	97	98	98	99	99	97	98	97	99			
[illegible] REFERENCE	°F	30	31	32	32	32	32	31	32	32	32	32	32	32			
TURB OUTLET	°F	78	292	355	357	350	360	355	355	365	365	365	355	354			

ALTITUDE EQUIPMENT DIVISION		
CALCULATED		
RECORDED		
DRAWN		
CHECKED		
APPROVED		

NASA GAS GENERATOR
5 HR ENDURANCE TEST
SER # P-A

AiResearch Manufacturing Company of Arizona

1a

FIGURE 75

NASA GAS GENERATOR ACCEPTANCE TEST LOG SHEET

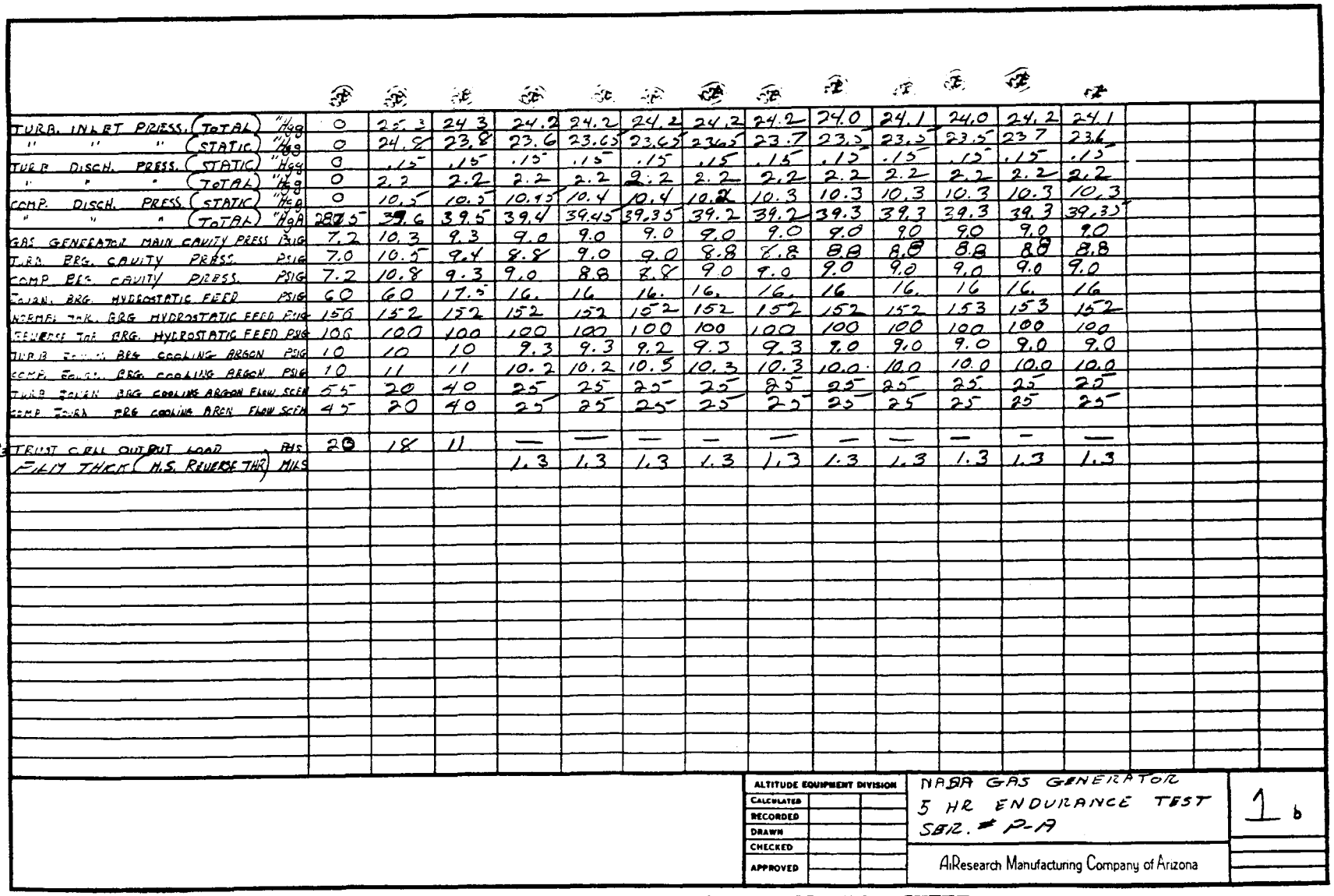

TURB. INLET PRESS. (TOTAL) "Hg	0	25.3	24.3	24.2	24.2	24.2	24.2	24.2	24.0	24.1	24.0	24.2	24.1
" " " (STATIC) "Hg	0	24.8	23.8	23.6	23.65	23.65	23.65	23.7	23.5	23.5	23.5	23.7	23.6
TURB DISCH. PRESS. (STATIC) "Hg	0	.15	.15	.15	.15	.15	.15	.15	.12	.15	.12	.15	.15
" " " (TOTAL) "Hg	0	2.2	2.2	2.2	2.2	2.2	2.2	2.2	2.2	2.2	2.2	2.2	2.2
COMP. DISCH. PRESS. (STATIC) "Hg	0	10.5	10.5	10.45	10.4	10.4	10.2	10.3	10.3	10.3	10.3	10.3	10.3
" " " (TOTAL) "Hg	28.5	39.6	39.5	39.4	39.45	39.35	39.2	39.2	39.3	39.3	39.3	39.3	39.35
GAS GENERATOR MAIN CAVITY PRESS PSIG	7.2	10.3	9.3	9.0	9.0	9.0	9.0	9.0	9.0	9.0	9.0	9.0	9.0
TURB. BRG. CAVITY PRESS. PSIG	7.0	10.5	9.4	8.8	9.0	9.0	8.8	8.8	8.8	8.8	8.8	8.8	8.8
COMP. BRG. CAVITY PRESS. PSIG	7.2	10.8	9.3	9.0	8.8	8.8	9.0	9.0	9.0	9.0	9.0	9.0	9.0
TURBN. BRG. HYDROSTATIC FEED PSIG	60	60	17.5	16.	16	16.	16.	16.	16	16.	16	16	16
NORMAL TURB. BRG HYDROSTATIC FEED PSIG	156	152	152	152	152	152	152	152	152	152	153	153	152
REVERSE TURB. BRG. HYDROSTATIC FEED PSIG	106	100	100	100	100	100	100	100	100	100	100	100	100
TURB TURBN. BRG COOLING ARGON PSIG	10	10	10	9.3	9.3	9.2	9.3	9.3	9.0	9.0	9.0	9.0	9.0
COMP. TURBN. BRG. COOLING ARGON PSIG	10	11	11	10.2	10.2	10.5	10.3	10.3	10.0	10.0	10.0	10.0	10.0
TURB TURBN BRG COOLING ARGON FLOW SCFM	55	20	40	25	25	25	25	25	25	25	25	25	25
COMP TURBN BRG COOLING ARGN FLOW SCFM	45	20	40	25	25	25	25	25	25	25	25	25	25
THRUST CELL OUTPUT LOAD LBS	20	18	11	—	—	—	—	—	—	—	—	—	—
FILM THKN (M.S. REVERSE THR) MILS				1.3	1.3	1.3	1.3	1.3	1.3	1.3	1.3	1.3	1.3

STRAIN GAGE #3

ALTITUDE EQUIPMENT DIVISION		
CALCULATED		
RECORDED		
DRAWN		
CHECKED		
APPROVED		

NASA GAS GENERATOR
5 HR ENDURANCE TEST
SBIR. # P-A

AiResearch Manufacturing Company of Arizona

1 b

FIGURE 76
NASA GAS GENERATOR ACCEPTANCE TEST LOG SHEET

UNIT ASSEMBLY 699300, SERIAL #P-A

PX1959

AIRESEARCH MANUFACTURING COMPANY OF ARIZONA

DATE 9-9-65 TECH. RAS
LOCATION D-107 ENG. WS
JOB TYPE Acceptance Test SUBJECT: NASA GAS GENERATOR

TAPE LOG SHEET

RECORDER TYPE FR-600 TAPE NO. 800 FM CENTER FREQUENCY 27KC

RWO 3409-27136-16-1002 RWO 6701 TAPE SPEED 15 IPS

TRACK	EVENT	TRACK	EVENT
1	DR FM SPEED - COMMENTARY	8	DR FM
2	DR FM WAYNE-KERR PROBE #21	9	DR FM COMPRESSOR END
3	DR FM " " " #22	10	DR FM
4	DR FM " " " #23	11	DR FM TURBINE END
5	DR FM " " " #24	12	DR FM
6	DR FM " " " #25	13	DR FM NORMAL THRUST SURFACE
7	DR FM " " " #26	14	DR FM REVERSE THRUST SURFACE

FOOTAGE	TIME	LOG
		CALIBRATE CHANNELS 2-7 FOR ONE VOLT
	1020	RUN UP TO 20,000 RPM TO STABILIZE UNIT
DP #1	1030	RUN UP TO 38,500 RPM
DP #2	1042	RUN HYDRODYNAMIC ON JOURNALS
DP #3	1115	STEADY STATE RUNNING HYDRODYNAMIC @ 38,500 RPM
DP #4	1145	
DP #5	1215	
DP #6	1245	
DP #7	1315	
DP #8	1345	
DP #9	1415	
DP #10	1445	
DP #11	1515	
DP #12	1545	
DP #13	1547	ADD HYDROSTATIC AIR AND DECREASE SPEED TO 20,000 RPM
DP #14	1555	STEADY STATE AT 20,000 RPM
DP #15	1557	
DP #16	1559	
DP #17	1601	
	1602	ROLL DOWN

Page 1 of 2

AiResearch Manufacturing Company of Arizona

INSTRUMENTATION

OSCILLOGRAPH RECORDING LOG

Unit Type: NASA GAS GEN RWO: 6701 Page No.: 1

Test Location: CELL D-107 RWO: 3409-27136-16-1002 Recorder No.: 6

Record Number	Date	Time	Tech.	Event	Remarks	Unit P/N	Spot Checked By
	9-9		RAS		NASA SHIPPING UNIT	P-A	
00390		1020			RUN UP TO 20,000 RPM		QC20
00391		1030		DP NO. 1	RUN UP TO 38,500 RPM		
00392		1042		DP NO. 2	RUN HYDRODYNAMIC ON JOURNALS		QC21
00393		1115		DP NO. 3	HYDRODYNAMIC AT 38,500 RPM		QC22
00394		1145		DP NO. 4	HYDRODYNAMIC AT 38,500 RPM		
00395		1215		DP NO. 5	HYDRODYNAMIC AT 38,500 RPM		
00396		1245		DP NO. 6	HYDRODYNAMIC AT 38,500 RPM		
00397		1315		DP NO. 7	HYDRODYNAMIC AT 38,500 RPM		
00398		1345		DP NO. 8	HYDRODYNAMIC AT 38,500 RPM		
00399		1415		DP NO. 9	HYDRODYNAMIC AT 38,500 RPM		
00400		1445		DP NO.10	HYDRODYNAMIC AT 38,500 RPM		
00401		1515		DP NO.11	HYDRODYNAMIC AT 38,500 RPM		QC23
00402		1535		DP NO.12	HYDRODYNAMIC AT 38,500 RPM		
00403		1547		DP NO.13	ADDED HYDROSTATIC ARGON AND REDUCE SPEED TO 20,000 RPM		QC25
00404		1555		DP NO.14	STEADY STATE AT 20,000 RPM		
00405		1557		DP NO.15	STEADY STATE AT 20,000 RPM		
00406		1559		DP NO.16	STEADY STATE AT 20,000 RPM		
00407		1601		DP NO.17	STEADY STATE AT 20,000 RPM		
00408		1602			ROLL DOWN		QC24

PX1406

PX1403

AiResearch Manufacturing Company of Arizona

OSCILLOGRAPH RECORDING DATA

Unit Type: NASA GAS GEN Test Location: D-107 Technician: [illegible] Tape Speed: 85 in/sec. 1 Calve Volts: 7.0 Cart No: 6

Job Title: ACCEPTANCE TEST RWO: 6701 Engineer: [illegible] Paper Type: 12" W-4 8 Calve Volts: 7.5 Recorder No: 6

Date: 9-9-65 RWO: 3409-27136-16-1002 Requested By: [illegible] Timing Lines: 1 per Sec. Timing Volts: 0 Record No: 00390 To 00408

UNIT ASSEMBLY 699300, SERIAL NO. P-A

Trace No.	Parameter	Console Chan	Calibration	Galvanometer Ref	Type	Damping	Transducer Cal. Pot.	Re Type	S/N	Range	Accuracy End	Bnd	Spec	Trns	Recorded	Trans Cable	Patch No.	Remarks
1	SPEED	TACH	10,000 RPM/IN	0.8											% ors			
															% ors			
2	THERMOCOUPLE NO. 1	T-1	200°F/IN 0°F AT	1.0											% ors			
4	THERMOCOUPLE NO. 2	T-2	200°F/IN 0°F AT	1.0											% ors			
6	THERMOCOUPLE NO. 4	T-3	200°F/IN 0°F AT	1.0											% ors			
7	THERMOCOUPLE NO. 6	T-4	200°F/IN 0°F AT	2.0											% ors			
8	THERMOCOUPLE NO. 7	T-5	200°F/IN 0°F AT	2.0											% ors			
9	THERMOCOUPLE NO. 10	T-6	200°F/IN 0°F AT	2.0											% ors			
11	THERMOCOUPLE NO. 11	T-7	200°F/IN 0°F AT	3.0											% ors			
13	THERMOCOUPLE NO. 13	T-8	200°F/IN 0°F AT	3.0											% ors			
14	THERMOCOUPLE NO. 14	T-9	200°F/IN 0°F AT	3.0											% ors			
15	THERMOCOUPLE NO. 15	T-10	200°F/IN 0°F AT	4.0											% ors			
16	THERMOCOUPLE NO. 16	T-11	200°F/IN 0°F AT	4.0											% ors			
18	THERMOCOUPLE NO. 18	T-12	200°F/IN 0°F AT	4.0											% ors			
26	THERMOCOUPLE NO. 19	T-1A	200°F/IN 0°F AT	5.0											% ors			
27	THERMOCOUPLE NO. 20	T-2A	200°F/IN 0°F AT	5.0											% ors			
28	THERMOCOUPLE NO. 21	T-3A	200°F/IN 0°F AT	5.0											% ors			
29	THERMOCOUPLE NO. 22	T-4A	200°F/IN 0°F AT	6.0											% ors			
															% ors			
31	TURBINE BRG. LOAD	ATT NO.1	10 LBS/IN	6.0			345#"- 14 LB		56K	INCREASING LOAD					% ors			ZERO W/NORMAL PRELOAD
33	COMPR BRG.LOAD	ATT NO.2	10 LBS/IN	7.0			335#"- 8 LB		56K	INCREASING LOAD					% ors			ZERO W/NORMAL PRELOAD
34	THRUST BRG.LOAD	ATT NO.3	200#"/IN	8.0			195#"		100K	CAL IN HYDRODYNAMIC DIRECTION					% ors			ZERO-ROTOR WT.
QC26															% ors			
															% ors			
															% ors			

NASA GAS GENERATOR ACCEPTANCE TEST
TAPE AND OSCILLOGRAPH LOG SHEETS
FIGURE 77

APPENDIX I

Glossary

The following is a list of terms used throughout the report:

g = conversion factor = 32.2 ft lb per lb sec^2.

$\overset{o}{m}$ = molal gas flow rate, lbs mol per sec.

r_c = compressor pressure ratio

r_{t_1} = gas-generator turbine pressure ratio

r_{t_2} = power-turbine pressure ratio

C = difference between bearing shoe radius and journal radius, inches

D_c = compressor-wheel diameter, inches

D_{t_1} = gas-generator turbine-wheel diameter, inches

E_R = recuperator effectiveness

L = bearing axial length, inches

M = molecular weight, lbs per lb mol

N_1 = gas-generator shaft speed, rpm

N_2 = power-turbine shaft speed, rpm

N_{S_c} = compressor shaft speed

$N_{S_{t_1}}$ = gas-generator turbine specific speed

$N_{S_{t_2}}$ = power-turbine specific speed

P_1 = compressor inlet pressure, lbs per sq ft

P_3 = gas-generator turbine inlet pressure, lbs per sq ft

R = bearing journal radius, inches

R_1 = universal gas constant = 1545 ft-lbs per lb-mol ^oR

T_1 = compressor inlet temperature, $^{\circ}R$

T_3 = gas-generator turbine-inlet temperature, $^{\circ}R$

W = mass flow rate, lbs per sec

$\beta = \dfrac{\text{turbine pressure ratio}}{\text{compressor pressure ratio}} = \dfrac{r_{t_1} \times r_{t_2}}{r_c}$

δ = inlet pressure, psia/14.7 psia

γ = ratio of gas specific heats = 1.667 for monatomic gases

$\theta_1 = \gamma - 1/\gamma$

θ = inlet temperature, $^{\circ}R/518.7^{\circ}R$

η_c = compressor adiabatic efficiency

$\eta_{cy} = \dfrac{\text{power-turbine shaft power output}}{\text{gas-cycle input rate}}$

η_{t_1} = gas-generator turbine adiabatic efficiency

η_{t_2} = power-turbine adiabatic efficiency